TRANSPORT AND PHASE TRANFER CATALYSIS IN GAS-EXPANDED LIQUIDS

A Thesis
Presented to
The Academic Faculty

by

Natalie Brimer Maxey

In Partial Fulfillment
of the Requirements for the Degree
Doctor of Philosophy in the
School of Chemical and Biomolecular Engineering

Georgia Institute of Technology
May 2006

TRANSPORT AND PHASE TRANFER CATALYSIS IN GAS-EXPANDED LIQUIDS

Approved by:

Dr. Charles Eckert, Advisor
School of Chemical and Biomolecular Engineering
Georgia Institute of Technology

Dr. Charles Liotta, Advisor
School of Chemistry and Biochemistry
Georgia Institute of Technology

Dr. William Koros
School of Chemical and Biomolecular Engineering
Georgia Institute of Technology

Dr. Charlene Bayer
Georgia Tech Research Institute
Georgia Institute of Technology

Dr. Carson Meredith
School of Chemical and Biomolecular Engineering
Georgia Institute of Technology

Date Approved: March 30, 2006

For Maddy
I learned the most from my time with you.

Madeline Grace Maxey
July 16, 2003-August 21, 2004

ACKNOWLEDGEMENTS

I would like to thank my advisors, Professor Charles Eckert and Professor Charles Liotta for their instruction, guidance, and support over the years. I have learned a great deal about working with groups of people from Chuck's ability to mesh varied ideas and areas of expertise to form plans that lead to solutions. I must also say that without his support and interest in each of his students as a person, my experience in graduate school would have been very different. Charlie's enthusiasm, creativity, and general level of knowledge about his field are truly inspirational, and his humorous approach to every situation makes him a joy to work with. The rich learning and working environment created by the combination of these personalities in the joint group has benefited me greatly.

I also thank my committee members, Dr. William Koros, Dr. Carson Meredith, and Dr. Charlene Bayer for your interest and support in my work.

I would also like to thank all of the Eckert-Liotta research group members, both past and present. The easy camaraderie in the group fosters a spirit of teamwork that makes learning to do research a pleasure. These past few years have not been the easiest time to know me, and I cannot thank each person enough for giving me a place to feel normal and productive. I am especially grateful to the post-doctoral researchers whose advice has been invaluable, including Josh Brown, David Bush, and Jason Hallett. I also thank the undergraduate researchers who have helped with the day-to-day work of my projects: Greg Robbins, Kimberly Buckner, Kristen Kitigawa, Megan Shenstone,

Christopher Dumler, and Laura Nunez. I also thank Deborah Babykin, who makes all of us more productive.

I must also gratefully acknowledge the love and support of my parents, sisters, and extended family. I thank them for instilling in me a love of learning and education, the confidence to dream big, and the perseverance to follow through. I also thank my mother- and father-in-law for their love and support and for making me a real part of their wonderful family.

Finally, I thank my husband and best friend, Kirk, for his unending confidence in me, his unique ability to make me laugh when I need to, and his complete, unswerving devotion to our marriage and family. I cannot imagine having done this without his support. I also thank my daughter Madeline, whose example of smiling and shining through difficulties I will always strive to follow. I am also very thankful to our newest family member, who has given me renewed healing and a sense of hope for the future. I am truly blessed and thank God for the impact each of them have had on my life.

TABLE OF CONTENTS

LIST OF TABLES

LIST OF FIGURES

LIST OF ABBREVIATIONS

GXL	gas-expanded liquid
CO_2	carbon dioxide
PTC	phase-transfer catalysis
THxAB	tetrahexylammonium bromide
BPB	bromophenol blue

SUMMARY

Gas-expanded liquids (GXL) are a new and benign class of liquid solvents that are intermediate in physical properties between normal liquids and supercritical fluids and therefore may offer advantages in separations, reactions, and advanced materials. Phase-transfer catalysis (PTC) is a powerful tool in chemistry that facilitates interaction and reaction between two or more species present in immiscible phases and offers the ability to eliminate the use of frequently expensive, environmentally undesirable, and difficult to remove polar, aprotic solvents. The work presented here seeks to further characterize the transport properties of GXLs and apply these new solvents to PTC systems, which could result in both greener chemistry and improved process economics.

The transport properties of GXL are characterized by the measurement of diffusivities by the Taylor-Aris dispersion method and calculation of solvent viscosity based on those measurements. The measurement of these bulk properties is part of a larger effort to probe the effect of changes in the local structure surrounding a solute on the solution behavior. The two technologies of PTC and GXL are combined when the distribution of a phase-transfer catalyst between GXL and aqueous phases is measured and compared to changes in the kinetics of a reaction performed in the same system. The results show that increased reaction rates and more efficient catalyst recovery are possible with GXL solvents.

CHAPTER 1

INTRODUCTION

Gas-expanded liquids (GXL) are a new and benign class of liquid solvents formed by the swelling of an organic solvent with a gas, usually carbon dioxide (CO_2) at pressures below the critical pressure of the mixture. These solvents are intermediate in physical properties between normal liquids and supercritical fluids and therefore may offer advantages in separations, reactions, and advanced materials. Phase-transfer catalysis (PTC) is a powerful tool in chemistry that facilitates interaction and reaction between two or more species present in immiscible phases. It offers the ability to eliminate the use of frequently expensive, environmentally undesirable, and difficult to remove polar, aprotic solvents. Combining these technologies could result in both greener chemistry and improved process economics.

In Chapter 2, some background on phase transfer catalyzed processes and the properties and applications of gas-expanded liquids is provided.

In Chapter 3, the diffusivities of a series of nitrogen-containing molecules are measured in GXLs by the Taylor-Aris dispersion technique. Diffusion coefficients increase with added CO_2, as expected. Unexpectedly, the results suggest that diffusion coefficients are impacted more strongly by size and shape of solute molecule and less strongly by polarity or chemical make-up; thus diffusion is a truly bulk property with no discernable effects in the cybotactic region. Using the appropriate estimation techniques, diffusion coefficients are also used successfully to determine viscosity of GXLs.

Chapter 4 describes the distribution behavior of a phase-transfer catalyst, tetrahexylammonium bromide, between water and CO_2-expanded toluene. Changes in the density and polarity/polarizability of the GXL phase cause the catalyst distribution to first decrease slightly and the increase substantially into the aqueous phase. This change in distribution results in significant potential savings in water usage for recovery of the catalyst by extraction.

In Chapter 5, the effect on kinetics of the phase-transfer catalyzed nucleophilic displacement of benzyl bromide by potassium thiocyanate with tetrahexylammonium bromide in the same aqueous/CO_2-expanded toluene system used in Chapter 4 is presented. A minimum in rate constant is observed, suggesting two competing effects on the rate: a heterogeneous mechanism that is enhanced and a homogeneous mechanism that is slowed by added CO_2.

Chapter 6 includes conclusions and recommendations for further research efforts in the various investigations presented in this thesis. These include ideas for reversible emulsions, other PTC reactions in GXL/aqueous systems, and enantioselective PTC reactions.

Appendix A discusses attempts at performing enantioselective PTC alkylations in SCF CO_2. The results were racemic mixtures in both cases. These findings are consistent with literature data for PTC reactions with chiral catalysts, which showed that no enantiomeric excesses are achieved for solid-liquid conditions, while liquid-liquid reactions are typically more successful.

Appendix B includes work toward the development of air filter media with chemical functionalities that react with components in an inlet air stream to remove

unwanted chemicals and odors. The results show that the basic premise of using a gel containing ion exchange resin sequestering agents holds promise of being successful. A working filter was eventually designed and tested, but has not been implemented in industry yet.

CHAPTER 2

BACKGROUND ON PHASE-TRANSFER CATALYSIS AND GAS-EXPANDED LIQUID SOLVENTS

One of the largest areas of research and potential impact in the search to find greener, more sustainable solutions in chemical technology is the development of safer, more tunable solvents, such as gas-expanded liquids, which are still being characterized and extensively studied. Combining this technology with the benefits of phase transfer catalysis, which offers the ability to eliminate the use of frequently expensive, environmentally undesirable, and difficult to remove polar, aprotic solvents could result in both greener chemistry and improved process economics.

Phase-Transfer Catalysis

Phase-transfer catalysis (PTC) is a powerful tool in chemistry that facilitates interaction and reaction between two or more species present in immiscible phases (Starks, Liotta et al. 1994). In PTC, a phase-transfer agent is used in catalytic amounts to transfer one of the species to a location where it can quickly react with another species.

PTC Fundamentals

While the idea of PTC is quite general, the typical PTC mechanism, as illustrated in Figure 2.1, involves transfer of anions from an aqueous or solid phase to an organic phase (Starks 1971). Two general steps are involved in this catalytic sequence. The first step is the transfer of the anion from the aqueous to the organic phase. This step includes distribution of the catalyst between the two phases, ion exchange between the catalyst

and reacting salt, and transfer of the catalyst-ion complex to the organic phase. The second step is the intrinsic or organic phase reaction or sequence of reactions.

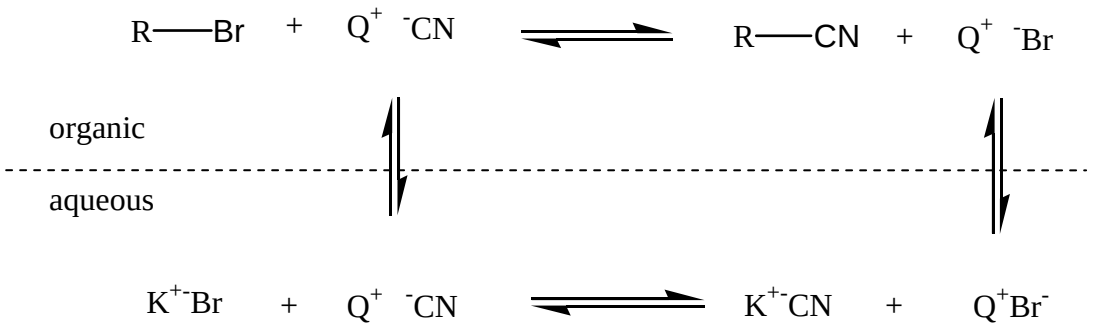

Figure 2.1: Schematic of PTC cyanide displacement (Starks 1971).

Many factors affect the rate of one or both of these steps. If one step is much slower than the other, it is said to be the limiting step. The PTC reaction rate matrix, Figure 2.2, shows the four types of systems possible. In it, the transfer rate is plotted on the x-axis and the intrinsic reaction rate on the y-axis. Midpoint lines divide the graph into quarters. In the lower-right corner, the transfer rate is fast, but the intrinsic reaction is slow. This is the intrinsic reaction rate limited region. To improve the overall rate for a reaction in this region, one must improve the intrinsic rate. The upper-left corner is the transfer rate limited region. Here, the intrinsic reaction rate is fast, but the transfer rate is slow. Improving the overall rate in this region requires improving mass transport through agitation (Ragaini, Chiellini et al. 1988) or solvent choice (Starks and Owens 1973). The upper right corner is the fast region, in which both the reaction and transfer have high rates. Almost any catalyst in any set of conditions will work here. The lower left corner is the slow region, where both the intrinsic reaction and the transfer steps are slow. Improving the rates in this region usually requires more extreme conditions or creative use of co-catalysts (Dehmlow, Thieser et al. 1985).

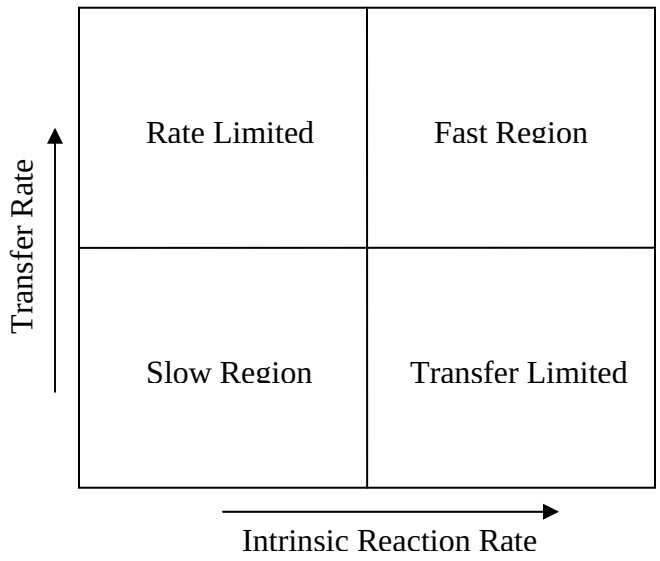

Figure 2.2: PTC Reaction Rate Matrix

PTC is performed in a wide variety of phase combinations. The example shown above is a liquid-liquid system; however, solid-liquid, solid-liquid-omega phase, solid-liquid-liquid, gas-liquid-solid, and liquid-liquid-liquid systems are also used (Yadav 2004). The use of microwave irradiation in either solid-liquid or liquid-liquid PTC systems has also become popular (Loupy, Petit et al. 2002).

PTC Catalysts

The most common catalysts for PTC systems are quaternary ammonium and phosphonium salts, crown ethers and cryptands, and polyethylene glycol and its derivatives (Starks, Liotta et al. 1994). Catalysts have also been found for special circumstances such as when high temperature is necessary (Brunelle 1987) or when a chiral product is desired (Dolling, Davis et al. 1984). When choosing a catalyst for a PTC reaction, one must consider structure-activity relationships, stability and catalyst separations considerations, and in industrial settings, cost, toxicity, availability, recyclability, and waste treatment.

Quaternary ammonium salts (Figure 2.3) are the most commonly used phase-transfer catalysts. Two important structural aspects of the catalyst should be considered when choosing a catalyst of this type. These are the distribution of the catalyst and reactive species between the phases and the anion-activating versus accessibility properties of the catalyst (Starks, Liotta et al. 1994). A quaternary ammonium cation with longer, bulkier alkyl groups attached activates its associated anion by increasing the distance separating the ion pair. Quaternary cations with one large group and three small groups have a cation center that is highly accessible to the associated anion (Starks and Liotta 1978). Activating quaternary salts are generally best for simple displacement reactions, especially those involving smaller anions, whereas accessible catalysts are better for reactions involving strong bases that require transfer of hydroxide ion (Sirovskii, Velichko et al. 1985).

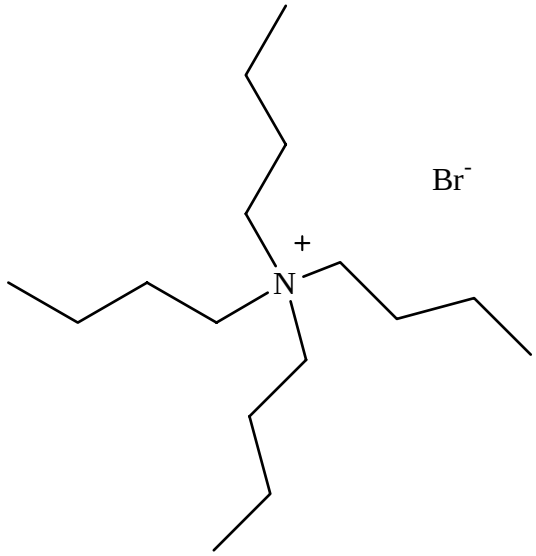

Figure 2.3: Typical quaternary ammonium salt structure—tetrabutylammonium bromide

For the quaternary ammonium cation, shorter alkyl groups tend to cause the catalyst to partition more into the aqueous phase, while longer alkyl groups allow more of it to reside in the organic phase (Starks, Liotta et al. 1994). The distribution of the catalyst-anion pair between the aqueous and organic phases can have a significant impact on the overall reaction rate since the anion needs to be present in the organic phase (where the reaction is occurring) in sufficient quantity for the reaction to proceed at a reasonable rate (Herriott and Picker 1975). At the same time, it cannot have so much organic character that it does not approach the interface at all. In general, this distribution depends strongly on catalyst structure for transfer of small anions, such as chloride, bromide, and cyanide, and less so for anions that have more organic quality themselves.

Catalyst distribution is also related to the choice of organic phase solvent (Brandstrom 1977). Higher polarity solvents allow greater distribution of the catalyst to the organic phase. The distribution of tetrabutylammonium bromide in a selection of solvents is shown in Table 2.1.

Table 2.1: Effect of solvent on distribution of tetrabutylammonium bromide between organic and aqueous phases (Brandstrom 1977).

Solvent	Distribution constant, K $K = [Q^+Br^-]_{org}/[Q^+]_{aq}[Br^-]_{aq}$
benzene	<0.1
diethyl ether	<0.1
chlorobenzene	<0.1
o-dichlorobenzene	<0.1
ethyl acetate	0.2
n-chlorobutane	<0.1
dichlorobutane	0.3
dichloropropane	2.9
dichloroethane	6.1
dichloromethane	35.0
chloroform	47.0
carbon tetrachloride	<0.1
3-pentanone	1.1
2-butanone	14.0
n-butanol	69.0
nitropropane	9.0
nitromethane	168.0

PTC Applications

PTC is used for a number of important industrial applications. In the early 1990s, an estimated 500 industrial processes, contributing to at least $10 billion/year in sales of products, were being performed (Starks, Liotta et al. 1994). These processes include a wide variety of industries, including polymers, pharmaceuticals, agricultural chemicals, monomers, general chemicals, flavors and fragrances, dyes, surfactants, and explosives. The many benefits of PTC, such as high yield with increased reaction rate, mild reaction conditions, and flexibility of solvent choice, make it very attractive in an industrial setting.

Most of the drawbacks to using PTC industrially involve the catalyst—its toxicity, cost, availability, and separation. Therefore, an important consideration for industrial use of PTC is separation and recovery of the catalyst from the products of reaction. The use of insoluble (supported) catalysts largely avoids this problem (Yadav 2004). However, heterogeneous catalysis also has disadvantages such as lower activity and selectivity. When the use of soluble catalysts is most appropriate, the most commonly used methods of separation on an industrial scale are extraction and distillation (Zaidman, Sasson et al. 1985).

Recently Xie, et al reported the enhanced aqueous extraction of phase transfer catalysts using carbon dioxide as an antisolvent to increase the catalyst partitioning into the aqueous phase, as shown in Figure 2.4 (Xie, Brown et al. 2002). Reductions of 95% or more in wash water volumes are possible with an aqueous extraction enhanced with 50 bar of CO_2, according to this work.

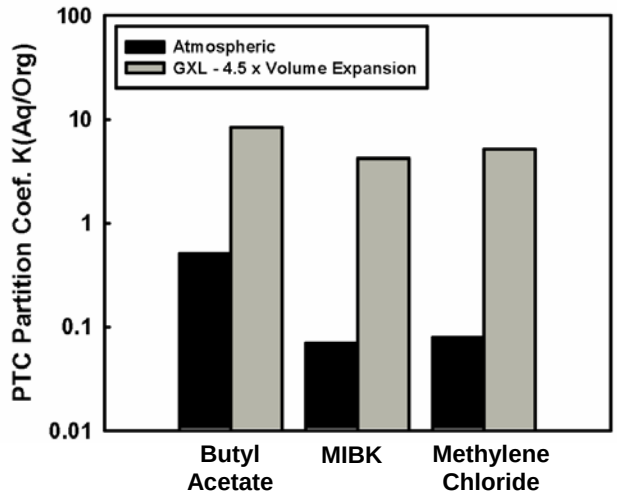

Figure 2.4: Tetrabutylammonium picrate distribution coefficient as a function of CO_2 expansion at room temperature (Xie, Brown et al. 2002).

Supercritical fluids have been studied extensively as benign alternatives to conventional organic solvents that may also offer improvements in reaction rate, product selectivity, and separations. Dillow, et al reported the first example of PTC in supercritical fluids—the nucleophilic displacement of benzyl chloride with bromide and cyanide ions (Dillow, Brown et al. 1998). The alkylation and cycloaklyation of phenylacetonitrile have also been reported (Wheeler, Lamb et al. 2002). In these cases, the results suggested the formation of a third catalyst-rich phase on the surface of the salt, called the "omega phase," in which the reaction actually occurred. This phase has also been shown to be important in other PTC reactions (Regen 1976). In this system, the substrate and product partition in and out of the omega phase, which has enough organic quality to solubilize them and enough ionic quality to also support the reactant ions. The supercritical fluid, with its increased diffusivity, facilitates this transport better than a liquid solvent.

The production of chiral molecules for pharmaceuticals, a high-value product with an inherent need for high purity, is a natural fit for the benefits of PTC. Several examples of enantioselective PTC reactions have been reported in the literature, mostly catalyzed by cinchona-alkaloid-derived quaternary ammonium salts (Dolling, Davis et al. 1984; Dolling, Hughes et al. 1987). Alkylations of indanones have been reported using a variety of N-benzylcinchoninium halides with enantiomeric excesses (e.e.'s) of up to 94% (Hughes, Dolling et al. 1987). This same group also reported alkylations using a similar catalyst with a fluorous group attached and an asymmetric modification of the Robinson annulation. Asymmetric Michael additions have also been reported with more modest e.e.'s (Diez-Barra, de la Hoz et al. 1998).

Gas-Expanded Liquids

Solvent choice is a major concern in chemical processing. For reactions, the solvent properties that must be considered are those that affect the solvation of reactants and the ability to transport them through solution, such as density, viscosity, diffusivity, and any specific interactions. The potential impact on human health and the environment and the cost associated with using and recycling the solvent are also important considerations. For these reasons, the use of CO_2 as an alternative to traditional organic solvents has been an extensive area of research over the last several decades. Supercritical fluid (SCF) CO_2 has been used for extractions, reactions (Dillow, Brown et al. 1998), catalyst recycling, and in polymer processing (Kazarian, Vincent et al. 1996). The advantages of using SCF CO_2 are generally vastly improved mass transfer rates and simplicity of solvent removal. The disadvantages of these processes are solubilities that are usually less than in liquids and high capital costs for the required process equipment.

The limited solubilities of most compounds seen in SCFs has led to the use of co-solvents (1–5% organic modifier) such as methanol and acetone, which have also been studied extensively. SCF systems with added co-solvents still have the benefits of easier mass transfer and solvent removal, but also have increased ranges of solvent power (Tomasko, Knutson et al. 1993). Then main disadvantage of these systems is the increase in the critical pressure of the mixture that results from adding co-solvent, which has detrimental effects on both economic and processing variables. These solvents have been used for improved reactions (Caravati, Grunwaldt et al. 2006) as well as the extraction of natural compounds for food and cosmetics applications (Han, Cao et al. 2005; Kopcak and Mohamed 2005).

Gas-expanded liquids (GXL) are a new and benign class of liquid solvents formed by the swelling of an organic solvent with a gas, usually carbon dioxide (CO_2) at pressures below the critical pressure of the mixture (Eckert, Liotta et al. 2004). These solvents are intermediate in physical properties between normal liquids and supercritical fluids and therefore may offer advantages in separations, reactions, and advanced materials. In general, liquid CO_2 is a poor solvent, whereas typical organics are better solvents, so a range of solvent properties is accessible in these highly tunable solvents at moderate pressures (30-80 bar). Since separations typically represent 60-80% of the total cost of a chemical process, the ability to reduce separations costs represents one of the most significant processing advantages inherent to GXLs. The transport properties are similarly tunable between those of SCFs and traditional organic solvents. A pictoral comparison of the solvent power and transport properties of these systems is shown in Figure 2.5.

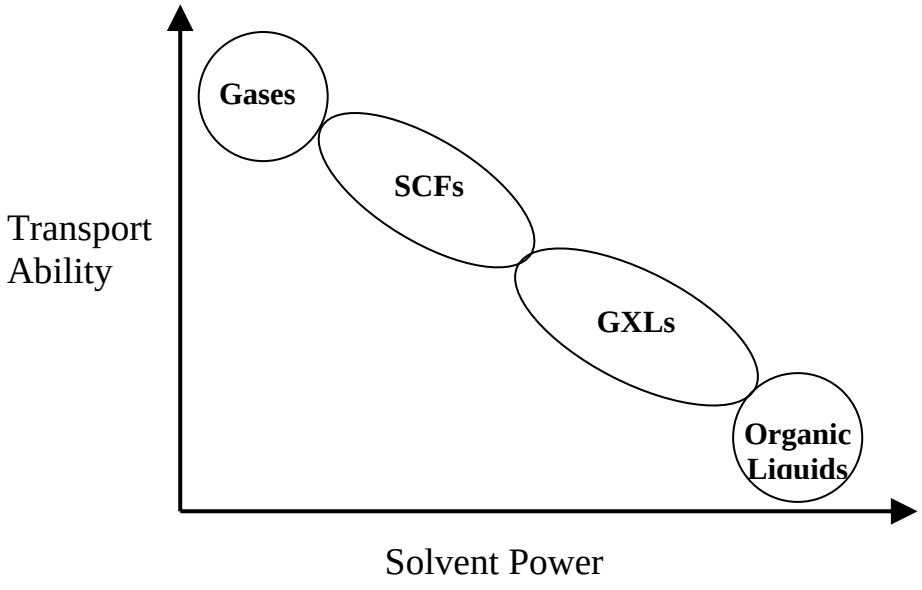

Figure 2.5: Relative solvent power and transport ability of different solvent types.

GXL Applications

Gas-antisolvent (GAS) crystallization is one highly successful application of GXLs (Winters, Knutson et al. 1996). The advantage of GAS over traditional crystallization processes is the potential to nucleate crystals throughout the solution, leading to more uniform particle size. GXLs have also been used as the mobile phase in HPLC, where they are known as "enhanced fluidity liquids." Some of those applications include reversed-phase HPLC, size-exclusion chromatography, and chiral HPLC separations.

The tunability of GXLs has also been exploited to separate and recycle homogeneous catalysts. In these systems, the reaction is run homogeneously, and the organic solvent is subsequently expanded, inducing immiscibility and allowing heterogeneous separation and product recovery and catalyst recycling. This approach has been applied to fluorous biphasic chemistry and organic-aqueous tunable solvents (OATS) for enzyme reactions (Lu, Lazzaroni et al. 2004). Hydrogenation reactions have also been performed in these systems to take advantage of their increased gas solubility.

CO_2 has also been shown to be both reactant and solvent for reactions in GXL. Methylcarbonic acid is formed in CO_2-expanded methanol, and peroxycarbonic acid is formed from hydrogen peroxide and CO_2. These acids can be formed reversibly in-situ for catalysis and do not require neutralization, regeneration, or waste disposal. Methylcarbonic acids have been used to catalyze acetal formation (Xie, Liotta et al. 2004) and for the production of terpineol from b-pinene (Chamblee, Weikel et al. 2004), and peroxycarbonic acids have been used to catalyze the epoxidation of cyclohexene.

CO_2-expanded liquids have also been used to form protecting groups for reaction intermediates. In CO_2-expanded THF, CO_2 reacts with primary amines to form solid carbamic acids and/or ammonium carbamates (Xie, Liotta et al. 2004). The amines are protected from hydrogenation, and can be easily separated and recovered upon gentle heating.

Conclusions

The use of GXL solvents in PTC systems offers the ability to not only replace potentially harmful and expensive solvents with safer alternatives, such as CO_2, but also to take advantage of better solvent properties and tunability. PTC affects more than 500 industrial processes, so the potential for environmental and economic impact is significant.

References

Brandstrom, A. (1977). "Principles of phase-transfer catalysis by quaternary ammonium salts." Advances in Physical Organic Chemistry **15**: 267-330.

Brunelle, D. J. (1987). "Stable catalysts for phase transfer at elevated temperatures." ACS Symposium Series **326**(Phase Transfer Catal.: New Chem., Catal, Appl.): 38-53.

Caravati, M., J.-D. Grunwaldt, et al. (2006). "Solvent-modified supercritical CO2: A beneficial medium for heterogeneously catalyzed oxidation reactions." Applied Catalysis, A: General **298**: 50-56.

Chamblee, T. S., R. R. Weikel, et al. (2004). "Reversible in situ acid formation for b-pinene hydrolysis using CO2 expanded liquid and hot water." Green Chemistry **6**(8): 382-386.

Dehmlow, E. V., R. Thieser, et al. (1985). "The extraction of alkoxide anions by quaternary ammonium phase transfer catalysis." Tetrahedron **41**(14): 2927-32.

Diez-Barra, E., A. de la Hoz, et al. (1998). "A study on the phase transfer catalyzed Michael addition." Tetrahedron **54**(9): 1835-1844.

Dillow, A. K., J. S. Brown, et al. (1998). "Supercritical Fluid Tuning of Reactions Rates: the Cis-Trans Isomerization of 4-4'-Disubstituted Azobenzene." Journal of Physical Chemistry A **102**(39): 7609-7617.

Dolling, U. H., P. Davis, et al. (1984). "Efficient catalytic asymmetric alkylations. 1. Enantioselective synthesis of (+)-indacrinone via chiral phase-transfer catalysis." Journal of the American Chemical Society **106**(2): 446-7.

Dolling, U. H., D. L. Hughes, et al. (1987). "Efficient asymmetric alkylations via chiral phase-transfer catalysis: applications and mechanism." ACS Symposium Series **326**(Phase Transfer Catal.: New Chem., Catal., Appl.): 67-81.

Eckert, C. A., C. L. Liotta, et al. (2004). "Sustainable Reactions in Tunable Solvents." Journal of Physical Chemistry B **108**(47): 18108-18118.

Han, H., W. Cao, et al. (2005). "Preparation of biodiesel from soybean oil using supercritical methanol and CO2 as co-solvent." Process Biochemistry (Oxford, United Kingdom) **40**(9): 3148-3151.

Herriott, A. W. and D. Picker (1975). "Phase transfer catalysis. Evaluation of catalysis." Journal of the American Chemical Society **97**(9): 2345-9.

Hughes, D. L., U. H. Dolling, et al. (1987). "Efficient catalytic asymmetric alkylations. 3. A kinetic and mechanistic study of the enantioselective phase-transfer methylation of 6,7-dichloro-5-methoxy-2-phenyl-1-indanone." Journal of Organic Chemistry **52**(21): 4745-52.

Kazarian, S. G., M. F. Vincent, et al. (1996). "Specific Intermolecular Interaction of Carbon Dioxide with Polymers." Journal of the American Chemical Society **118**(7): 1729-36.

Kopcak, U. and R. S. Mohamed (2005). "Caffeine solubility in supercritical carbon dioxide/co-solvent mixtures." Journal of Supercritical Fluids **34**(2): 209-214.

Loupy, A., A. Petit, et al. (2002). "Microwave and phase-transfer catalysis." Microwaves in Organic Synthesis: 147-180.

Lu, J., M. J. Lazzaroni, et al. (2004). "Tunable Solvents for Homogeneous Catalyst Recycle." Industrial & Engineering Chemistry Research **43**(7): 1586-1590.

Ragaini, V., E. Chiellini, et al. (1988). "Phenylacetonitrile alkylation with different phase-transfer catalysts in continuous flow and batch reactors." Industrial & Engineering Chemistry Research **27**(8): 1382-7.

Regen, S. L. (1976). "Triphase catalysis. Kinetics of cyanide displacement on 1-bromooctane." Journal of the American Chemical Society **98**(20): 6270-4.

Sirovskii, F. S., S. M. Velichko, et al. (1985). "Alkaline dehydrochlorination reactions of pentachloropropane. III. Correlation between structure and catalytic activity of quaternary ammonium salts (QAS) in alkaline dehydrochlorination of 1,1,2,2,3-pentachloropropane." Kinetika i Kataliz **26**(6): 1478-81.

Starks, C. M. (1971). "Phase-transfer catalysis. I. Heterogeneous reactions involving anion transfer by quaternary ammonium and phosphonium salts." Journal of the American Chemical Society **93**(1): 195-9.

Starks, C. M. and C. Liotta (1978). Phase Transfer Catalysis: Principles and Techniques.

Starks, C. M., C. L. Liotta, et al. (1994). Phase-Transfer Catalysis: Fundamentals, Applications, and Industrial Perspectives.

Starks, C. M. and R. M. Owens (1973). "Phase-transfer catalysis. II. Kinetic details of cyanide displacement on 1-halooctanes." Journal of the American Chemical Society **95**(11): 3613-17.

Tomasko, D. L., B. L. Knutson, et al. (1993). "Spectroscopic study of structure and interactions in cosolvent-modified supercritical fluids." Journal of Physical Chemistry **97**(45): 11823-34.

Wheeler, C., D. R. Lamb, et al. (2002). "Phase-Transfer-Catalyzed Alkylation of Phenylacetonitrile in Supercritical Ethane." Industrial & Engineering Chemistry Research **41**(7): 1763-1767.

Winters, M. A., B. L. Knutson, et al. (1996). "Precipitation of Proteins in Supercritical Carbon Dioxide." Journal of Pharmaceutical Sciences **85**(6): 586-594.

Xie, X., J. S. Brown, et al. (2002). "Phase-transfer catalyst separation by CO2 enhanced aqueous extraction." Chemical Communications (Cambridge, United Kingdom)(10): 1156-1157.

Xie, X., C. L. Liotta, et al. (2004). "CO2-Catalyzed Acetal Formation in CO2-Expanded Methanol and Ethylene Glycol." Industrial & Engineering Chemistry Research **43**(11): 2605-2609.

Xie, X., C. L. Liotta, et al. (2004). "CO2-Protected Amine Formation from Nitrile and Imine Hydrogenation in Gas-Expanded Liquids." Industrial & Engineering Chemistry Research **43**(24): 7907-7911.

Yadav, G. D. (2004). "Insight into Green Phase Transfer Catalysis." Topics in Catalysis **29**(3-4): 145-161.

Zaidman, B., Y. Sasson, et al. (1985). "General economic evaluation of the use of quaternary ammonium salts as catalysts in industrial applications." Industrial & Engineering Chemistry Product Research and Development **24**(3): 390-3.

CHAPTER 3

DIFFUSIVITIES IN GAS-EXPANDED LIQUIDS BY TAYLOR-ARIS DISPERSION

Transport properties, especially diffusion coefficients, are of great practical importance when developing processes for industrial applications. Designing and modeling potential GXL processes such as extractions and chromatography will require an understanding of these properties for success. Knowledge of these properties, and especially the trends in these properties with added CO_2 content, is also helpful to the continued research on these new and potentially promising solvents.

In this work, diffusion coefficients in CO_2-expanded methanol are measured using the Taylor-Aris dispersion method in a supercritical fluid chromatograph (Taylor 1953; Taylor 1954; Aris 1959). This technique introduces a pulse of solute into a solvent flowing under fully developed laminar flow conditions in a long, narrow tube (Figure 3.1). The narrow pulse disperses due to the radial velocity profile and radial and axial diffusion (Cussler and Editor 1996). The resulting concentration versus time profile from the end of the tube can then be fit using the proper models to determine the diffusion coefficient. Fast diffusion produces little dispersion, and slow diffusion produces more, as illustrated by the concentration profiles in Figure 3.2 (Cussler and Editor 1996). The reason for this is that in the slow diffusion case, the flow of fluid dominates and broadens the profile. When diffusion is fast, axial diffusion occurs outward (toward the slower-moving fluid) near the center of the velocity profile and inward (toward the faster-moving fluid) near the walls, keeping the concentration profile narrow.

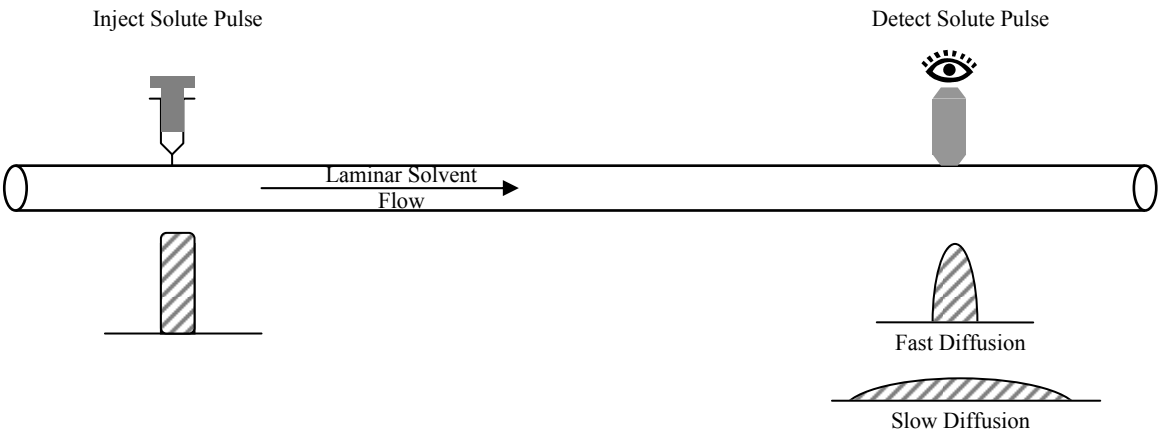

Figure 3.1: Taylor-Aris dispersion

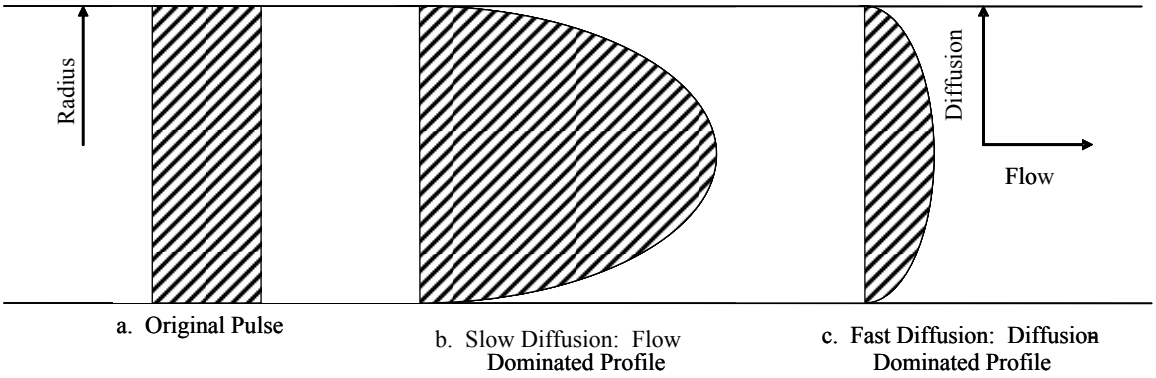

Figure 3.2: Dispersion of concentration profile

The concentration profile can be fit to Equation 3.1 below, where K is related to the diffusion coefficient, and is given by Equation 3.2 (Funazukuri and Ishiwata 1999) where L is the tube length, R is the tube internal radius, m is the amount of solute in the pulse in excess of that in the carrier stream, and u is the average velocity of the flowing fluid.

$$C(t) = \frac{m}{2\pi R^2 \sqrt{\pi K t}} \exp\left(\frac{-(L-ut)^2}{4Kt} \right) \quad \text{Eq 3.1}$$

$$K = \frac{R^2 u^2}{48D} + D \quad \text{Eq 3.2}$$

The assumptions necessary for this model are true when the time constant given by Equation 3.3 is greater than 5 (radial concentration profiles are virtually absent) and the product of the Dean number and the square root of the Schmidt number (Equation 3.4) is less than 10 (secondary flow due to coiled tube is negligible).

$$\tau = \frac{Dt}{R^2} > 5 \quad \text{Eq 3.3}$$

$$DeSc^{1/2} < 10 \quad \text{Eq 3.4}$$

Since this project is part of a larger effort to elucidate the cybotactic region of GXLs, solutes that might have specific interactions with the fluid were chosen. Since many data were available for diffusion coefficients of substitute benzenes in ambient organic alcohols (Lu, Kong et al. 1999; Gonzalez, Bueno et al. 2001) and the binary diffusion coefficient of benzene in CO_2-expanded methanol had been measured for the whole composition range (Sassiat, Mourier et al. 1987), we chose a series of nitrogen-containing ring compounds which all have different dipole moments. The diffusion coefficients of benzene, pyridine, pyrimidine, pyrazine and 1,3,5-triazine (Figure 3.3) were measured in CO_2-expanded methanol by the Taylor-Aris dispersion technique. These diffusion coefficients will be used to estimate the viscosity of the methanol/CO_2

mixtures by applying a variation of the Stokes-Einstein Equation that is valid for supercritical fluids (Woerlee 2001). The diffusion coefficients of these solutes in CO_2-expanded methanol will also be calculated using models developed by a collaborating researcher. Those results are beyond the scope of this particular study.

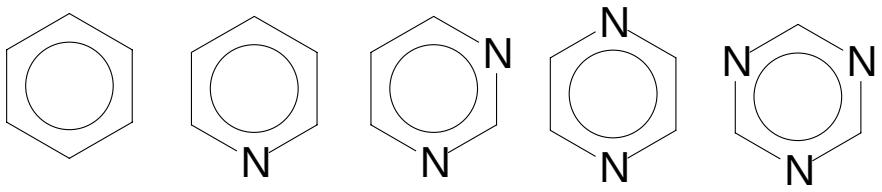

Figure 3.3: Solutes studied.

Experimental Methods

Materials

Methanol (HPLC) and all solutes (benzene, toluene, phenol, 2-naphthol, pyridine, pyrimidine, pyrazine and 1,3,5-triazine, analytical grade) were purchased from Sigma-Aldrich. Carbon dioxide was purchased from Airgas. All were used as received.

Apparatus

All data were measured in a supercritical fluid chromatograph (SFC) (Berger Instruments) fitted with an autosampler (Berger Instruments, Model 718) and UV detector (Hewlett Packard 1050 Series). Data were acquired via software (Berger Instruments SFC Chemstation Version 3.03). The column was replaced with 100 feet of coiled 1/16 inch tubing. The pumps were bypassed and replaced with syringe pumps (ISCO) to ensure a constant and controllable pulse-free flow. Pressure was maintained

with a back pressure regulator (TESCOM 26-1764-24). A schematic is shown in Figure 3-4.

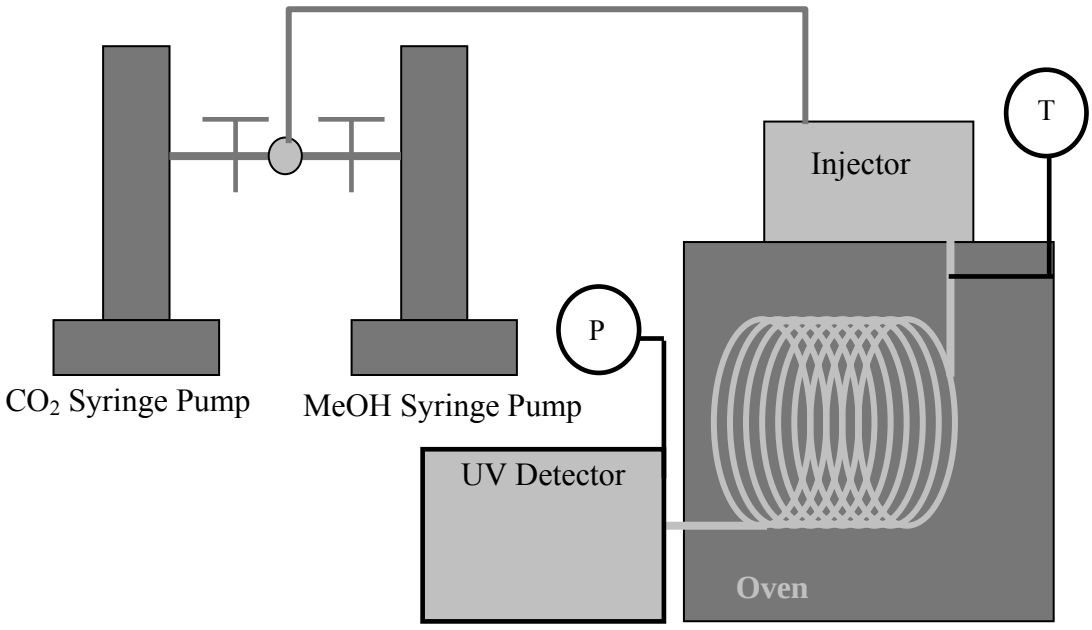

Figure 3.4: Supercritical fluid chromatograph.

Procedure

The procedure outlined below was validated via several diagnostics, the details of which can be found in Appendix C. Laminar flow is developed throughout the system by setting the total liquid flow rate to 0.2 ml-min^{-1} and allowing the system pressure to reach the desired pressure of 150 bar. Because the tube is coiled, it is important to note that laminar flow is not only determined by the Reynolds number, but also by the Dean and Schmidt numbers. Care had to be taken to choose a flow rate low enough such that $(De)(Sc)^{0.5} < 10$ (Bueno, Suarez et al. 1993). A known volume of solute in methanol solution is injected via a sample loop, with care taken to allow the mobile phase to flow through the loop for a short time; thus avoiding dispersion effects and tailing (Sassiat, Mourier et al. 1987). The pulse flows through the 100 feet of column before entering the

detector. The result is a Gaussian peak representing the concentration distribution of the initial pulse of solute that passes through the detector which has broadened based on the dispersion in the mobile phase.

The temporal variance of the Gaussian curve may be interpreted using Equation 3.7, where σ is the variance of the curve in length, D_{12} is the infinite dilution diffusion

$$\sigma^2 = \frac{2D_{12}L}{\bar{u}_0} + \frac{r_0^2\bar{u}_0^2}{24D_{12}} \qquad \text{Eq. 3.7}$$

coefficient of the solute (1) in the solvent (2), L is the length of the tube, $\bar{u}_0$ is the average velocity of the mobile phase, which is equal to the length divided by the retention time, and r_0 is the inner radius of the tube (Bueno, Suarez et al. 1993). The software package does not give a dispersion term, but rather gives the width of the peak at half its height, or $W_{1/2}$, which is 2.354σ. Furthermore, applying the "height of the theoretical plate" or "relative peak broadening" concept from Equation 3.8 to Equation 3.7 results in Equation 3.9 (Bueno, Suarez et al. 1993).

$$H = \sigma^2 / L = 1 / 2.354^2 W_{1/2}^2 L \qquad \text{Eq. 3.8}$$

$$D_{12} = \left(\frac{\bar{u}_0}{4}\right)\left\{H - \left[H^2 - \left(\frac{r_0}{3}\right)^{1/2}\right]\right\} \qquad \text{Eq. 3.9}$$

Once diffusion coefficients are measured, the viscosity, η, of the mobile phase can be estimated using a version of the Stokes-Einstein equation that is valid for supercritical fluids (Equation 3.10) where D_i is the diffusion coefficient of the chosen solute in the mobile phase, κ is Boltzmann's constant, T is absolute temperature and σ

$$D_i\eta = \frac{5}{9}\frac{\kappa T}{\pi\sigma_i}\frac{\sigma}{\sigma_i} \qquad \text{Eq. 3.10}$$

and σ_i are the average and individual collision diameters of the molecules, respectively (Woerlee 2001). It is important to note that while diffusion depends on the solute and solvent, viscosity is only measured with regard to the solvent. Since these measurements have a solute present, it is important to account for interactions between that solute and itself or the solvent. This occurs in the collision diameter terms.

Results and Discussion

Before any measurements in CO_2-expanded methanol were made, a variety of measurements such as variation of diffusion coefficients in pure methanol with regard to solute concentration, ISCO temperature, flow rate and pressure were performed to ensure the validity of the experimental method. Details of these validation procedures are presented in Appendix C. Furthermore, the diffusion coefficients of several solutes were measured in methanol and showed relatively good agreement with literature values (Table 3.1).

Table 3.1: Our data compared with literature data for several solutes in methanol.

	Lu, et. al.	Our Work	Our Work, Converted
Solute	298.2K, 1 bar ($D/10^{-5}$, cm^2/s)	313.2K, 100 bar ($D/10^{-5}$, cm^2/s)	298.2K and 1bar ($D/10^{-5}$, cm^2/s)
Benzene	2.61±0.02	2.9-3.1	2.44-2.61
Toluene	2.42±0.02	2.76-2.83	2.33-2.38
Phenol	1.69±0.02	1.9-2.0	1.60-1.68
2-Naphthol	1.45±0.01	1.67-1.73	1.41-1.46

Once we could be sure of our measurements on pure solvents, we attempted to reproduce the data of Sassiat et. al. (Sassiat, Mourier et al. 1987) for diffusion coefficients of benzene in CO_2-expanded methanol as shown in Figure 3.5. Diffusion coefficients of benzene in the GXL are shown as a function of mass fraction of carbon dioxide. It is important to note that the dashed line in the figure is a curved line connecting the points that was included to guide the eye and is not a mathematical fit. The cited authors made their measurements at 210 nm while we made ours at 254 nm. We determined that this was the most suitable detection wavelength for benzene for our system, but according to the data it does not seem to matter. Our data match that of the literature satisfactorily.

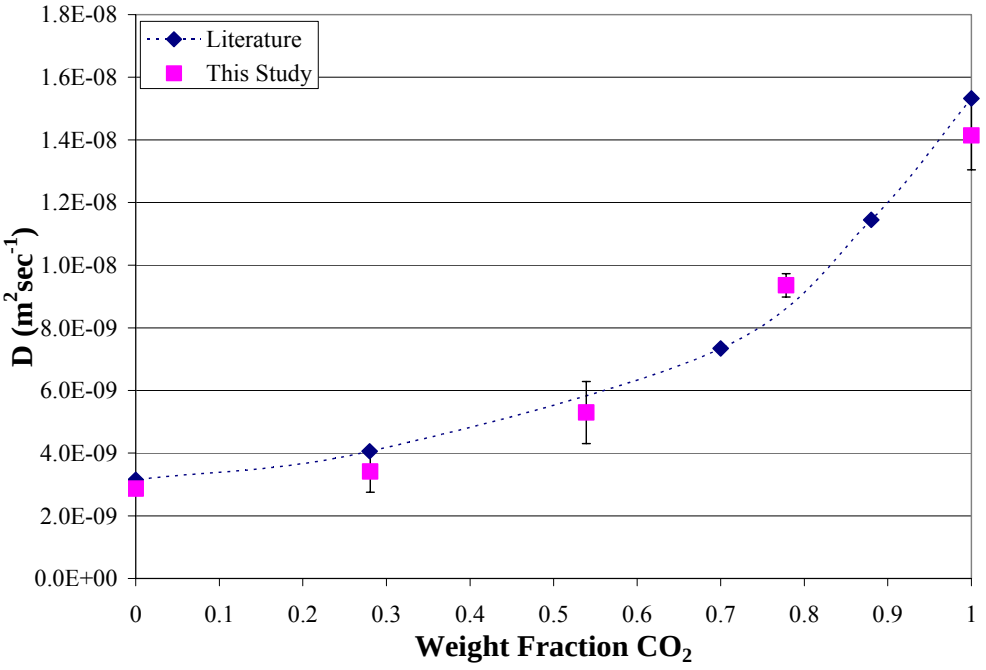

Figure 3.5: Diffusion coefficients of benzene in CO_2-expanded methanol as a function of weight fraction of CO_2, 313 K, 150 bar.

Data were measured for all solutes in the full range of methanol/CO_2 mixtures. Data are presented in two ways – separated by solute in Figure 3.6 and overlaid in figure 3.7 – in order to make it easier to understand the data. Several conclusions can be drawn from analysis of the data presented. All of the solutes studied behave in an expected manner; all diffuse faster as the amount of carbon dioxide is increased. What these graphs also tell us is that the differences in polarity of the solute molecules does not have an impact on the diffusion coefficients in CO_2-expanded methanol. Thus any inhomogeneities that may exist in the cybotactic region as a result of these different polarities are not manifested in the dispersion of a solute through these fluids. Therefore it seems that diffusivity has no discernable effects in the cybotactic region.

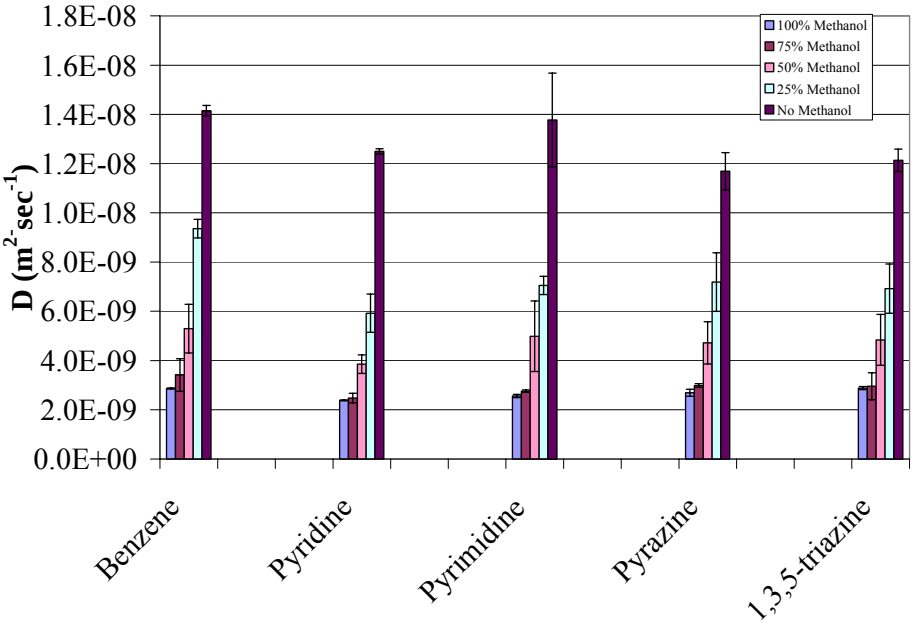

Figure 3.6: Diffusion coefficients of benzene, pyridine, pyrimidine, pyrazine and 1,3,5-triazine in CO_2-expanded methanol as a function of volume fraction of methanol, 313 K, 150 bar.

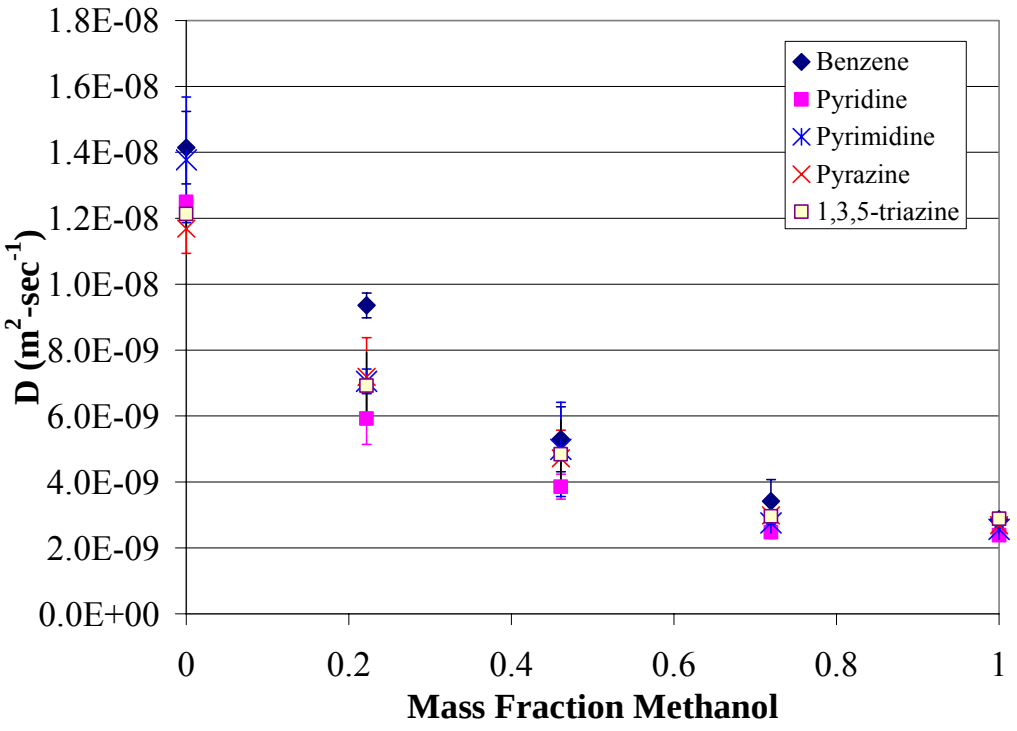

Figure 3.7: Diffusion coefficients of benzene, pyridine, pyrimidine, pyrazine and 1,3,5-triazine in CO_2-expanded methanol as a function of mass fraction of methanol, 313 K, 150 bar.

In order to strengthen the above conclusion, data of a variety of pseudoplanar compounds in an ambient ethanol were examined (Figure 3.8) (Chan and Chan 1992). While we show that polarity of the molecule has little impact on the diffusion of that molecule through a solvent, the authors of the cited study show that size and shape has an effect. Larger, bulkier molecules diffuse through solvents much more slowly than smaller molecules of similar shapes. Thus diffusion is governed more strongly by physical constraints – i.e., steric effects – than chemical interactions.

The Wilke-Chang equation (Equation 3.11) is an empirical relationship for diffusion coefficients in liquids based on the Stokes-Einstein equation (Hines and Maddox 1985). It captures this effect on diffusion of the size and shape of the solute in

the term V_A, which is the molar volume of the solute at the normal boiling point. No term for molecular interactions between the solute and solvent are included in this model, which is consistent with the idea that those interactions do not affect diffusion significantly.

$$D_{AB}^{o} = \frac{1.17 \times 10^{-13} \left(\xi_B M_B\right)^{1/2} T}{V_A^{0.6} \mu} \qquad \text{Eq. 3.11}$$

D_{AB}^{o} = interdiffusion coefficient in dilute solutions, m^2/s
μ = viscosity of solution, cP
V_A = molar volume of solute at the normal boiling point, m^3/kg-mol
M_B = molecular weight of solvent, kg/kg-mol
T = absolute temperature, K
ξ_B = association factor of solvent B

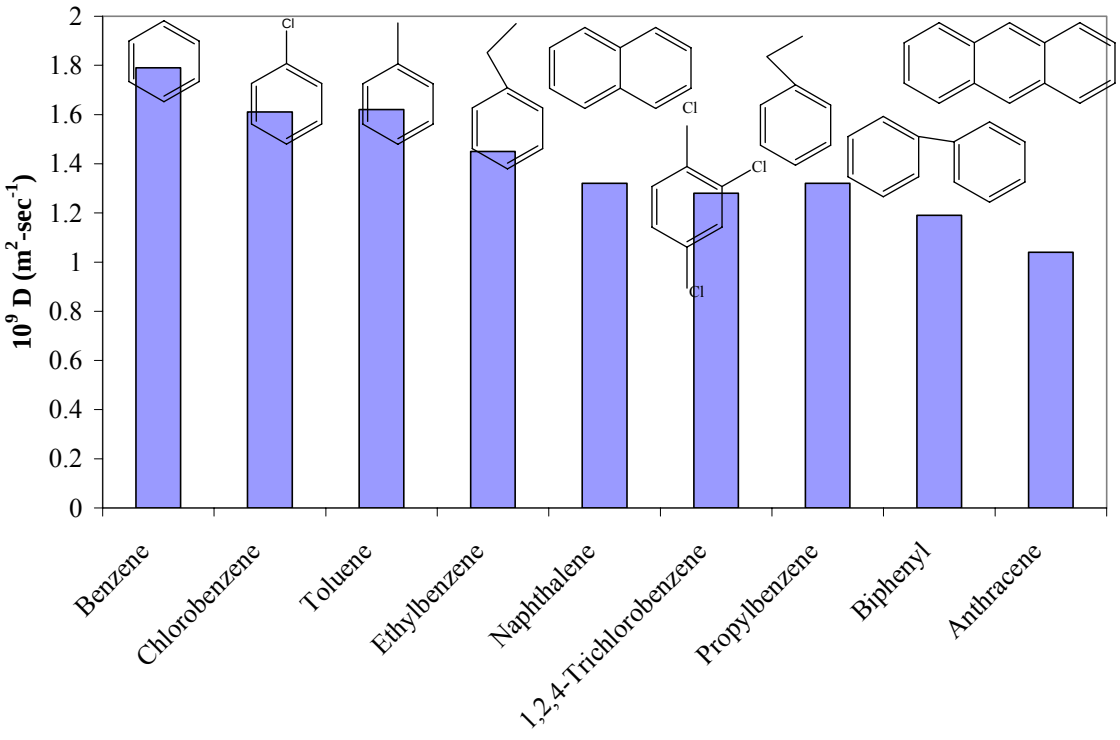

Figure 3.8: Diffusion coefficients of various pseudoplanar molecules in ethanol, 298.2 K, ambient pressure.

The modified Stokes-Einstein Equation mentioned above (Woerlee 2001) was applied using the measured diffusion coefficients of benzene in the assorted mixtures of methanol and carbon dioxide in order to estimate the viscosity of each mixture (Figure 3.9). Collision diameter values for benzene, methanol and carbon dioxide were taken from the literature (Hirschfelder, Curtiss et al. 1954) (Bird, Stewart et al. 1960) and the true average of the three numbers was used as the average collision diameter. The viscosity of methanol was taken from the DIPPR chemical data base and the viscosity of carbon dioxide was interpolated from experimental data (Fenghour, Wakeham et al. 1998). The calculation and the data are satisfactorily close at the end points, indicating that the equation works well enough to make a rough estimation of the mixture of CO_2-expanded methanol given the composition of the liquid phase and the diffusion coefficient at that composition.

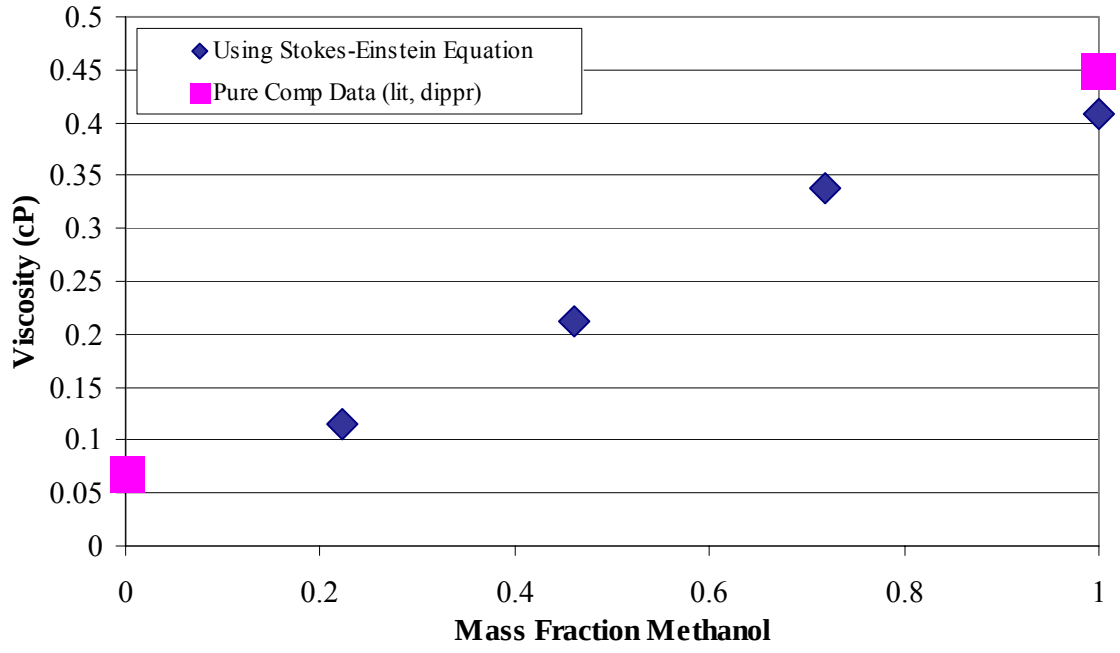

Figure 3.9: Viscosity of CO_2-expanded methanol as a function of mass fraction of methanol calculated from diffusion coefficients of benzene measured at 313 K, 150 bar via the Stokes-Einstein equation.

Calculating the viscosity from the diffusivity in this way does not account for the possibility that the viscosity of the GXL may not be a simple linear function of the methanol mass fraction. Direct measurement of the viscosity by some other means for comparison would be required to determine whether viscosity has any local effects.

Conclusions

The Taylor-Aris dispersion technique measures diffusion coefficients in CO_2-expanded methanol successfully. Addition of CO_2 expectedly increases the diffusion coefficient of the mixture. Unexpectedly, diffusion coefficients are impacted more strongly by size and shape of solute molecule and less strongly by polarity or chemical make-up; thus diffusion is truly a bulk property with no discernable effects in the cybotactic region. Using the appropriate estimation techniques, diffusion coefficients can be used successfully to determine viscosity of GXLs.

References

Aris, R. (1959). "Dispersion of a solute by diffusion, convection, and exchange between phases." Proc. Roy. Soc. (London) **A252**: 538-50.

Bird, R. B., W. E. Stewart, et al. (1960). Transport Phenomena.

Bueno, J. L., J. J. Suarez, et al. (1993). "Infinite dilution diffusion coefficients: benzene derivatives as solutes in supercritical carbon dioxide." Journal of Chemical and Engineering Data **38**(3): 344-9.

Chan, T. C. and M. L. Chan (1992). "Diffusion of pseudo-planar molecules: an experimental evaluation of the molecular effects on diffusion." Journal of the Chemical Society, Faraday Transactions **88**(16): 2371-4.

Cussler, E. L. and Editor (1996). Diffusion: Mass Transfer in Fluid Systems, Second Edition.

Fenghour, A., W. A. Wakeham, et al. (1998). "The Viscosity of Carbon Dioxide." Journal of Physical and Chemical Reference Data **27**(1): 31-44.

Funazukuri, T. and Y. Ishiwata (1999). "Diffusion coefficients of linoleic acid methyl ester, Vitamin K3 and indole in mixtures of carbon dioxide and n-hexane at 313.2 K, and 16.0 MPa and 25.0 MPa." Fluid Phase Equilibria **164**(1): 117-129.

Gonzalez, L. M., J. L. Bueno, et al. (2001). "Determination of Binary Diffusion Coefficients of Anisole, 2,4-Dimethylphenol, and Nitrobenzene in Supercritical Carbon Dioxide." Industrial & Engineering Chemistry Research **40**(16): 3711-3716.

Hines, A. L. and R. N. Maddox (1985). Mass Transfer: Fundamentals and Applications.

Hirschfelder, J. O., C. F. Curtiss, et al. (1954). Molecular Theory of Gases and Liquids.

Lu, J. G., R. Kong, et al. (1999). "Effects of molecular association on mutual diffusion: A study of hydrogen bonding in dilute solutions." Journal of Chemical Physics **110**(6): 3003-3008.

Sassiat, P. R., P. Mourier, et al. (1987). "Measurement of diffusion coefficients in supercritical carbon dioxide and correlation with the equation of Wilke and Chang." Analytical Chemistry **59**(8): 1164-70.

Taylor, G. (1953). "Dispersion of soluble matter in solvent flowing slowly through a tube." Proc. Roy. Soc.(London) **A219**: 186-203.

Taylor, G. (1954). "The dispersion of matter in turbulent flow through a pipe." Proc. Roy. Soc. (London) **A223**: 446-68.

Woerlee, G. F. (2001). "Expression for the Viscosity and Diffusivity Product Applicable for Supercritical Fluids." Industrial & Engineering Chemistry Research **40**(1): 465-469.

CHAPTER 4

DISTRIBUTION OF PHASE-TRANSFER CATALYSTS IN AQUEOUS/GAS-EXPANDED LIQUID SYSTEMS

The distribution of a phase-transfer catalyst between the two phases in a liquid-liquid PTC system can significantly affect the reaction taking place in the organic phase (Starks, Liotta et al. 1994). This distribution is affected by not only the structure and organic character of the catalyst, but also the solvent power of the organic phase solvent. Less polar (or polarizable) solvents are less able to support the ionic catalyst.

The addition of CO_2 to an immiscible aqueous/organic system has previously been shown to drive lipophilic quaternary ammonium salts into the aqueous phase, greatly changing the distribution coefficients (Xie, Brown et al. 2002). In this investigation, partitioning behavior of a phase transfer catalyst, tetrahexylammonium bromide (THxAB, Figure 4.1), between water and gas-expanded toluene was studied to determine the effect of CO_2 expansion on distribution. The organic solvent, toluene, was expanded with CO_2, resulting in a less polarizable organic phase, which can affect the ability of the phase to solubilize the ionic quaternary ammonium salt. PTC reactions were also performed in these systems to determine the effect of the GXL solvent on the kinetics. Those experiments are discussed in Chapter 5.

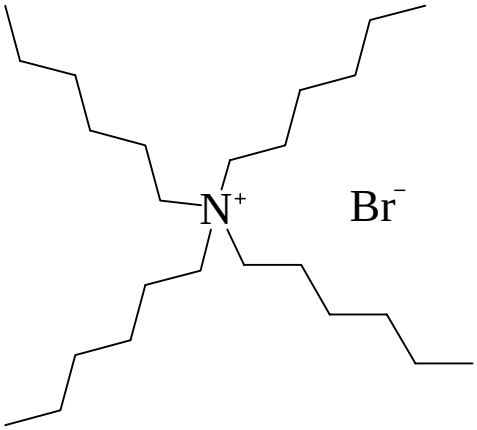

Figure 4.1: Structure of THxAB

Experimental Methods

Materials

CO_2 was purchased from Airgas (SFC/SFE grade) and dried using a gas filter (Matheson model 450B). Tetrahexylammonium bromide (99%), toluene (99.5% ACS grade reagent), bromophenol blue sodium salt (ACS reagent), sodium hydroxide (certified ACS), and sodium phosphate monobasic monohydrate (reagent ACS grade) were purchased from Acros and used as received. Distilled water was used for the aqueous phase.

Apparatus

Figure 4.2 shows a schematic of the reaction apparatus. All distribution experiments were performed in a windowed high-pressure stirred reactor (Parr model 4560). The reactor had a volume of 300 mL and was stirred by a blade impeller. Ethylene-propylene o-rings were used to seal the windows, and a Teflon gasket to seal the top of the reactor. Temperature (± 0.5°C), pressure (± 0.034 bar), and stirring rate

were monitored and controlled by the accompanying Parr 4842 controller. The reactor was fitted with a 2000 psi rupture disk.

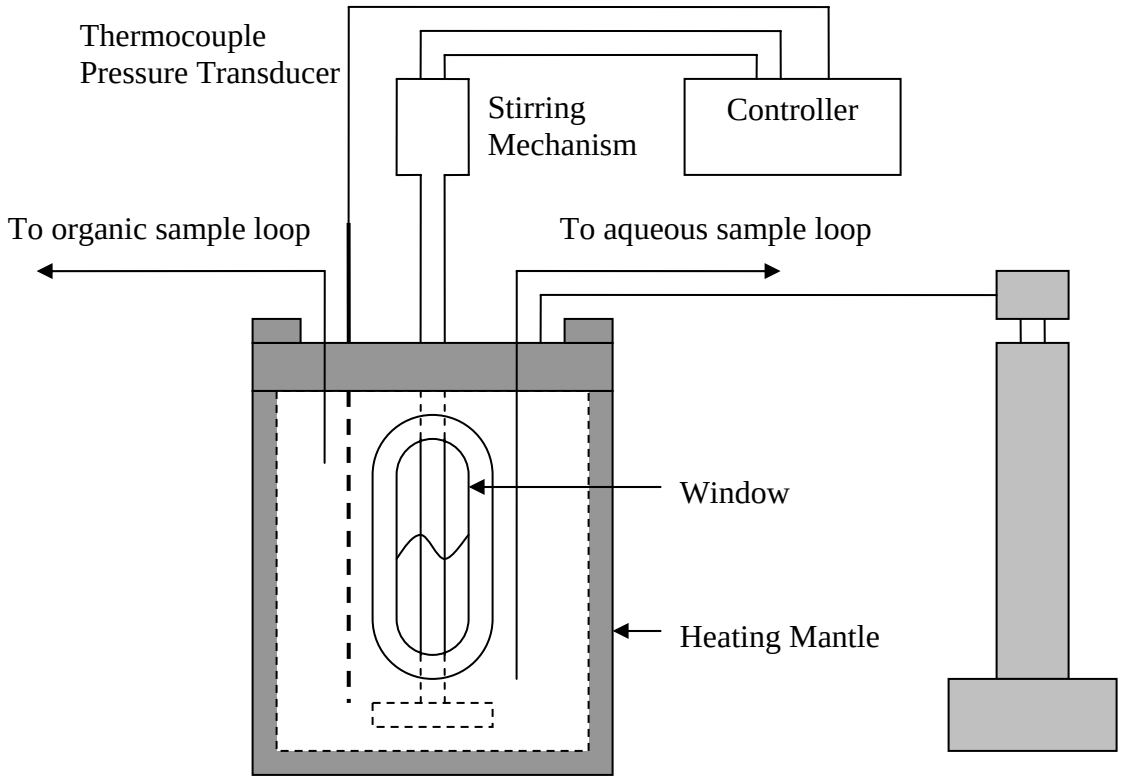

Figure 4.2: Partitioning experiment apparatus.

Both the organic (GXL) and aqueous phases were sampled using dip tubes attached to six-port sampling valves (Valco Instruments Co. Inc.) fitted with 239 and 246 microliter sample tubes, respectively. The reactor was pressurized with CO_2 using a high pressure syringe pump (Isco, Inc., Model 500D). An HPLC pump was used to flush the sample loops after each sample.

Procedure

The reactor was loaded with water, toluene, and THxAB and heated to 30^{o}C while stirring at approximately 400 rpm. Once the temperature had equilibrated, the reactor was pressurized with CO_2 and allowed to equilibrate again while stirring. Once the pressure had stopped changing, the reactor was allowed to stir for at least one hour to ensure equilibration of the concentrations. The stirrer was then switched off, and the phases were allowed to separate for at least one hour before sampling each separately.

Samples were taken in triplicate through the six-port valves, illustrated in Figure 4.3. For each sample, the valve was first switched to the position that allowed the reactor contents to flow through the sample loop and out to waste (position A). The valve to the waste reservoir was opened, and the reactor contents were allowed to flush for several seconds. The valve was then closed, containing the reactor contents in the loop, and the HPLC pump switched on to allow solvent, chloroform for the organic samples and buffered water solution for the aqueous samples, to flow into a volumetric flask (5 mL for the organic samples, 10 mL for the aqueous samples) through the sample collection tube. After a small amount of solvent was collected, the six-port valve was switched to the position that allowed the loop contents to be flushed through the sample collection tube by the solvent into the collection flask (position B). When the sample had been diluted to the appropriate volume, the HPLC pump was switched off.

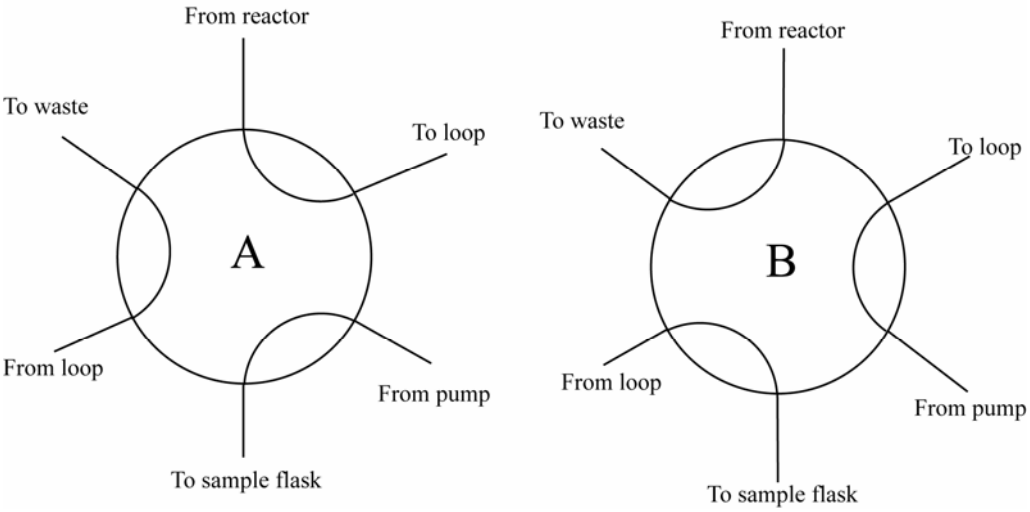

Figure 4.3: Sampling system

The samples were analyzed by an extraction-spectrophotometric technique outlined by Yamamoto (Yamamoto 1995). This technique involves complexing the quaternary ammonium catalyst with the dye bromophenol blue (BPB), extracting the complex into chloroform, and analyzing the chloroform phase by UV-vis spectroscopy. A Hewlett-Packard HP 8435 UV-vis instrument was used for this purpose. The response of the UV for a range of concentrations of THxAB was calibrated for sampling both the organic and aqueous phases. The details of this analytical technique can be found in Appendix D.

Results and Discussion

The partitioning experiments were performed at 30^{o}C and pressures of CO_2 varying from 25 to 60 bar. The reactor was loaded with 100 g distilled water, 0.18 g THxAB, and varying volumes of toluene to allow for expansion with CO_2 at several pressures for each loading. The experiments with no CO_2 were performed under nitrogen pressure to allow for pressurized sampling.

The pressure range used for these experiments was chosen based on the swelling phase behavior of CO_2 and toluene at 30°C, shown in Figure 4.4. Toluene does not expand significantly below 45 bar, but expands rapidly between 45 and 65 bar. It is expected that the properties of the GXL will have the widest range of solvent properties in this region, and therefore the distribution of the catalyst will also be affected most.

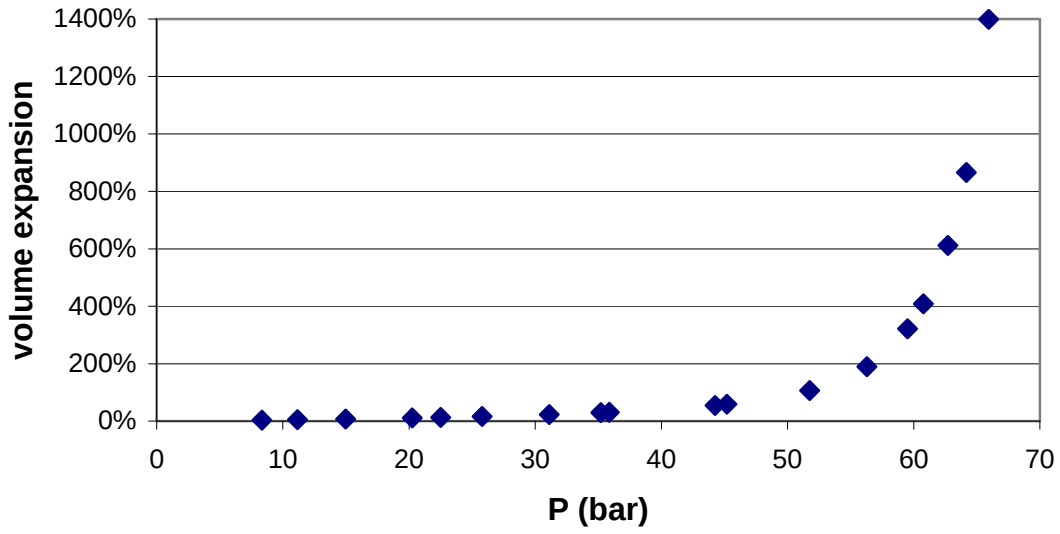

Figure 4.4: Swelling behavior of CO_2 in toluene at 30°C.

These conditions were also chosen to match as closely as possible the conditions used for the concurrent kinetics experiments using this system, which are described in Chapter 5. The reactants in those experiments, benzyl bromide and potassium thiocyanate were not included in the partitioning experiments. Since benzyl bromide is so similar to toluene, it would be expected to have little effect on the partitioning results. The salt, potassium thiocyanate, could have had a substantial effect on the phase behavior of the catalyst. Increasing ionic strength in the aqueous phase usually has a "salting out" effect on phase transfer catalysts, shifting the partitioning toward the organic phase

(Starks, Liotta et al. 1994). However, the potassium ion complexes more readily than the tetrahexylammonium ion with the BPB used for analysis of the catalyst concentration, making analysis of the catalyst difficult, especially since the salt concentration is 200 times that of the catalyst in the reaction system. Therefore, it was omitted from these experiments.

The distribution of the catalyst was calculated by dividing the mol fraction of THxAB measured in the aqueous phase by that measured in the GXL phase. A mass balance on the total THxAB in the system was performed, and the calculated mass was found to be within 15% of the mass measured into the reactor for each experiment.

The distribution results as a function of CO_2 pressure are found in Figure 4.5 below. The distribution decreases slightly until about 50 bar, when it begins to increase rapidly with added CO_2. This behavior is consistent with the swelling behavior for CO_2-toluene. At 60 bar, the ratio of the activity coefficients has increased to more than 10:1 from approximately 1:1 with no CO_2. At approximately 65 bar, the concentration of THxAB in the organic phase falls below the detection limit of the analytical technique, making accurate measurement of the distribution impossible by this method.

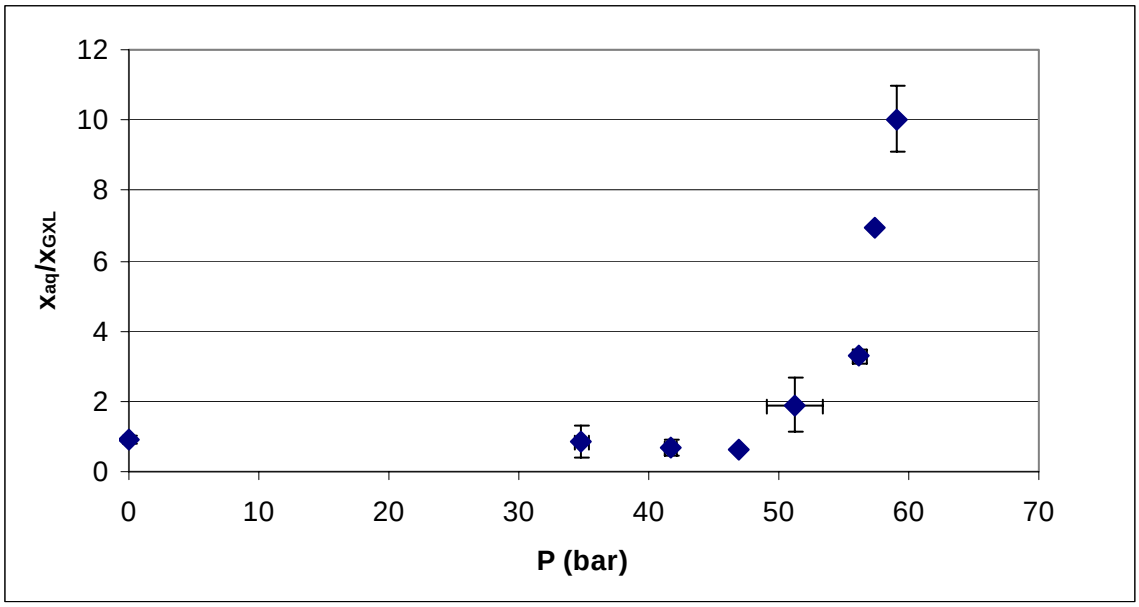

Figure 4.5: Distribution of THxAB between the GXL and aqueous phases as a function of CO_2 pressure.

The same results are compared to the density of the CO_2-expanded toluene phase and plotted against CO_2 mol fraction in the GXL in Figure 4.6. To calculate the swelling, CO_2 mol fractions and densities, data for the phase behavior of CO_2 and toluene (Fink and Hershey 1990) (Lazzaroni, Bush et al. 2005) was fit to the Patel-Teja equation of state (Patel and Teja 1982) with Mathias-Klotz-Prausnitz mixing rules (Mathias, Klotz et al. 1991) with the adjustable parameters $k_{12} = 0.099$ and $l_{12} = 0.056$. The density increases slightly with added CO_2 before decreasing dramatically after about 70% CO_2. This is in the same concentration range that the distribution starts to increase substantially.

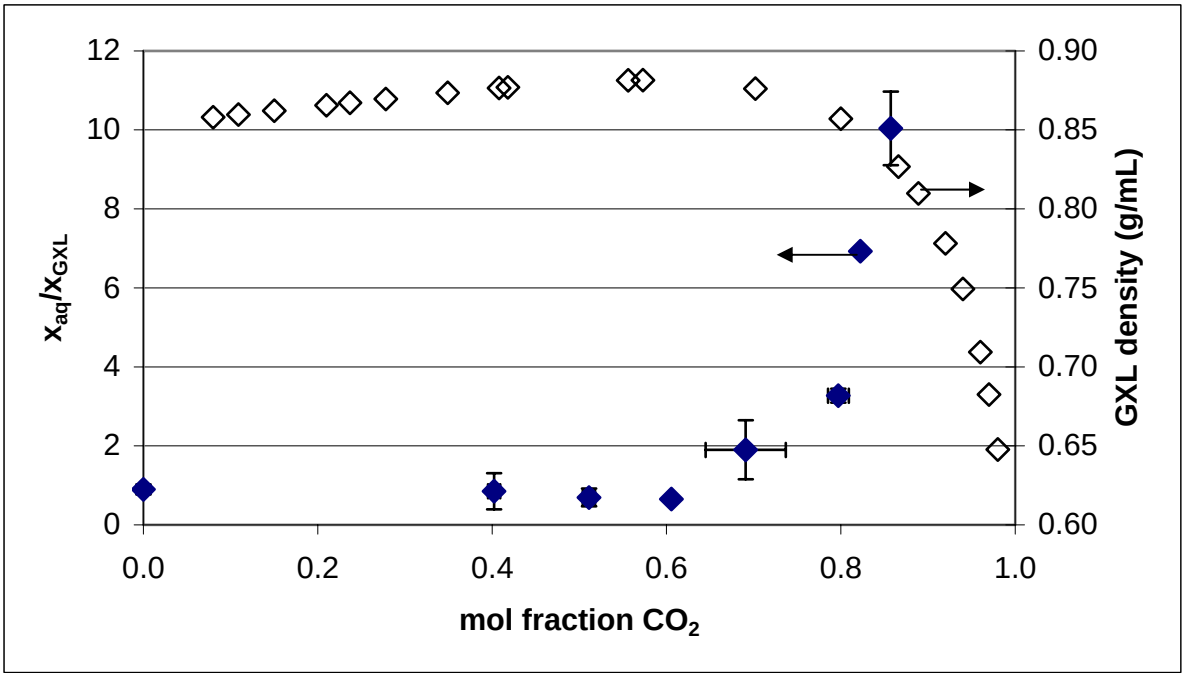

Figure 4.6: Distribution of THxAB as a function of CO_2 mol fraction compared to the density of CO_2-expanded toluene at 30°C.

The distribution is also shown with changes in density in Figure 4.7. When plotted this way, two trends develop. Initially, the distribution of the catalyst decreases only very slightly as the density increases. At CO_2 mol fractions higher than 60%, the distribution increases almost linearly with the decrease in density. As the solvent becomes less dense, it also becomes less able to solvate molecules in solution, so the catalyst distribution shifts to favor the aqueous phase more.

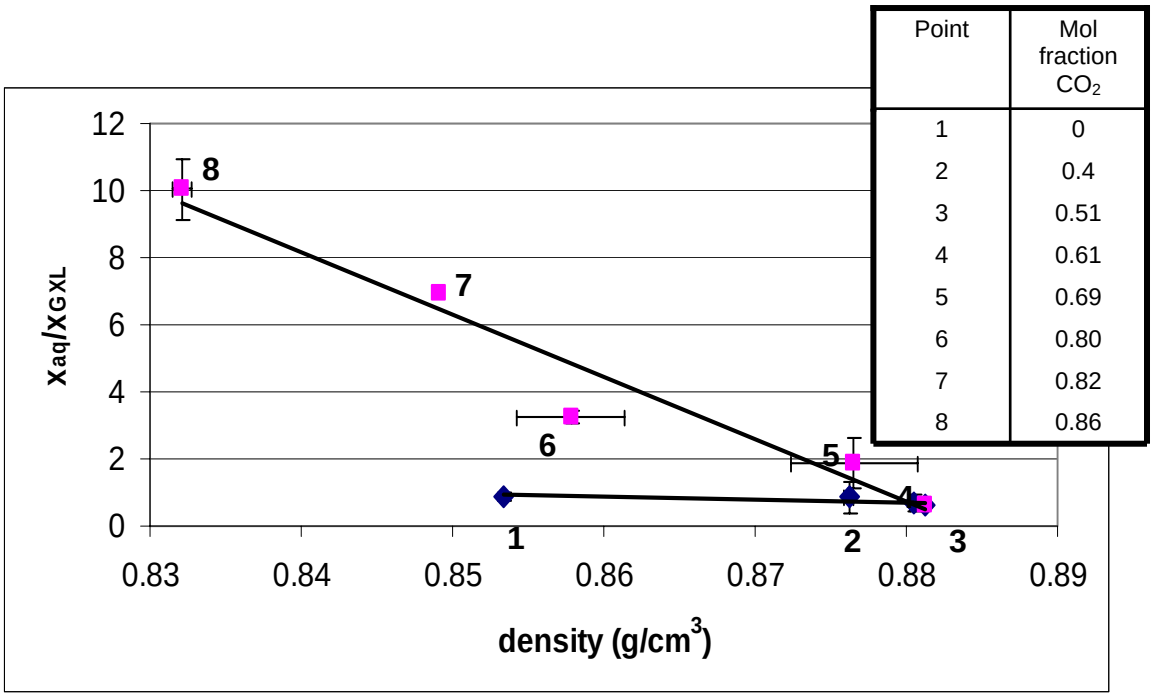

Figure 4.7: Distribution of THxAB as a function of CO_2-expanded toluene phase density.

Figure 4.8 compares the THxAB distribution to the change in the Kamlet-Taft parameter π* in CO_2-expanded toluene as a function of CO_2 mol fraction, also at 30°C. Kamlet-Taft parameters are based on characteristic solvatochromic responses of a group of nitroaromatic probe molecules to their solvent environments in solution (Reichardt 1990). These responses have been used to form scales of values that are commonly used to characterize and compare solvent properties. The parameter π* is a measure of the solvent's polarity and polarizability with a value of 0 for cyclohexane and 1 for dimethyl sulfoxide (DMSO). Neither toluene nor CO_2 are considered polar molecules, but pure toluene does have a π* value of 0.45 because toluene has some polarizability. The density of electrons in the conjugated system allows polar molecules to induce a dipole in toluene, which allows it to support polar or ionic molecules in solution more than would

otherwise be expected. CO_2 is neither polar nor polarizable, so as its concentration is increased in the solvent system, π^* decreases and the mixture becomes less able to support the ionic THxAB in solution. The result is an increase in the distribution of THxAB into the aqueous phase.

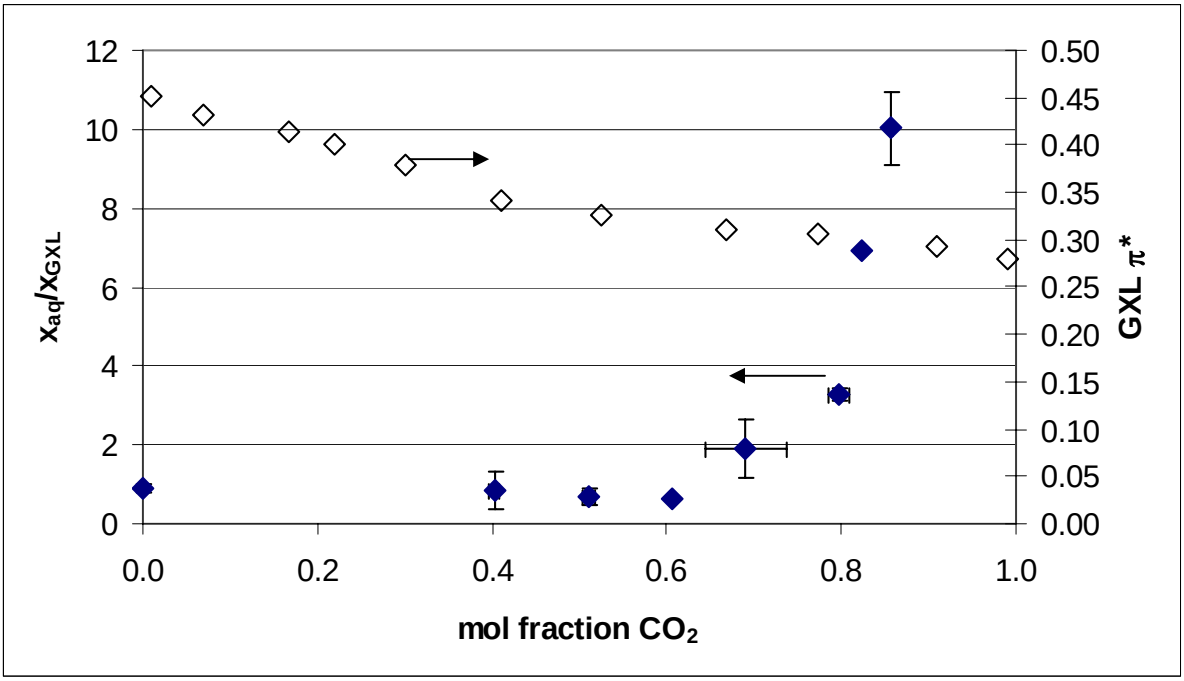

Figure 4.8: Distribution of THxAB compared to the π* value of the GXL phase.

The shift in partitioning of the THxAB into the aqueous phase can be used to enhance the efficiency of an aqueous extraction recovery of the catalyst, which is common industrially. The theoretical fraction of THxAB that can be recovered by a single equal-volume extraction is given by Equation 4.1 where *v* is the molar volume of each phase. Figure 4.9 shows the theoretical fraction recovered as a function of pressure, which increases to 97% at the highest pressure measured. The distribution of the catalyst into the aqueous phase is increasing exponentially in this concentration range, so it is possible that much higher recovery can be achieved with a relatively small increase in

pressure. The theoretical fraction recovered is highly sensitive to small changes in the distribution coefficient, so the minimum in the fraction recovered seen here is caused by the slight minimum in the distribution coefficient at those pressures.

$$rec = \frac{\frac{x_{aq}}{x_{org}}\frac{v_{GXL}}{v_{aq}}}{1+\frac{x_{aq}}{x_{org}}\frac{v_{GXL}}{v_{aq}}} \qquad \text{Equation 4.1}$$

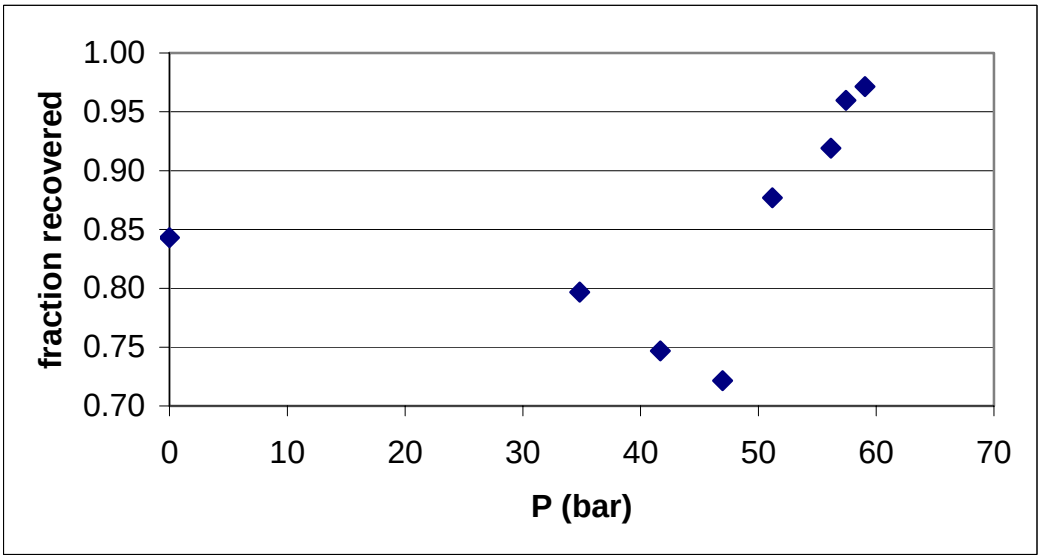

Figure 4.9: Theoretical fraction of THxAB recovered from a single equal-volume extraction with increasing CO_2 pressure.

The calculated volume of water required to recover 99% of the THxAB left in the organic phase after the equal volume extraction with a countercurrent extraction is 110 L water/ L organic phase fed (Wankat 1988). The volume of water necessary to achieve the

same outlet concentration of THxAB in the organic phase is shown in Figure 4.10 below. At 60 bar, the volume of water necessary is 2 L water/ L organic fed, a reduction of 98%. The initial increase in water requirements is a result of the initial decrease in the distribution of the catalyst. The maximum in this plot is also a result of the sensitivity of this calculation to changes in the distribution coefficient, as discussed above.

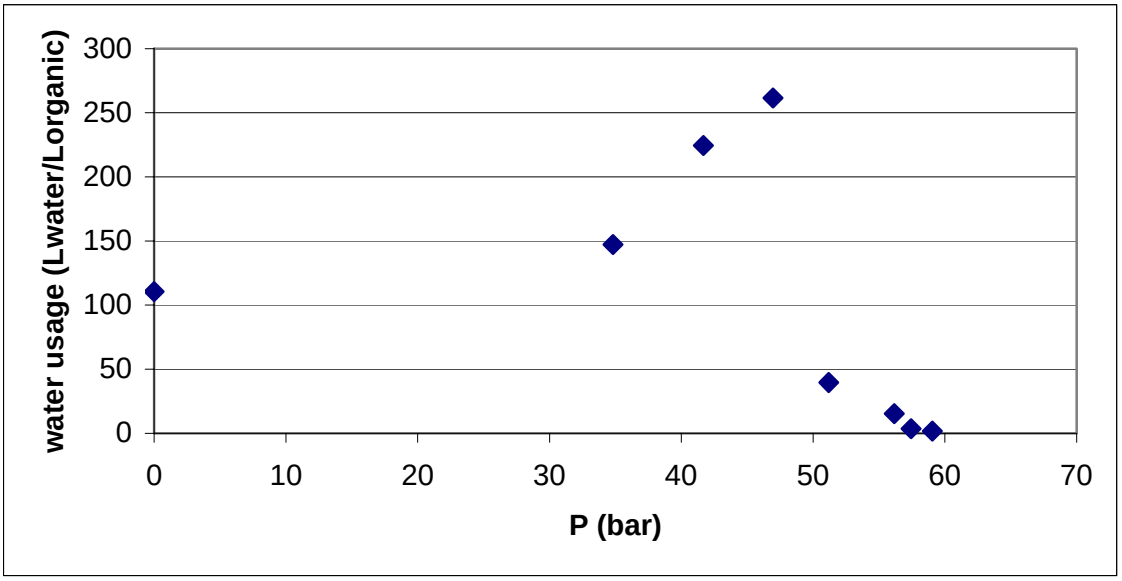

Figure 4.10: Comparison of the water usage of a countercurrent extraction system.

Conclusions

The distribution of THxAB between water and CO_2-expanded toluene as CO_2 mol fraction is increased has been measured. The distribution changes very little at CO_2 mol fractions less than 0.6. Above this amount of CO_2 in the GXL phase, the distribution of the catalyst into the aqueous phase increases dramatically. This increase corresponds to decreases in the density and π^* values of the GXL. This change in distribution can reduce water requirements for extraction and recovery of the catalyst by 98%.

References

Fink, S. D. and H. C. Hershey (1990). "Modeling the vapor-liquid equilibria of 1,1,1-trichloroethane + carbon dioxide and toluene + carbon dioxide at 308, 323, and 353 K." Industrial & Engineering Chemistry Research **29**(2): 295-306.

Lazzaroni, M. J., D. Bush, et al. (2005). "High-pressure vapor-liquid equilibria of some carbon dioxide + organic binary systems." Journal of Chemical and Engineering Data **50**(1): 60-65.

Mathias, P. M., H. C. Klotz, et al. (1991). "Equation-of-state mixing rules for multicomponent mixtures: the problem of invariance." Fluid Phase Equilibria **67**: 31-44.

Patel, N. C. and A. S. Teja (1982). "A new cubic equation of state for fluids and fluid mixtures." Chemical Engineering Science **37**(3): 463-73.

Reichardt, C. (1990). Solvents and Solvent Effects in Organic Chemistry. New York, Cambridge.

Starks, C. M., C. L. Liotta, et al. (1994). Phase-Transfer Catalysis: Fundamentals, Applications, and Industrial Perspectives.

Wankat, P. C. (1988). Separations in chemical engineering: equilibrium-staged separations. Englewood Cliffs, New Jersey, Prentice Hall PTR.

Xie, X., J. S. Brown, et al. (2002). "Phase-transfer catalyst separation by CO2 enhanced aqueous extraction." Chemical Communications (Cambridge, United Kingdom)(10): 1156-1157.

Yamamoto, K. (1995). "Sensitive determination of quaternary ammonium salts by extraction-spectrophotometry of ion associates with bromophenol blue anion and coextraction." Analytica Chimica Acta **302**(1): 75-9.

CHAPTER 5

PHASE-TRANSFER CATALYSIS IN GAS-EXPANDED LIQUIDS

Numerous factors affect the kinetics of liquid-liquid PTC reactions, including properties of the organic solvent such as polarity, polarizability, and transport ability (Starks, Liotta et al. 1994). The tunable nature of a GXL allows the spectrum of these properties to be probed, while keeping other experimental variables constant. Understanding the effect of using such a solvent in a PTC system on the rate of reaction could further elucidate the basic mechanisms involved in PTC as well as the nature of GXLs, which is critical to finding and developing new applications for each.

In this investigation, reaction kinetics of the phase-transfer catalyzed nucleophilic displacement of benzyl bromide by potassium thiocyanate with tetrahexylammonium bromide (THxAB) were studied to gain an understanding of the effect on reaction rate of using an aqueous/gas-expanded liquid PTC system (Figure 5.1). The organic solvent, toluene, was expanded with CO_2, resulting in a less polarizable organic phase with higher transport ability. This study was performed in conjunction with the distribution study reported in Chapter 4 to correlate the changes in catalyst distribution to any observed changes in kinetics.

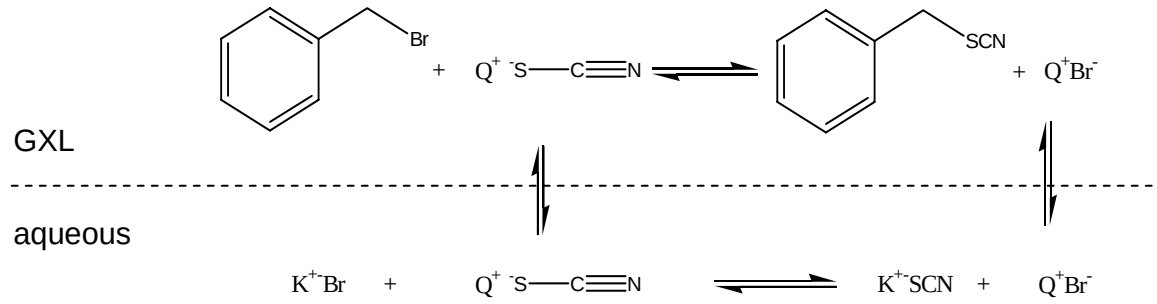

Figure 5.1: Phase-transfer catalyzed nucleophilic displacement of benzyl bromide by potassium thiocyanate with tetrahexylammonium bromide (THxAB)

Experimental Methods

Materials

CO_2 was purchased from Airgas (SFC/SFE grade) and dried using a gas filter (Matheson model 450B). Benzyl bromide (99%), benzyl thiocyanate (97%), potassium thiocyanate (98%), tetrahexylammonium bromide (99%), toluene (99.5% ACS grade reagent), and dodecane (99%) were purchased from Acros and used as received. Distilled water was used for the aqueous phase.

Apparatus

Figure 5.2 shows a schematic of the reaction apparatus. All distribution experiments were performed in a windowed high-pressure stirred reactor (Parr model 4560). The reactor had a volume of 300 mL and was stirred by a blade impeller. Ethylene-propylene o-rings were used to seal the windows, and a Teflon gasket sealed the top of the reactor. Temperature (± 0.5°C), pressure (± 0.034 bar), and stirring rate were monitored and controlled by the accompanying Parr 4842 controller. The reactor was fitted with a 2000 psi rupture disk.

The organic (GXL) phase was sampled using a dip tube attached to a six-port sampling valve (Valco Instruments Co. Inc.) fitted with a 243 microliter sample loop. The reactor was pressurized with CO_2 using a high pressure syringe pump (Isco, Inc., Model 500D). An HPLC pump was used to flush the sample loop after each sample.

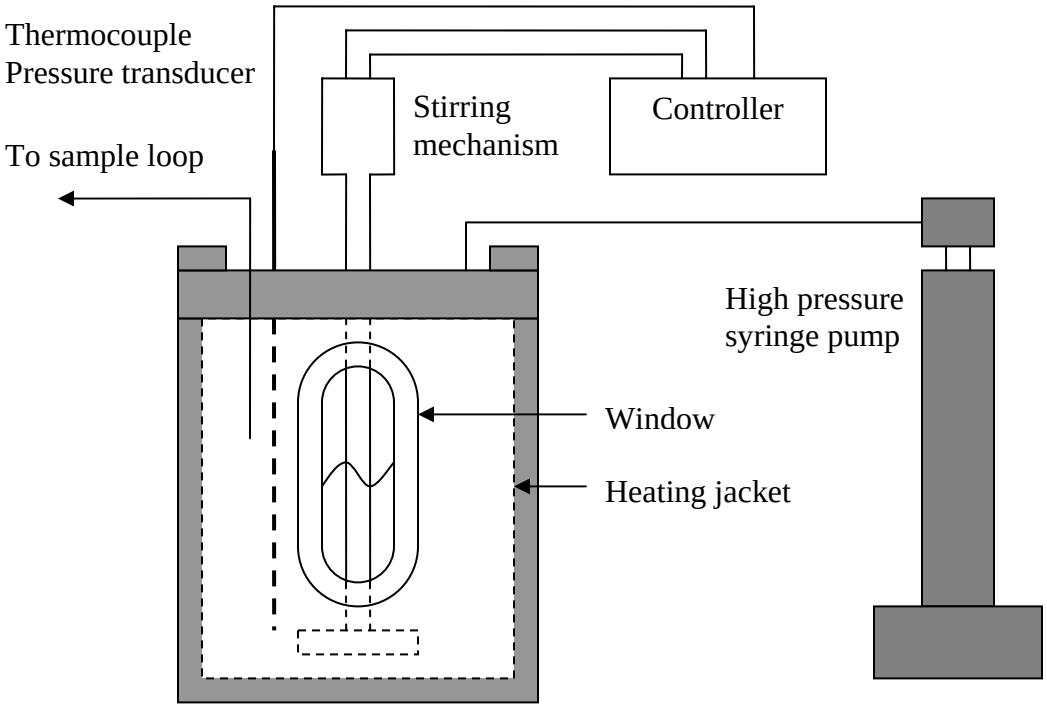

Figure 5.2: Schematic of PTC reaction apparatus

Procedure

The reactor was loaded with water, toluene, THxAB, potassium thiocyanate, and dodecane (used as an internal standard) and heated to 30^{o}C while stirring at approximately 400 rpm. Once the temperature had equilibrated, benzyl bromide (the limiting reagent) was added through a port on the reactor top by a syringe fitted with a long needle to ensure it was deposited into the solvents in the bottom of the reactor, as

opposed to the sides of the reactor. The reactor was closed and pressurized with CO_2 as quickly as possible to minimize the effect of equilibration on the initial rate data.

Samples were taken in triplicate at regular intervals through the six-port valve, illustrated in Figure 5.3. For each sample, the stirrer was turned off and the aqueous and organic phases were allowed to separate for 5 minutes, the interval experimentally determined to be required to get reproducible samples. Then the valve was switched to the position that allowed the reactor contents to flow through the sample loop and out to waste (position A). The valve to the waste reservoir was opened, and the reactor contents were allowed to flush for several seconds. The valve was then closed, containing the reactor contents in the loop, and the HPLC pump switched on to allow solvent, toluene in this case, to flow into a 5 mL flask through the sample collection tube. After a small amount of toluene was collected, the six-port valve was switched to the position that allowed the loop contents to be flushed through the sample collection tube by the toluene into the collection flask (position B). When the sample had been diluted to 5 mL, the HPLC pump was switched off.

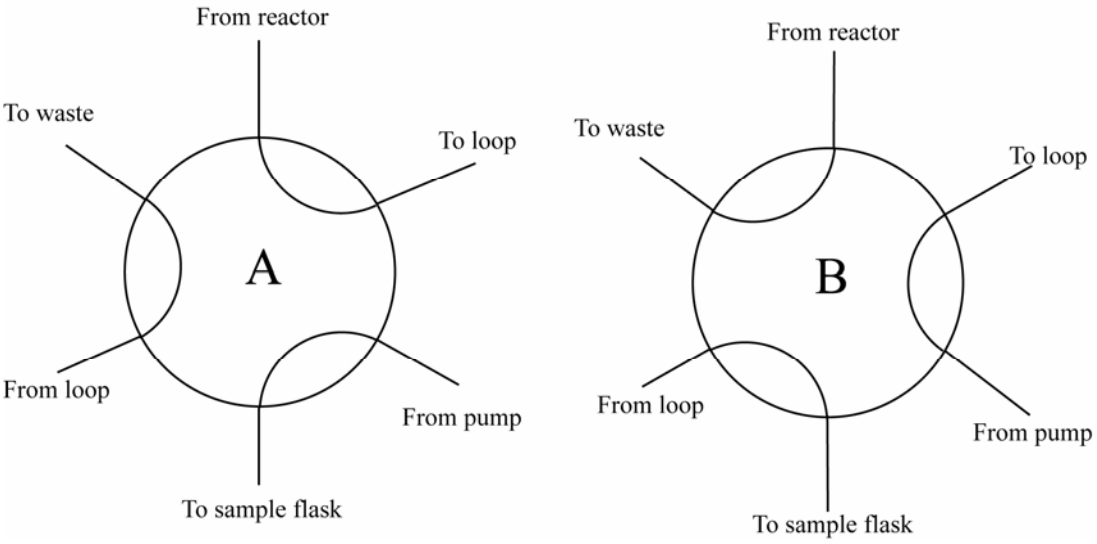

Figure 5.3: Sampling valve system

The samples were analyzed by a gas chromatograph (Hewlett-Packard model 6890) with an HP-5 column and an FID detector. The responses of benzyl bromide, benzyl thiocyanate, and dodecane were calibrated prior to analysis. The ratio of the responses of benzyl bromide (reactant) plus benzyl thiocyanate (product) to that of dodecane (internal standard) was used as a check of the mass balance that did not require the volume of the expanded organic phase.

Results and Discussion

The reactions were performed at 30^{o}C and pressures of CO_2 varying from 25 to 65 bar. Reactions were also performed with no CO_2 present under nitrogen pressure to allow sampling. In all cases, the volumes of the aqueous and organic phases were equal, and the initial concentration of benzyl bromide in the organic phase was approximately the same. Potassium thiocyanate was used in 10 times excess of the benzyl bromide to ensure pseudo-first order kinetics. Three concentrations of THxAB were used: 0, 5, and 10 mol% based on benzyl bromide, the limiting reactant. The experiments with no CO_2 were performed under nitrogen pressure to allow for pressurized sampling. Benchtop experiments were also performed to verify the validity of the nitrogen experiments.

For each sample, conversion of benzyl bromide was calculated based on the ratio of the GC responses for both the benzyl bromide and benzyl thiocyanate. This conversion data was fit to a model for pseudo-first order plus equilibrium kinetics, since the displacement reaction has been shown to be reversible (Grilly 2005). Equations 5.1-5.4 below show the appropriate equations and boundary conditions required for this model (Moore and Pearson 1981). The data was fit to Equation 5.5 using a non-linear

regression tool to calculate the adjustable parameters x_e, the conversion at equilibrium, and k_1, the pseudo-first order rate constant for the forward reaction. Data for conversion of benzyl bromide as a function of time are shown in Figure 5.4. The fit of the pseudo-first order plus equilibrium model is also shown, with good correlation.

$$A \rightleftharpoons B \qquad \text{Equation 5.1}$$

$$\frac{dC_A}{dt} = -k_1 C_A + k_{-1} C_B \qquad \text{Equation 5.2}$$

$$\frac{dx}{dt} = k_1 (1 - x) - k_{-1} x \qquad \text{Equation 5.3}$$

$$\left.\frac{dx}{dt}\right|_{x=x_e} = 0 = k_1 (1 - x_e) - k_{-1} x_e \qquad \text{Equation 5.4}$$

$$x_e \ln\left(1 - \frac{x}{x_e}\right) = k_1 t \qquad \text{Equation 5.5}$$

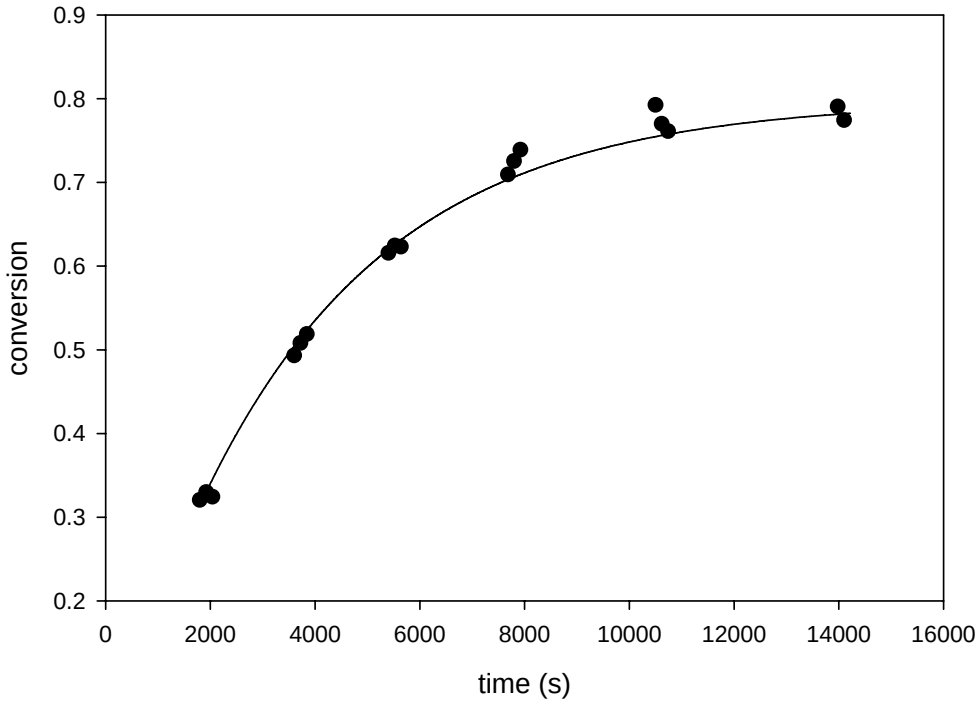

Figure 5.4: Raw data and model regression for conversion of benzyl bromide as a function of time. For this data, x_e = 0.798 and k_1 = 2.215E-04.

The pressure range used for these experiments was chosen based on the phase behavior of CO_2 and toluene at 30°C, shown in Chapter 4. Toluene does not expand significantly with CO_2 below 45 bar, but expands rapidly between 45 and 65 bar. It is expected that the properties of the GXL will have the widest range of variability in this region and therefore the kinetics of the reaction will also be affected most at those pressures.

The calculated rate constants as a function of CO_2 mol fraction are shown in Figure 5.5. With no catalyst present, the rate constant increases monotonically with added CO_2. With 5% catalyst (compared to the substrate, benzyl bromide), the rate constant first decreases slightly before increasing again between 50 and 90%. The data taken at 10% catalyst are consistent with the behavior at 5%.

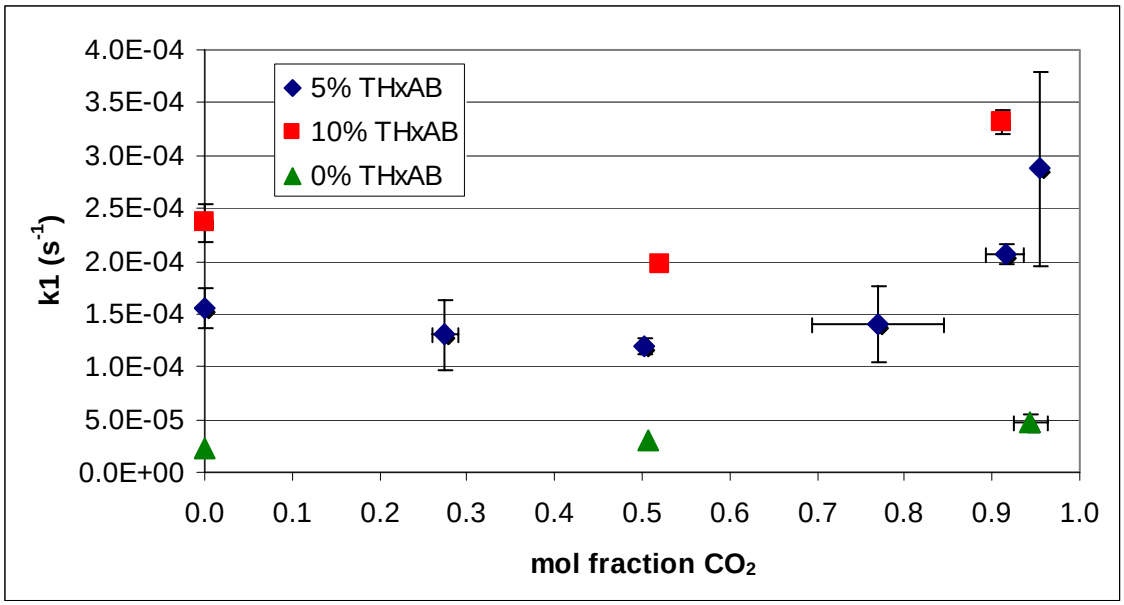

Figure 5.5: Pseudo-first order rate constants of the displacement of benzyl bromide with potassium thiocyanate catalyzed by THxAB at 30°C in an aqueous/CO_2-expanded toluene system.

When each set of data is normalized compared to the value of k_1 for each catalyst concentration in pure toluene, the data for the catalyzed reactions collapse to one curve (Figure 5.6). With no catalyst, the rate constant begins to increase at lower pressures than with 5 or 10% catalyst. At 95% CO_2, the normalized rate constants are all approximately the same. The minimum in the rate of the catalyzed reaction indicates that there must be at least two competing effects on the rate. The absence of a minimum in the rate constant when there is no catalyst present suggests that the effect that causes the rate to decrease involves the catalyst, while the effect that causes the rate to increase is general to the system or the reaction itself.

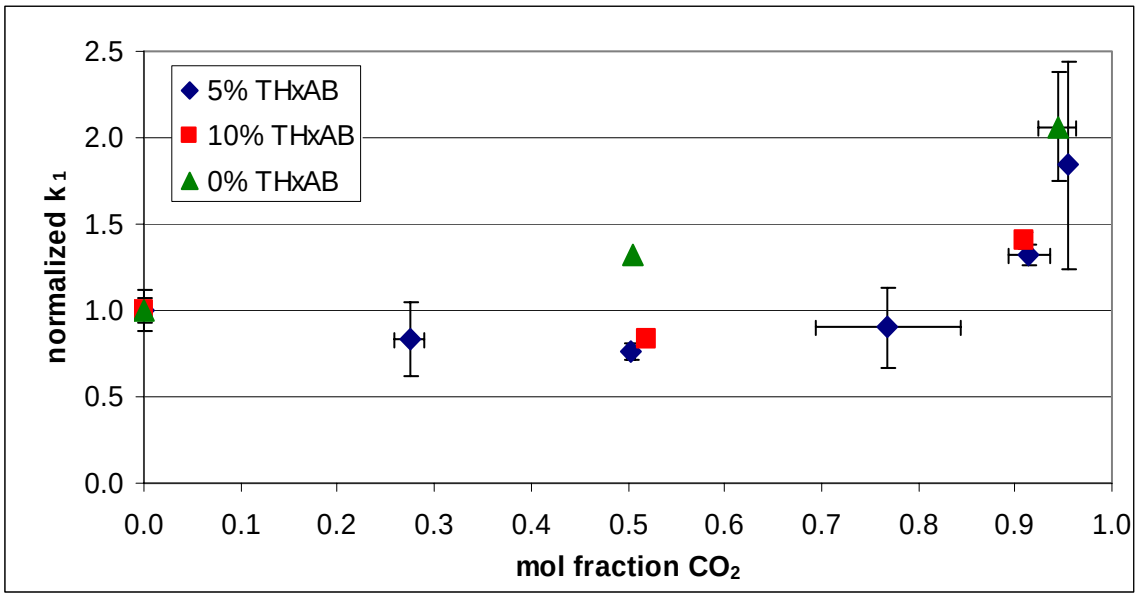

Figure 5.6: Rate constants normalized to values in pure toluene for each catalyst concentration.

Figure 5.7 compares the trend in the rate constants to the distribution data for this system reported in Chapter 4. While it seems plausible that the change in distribution could be causing the changes in rate, the sharp increase in the distribution occurs at a lower mol fraction than the increase in the rate constants. This suggests that some other effect of adding CO_2 is actually causing both trends.

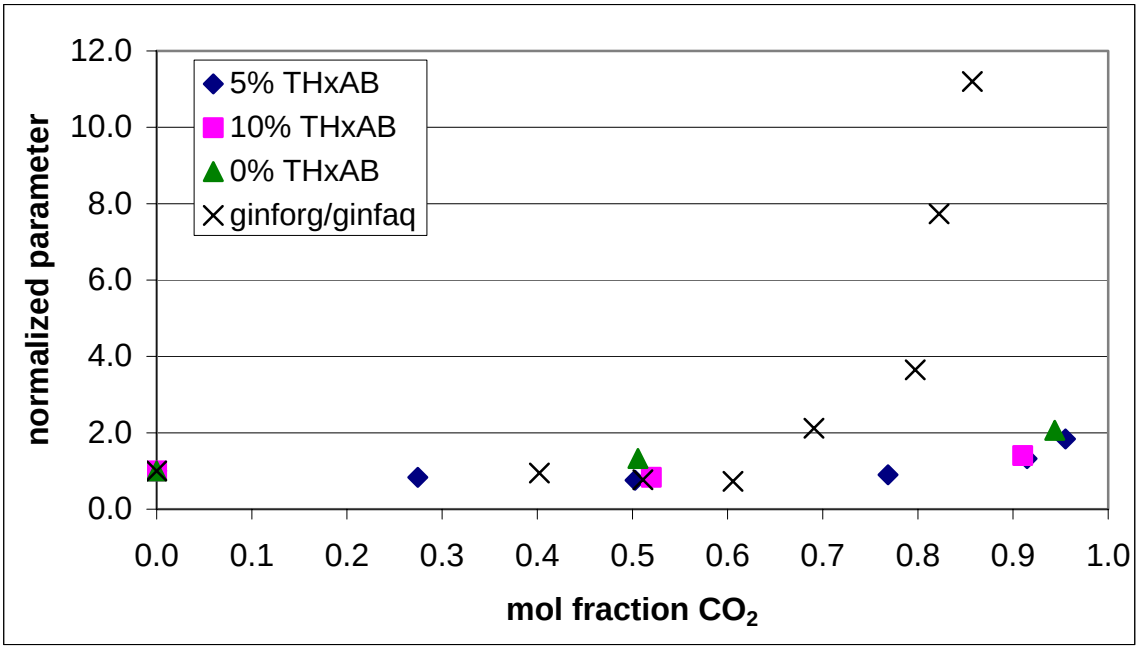

Figure 5.7: Rate constant and distribution data as a function of CO_2 mol fraction normalized to the values in pure toluene for each.

A model which is consistent with these results involves two mechanisms for the displacement reaction that are occurring in parallel. In the case where no catalyst is present, the only location for the reaction to occur is at the organic-aqueous interface since benzyl bromide and potassium thiocyanate are virtually insoluble in water and toluene, respectively. When THxAB is present, it catalyzes the heterogeneous interfacial reaction, increasing the rate, but distribution of the catalyst into the organic phase also allows the reaction to occur homogeneously, further increasing the observed rate.

This rate of this reaction run homogeneously in methyl sulfoxide (DMSO) has been shown to decrease with added CO_2 (Grilly 2005). This is consistent with a decrease in the ability of the solvent to stabilize the polar transition state (Figure 5.8) of this S_N2 reaction when CO_2 is added. The initial decrease in the rate of the reactions with 5 and

10% THxAB could be attributed to a decrease in the homogeneous rate due to decreased solvent power, as well.

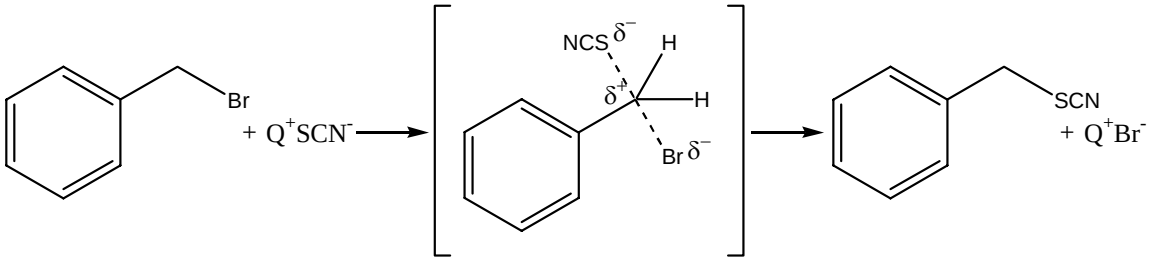

Figure 5.8: Homogeneous displacement reaction with polar transition state shown.

There are two factors that could cause the heterogeneous reaction rate to increase with added CO_2. The first is seen in the uncatalyzed reaction. As CO_2 is added to the GXL phase, the diffusivity in that phase increases by roughly an order of magnitude, as seen in Chapter 3. Faster diffusion of the reactant and product molecules to the interface could speed up the reaction. However, there must also be a second effect promoting this reaction that involves the catalyst, since the catalyzed reactions are much faster than the uncatalyzed.

Symmetric quaternary ammonium salts have been reported to show interfacial activity in organic-water systems (Vendegrift, Lewey et al. 1980). Sasson, et al correlated an increase in the rate constant of a phase-transfer catalyzed alkylation reaction to increases in surface pressures, defined as the difference in interfacial tension between systems where the catalyst is present and those where it is not (Mason, Magdassi et al. 1990). The surface pressure of THxAB was measured to be approximately 12 dynes/cm^2 in each of the solvent systems studied. The addition of CO_2 when catalyst is present could enhance this effect by increasing the interfacial volume, where the heterogeneous reaction is occurring (Figure 5.9). Since the catalyst is ionic, yet also organic in

character, neither the CO_2-expanded toluene nor the water phase is particularly attractive to it. The interfacial volume could increase as catalyst accumulates in that region, promoting the interaction of the catalyst with the reactant molecules and enhancing the reaction rate.

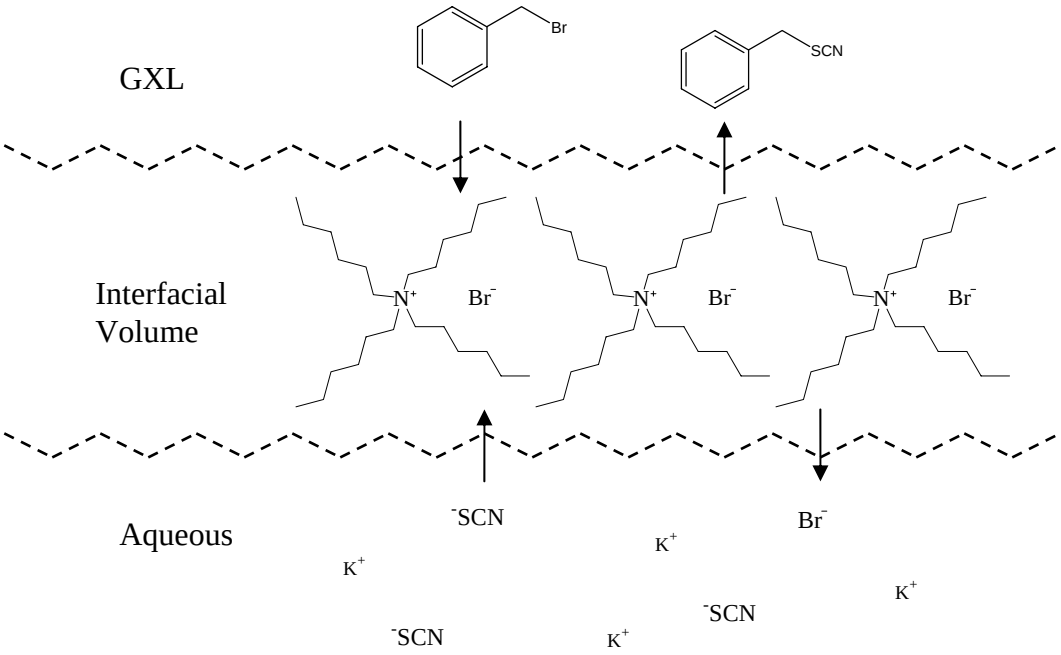

Figure 5.9: Schematic of interfacial volume.

The calculated values for the equilibrium conversion as a function of CO_2 mol fraction are shown in Figure 5.10. The decrease in the equilibrium conversion at high CO_2 concentration is consistent with a change in the dominant mechanism for the reaction.

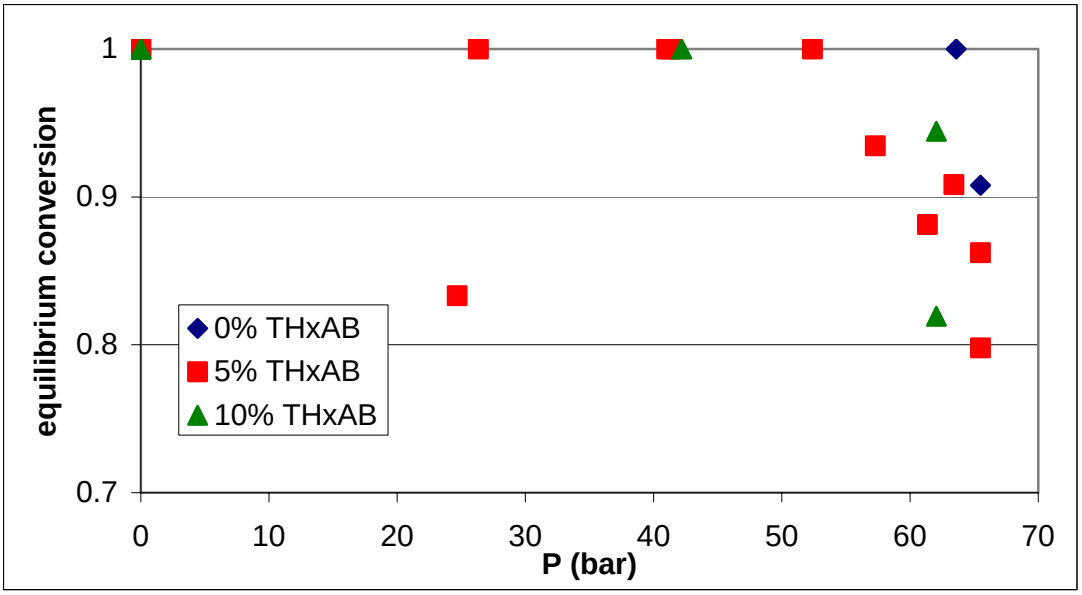

Figure 5.10: Equilibrium conversion as a function of CO_2 mol fraction.

Conclusions

The pseudo-first order rate constant of the phase-transfer catalyzed nucleophilic displacement of benzyl bromide by potassium thiocyanate with tetrahexylammonium bromide (THxAB) were measured in a CO_2-expanded toluene/aqueous system and shown to first decrease and then increase to approximately double the value in pure toluene at 95 mol% CO_2. The change in catalyst distribution does not seem to correlate with the changes in kinetics. Instead, the minimum in the rate constant suggests two competing effects on the rate: a heterogeneous mechanism that is enhanced and a homogeneous mechanism that is slowed by added CO_2.

References

Grilly, J. D. (2005). Switchable Solvents for Novel Chemical Processing. Chemical Engineering. Atlanta, Georgia, Georgia Institute of Technology. **Master of Science**.

Mason, D., S. Magdassi, et al. (1990). "Interfacial activity of quaternary salts as a guide to catalytic performance in phase-transfer catalysis." Journal of Organic Chemistry **55**(9): 2714-17.

Moore, J. W. and R. G. Pearson (1981). Kinetics and Mechanism. New York, John Wiley & Sons.

Starks, C. M., C. L. Liotta, et al. (1994). Phase-Transfer Catalysis: Fundamentals, Applications, and Industrial Perspectives.

Vendegrift, G. F., S. M. Lewey, et al. (1980). "Interfacial activity of liquid-liquid extraction reagents. II. Quaternary ammonium salts." Journal of Inorganic and Nuclear Chemistry **42**(1): 127-30.

CHAPTER 6

CONCLUSIONS AND RECOMENDATIONS

Diffusivities in Gas-expanded Liquids

In this work, the diffusivities of a series of compounds have been measured in CO_2-expanded methanol and used to calculate the viscosity of the GXL over the range of CO_2 concentration. The Taylor-Aris method was proved successful for measuring these diffusivities and viscosities, and could readily be applied to the measurement of other compounds and solvent mixtures of specific interest. Diffusivity was found to be truly a bulk property, with no observable effects of changes in the cybotactic region around the solute. As part of a larger effort to use the synergism of laboratory and simulation work to probe the local solvent structure surrounding solutes in GXL, simulations of the cybotactic regions of these systems are in progress by another researcher. Those results will be combined with the results shown here to determine what their comparison reveals about the relationship between local solvation and bulk properties.

Phase-Transfer Catalysis and Gas-Expanded Liquids

In this work, the distribution of a symmetric quaternary ammonium phase-transfer catalyst, tetrahexylammonium bromide, was measured between CO_2-expanded toluene and water. As expected, the catalyst distribution shifted first slightly to the GXL phase and then more toward the aqueous phase as the amount of CO_2 in the GXL phase was increased.

The kinetics of the phase-transfer catalyzed nucleophilic displacement of benzyl bromide by potassium thiocyanate with THxAB were measured in the same system to correlate changes in distribution with changes in rate. The pseudo-first order rate constant for the reaction also first decreased and then increased with added CO_2, but it was concluded that the trend in rate was not caused by the changes in distribution. We suggest that the minimum was caused two by competing effects on the observed rate. The first effect is a decrease in the rate constant of the homogeneous reaction caused by solvent effects on the polar transition state, and the second is an increase in the observed rate constant of the heterogeneous interfacial reaction caused by accumulation of the catalyst at the interface.

Overall, it was found that the reaction rate doubled at conditions where the volume of water required for recovery of the catalyst was cut by approximately 98%, which is definitely a positive result for industrial applications. Still, the higher cost of implementation of high-pressure equipment would have to be weighed against the economic benefits of increased production, better catalyst recovery, and reduced water requirements for a specific process before using a GXL in these systems can be deemed profitable.

One simple set of experiments that would help to support the theory that the kinetic results are caused by changes in parallel mechanisms is to vary the stirring speed of the reactor. In regimes where the homogeneous reaction is dominant, changing the stirring speed will have little effect on the rate constant. When the heterogeneous reaction dominates, the rate constant will increase with increased agitation.

Clearly, a multitude of other catalysts, reactions, and solvent combinations could be tried in this system. Catalysts with shorter (methyl, ethyl, propyl) alkyl chains distribute predominantly into the aqueous phase in normal organic/aqueous systems, and are usually not good phase-transfer catalysts (Starks, Liotta et al. 1994). Adding CO_2 to these systems would not be expected to have much effect. Tetrabutylammonium salts also distribute mostly into the aqueous phase, but have the unique property of forming third catalyst-rich phases in low polarity solvents. Adding CO_2 could enhance this effect, and may lead to higher reaction rates at lower overall catalyst concentrations. Higher tetraalkylammonium salts (dodecyl and larger) tend to distribute highly into the organic phase and rarely approach the interface, reducing reaction rates in normal organic/aqueous systems. Adding CO_2 would probably increase reaction rates in these systems, as more of the catalyst is distributed into the aqueous phase where anion exchange occurs.

Most simple displacement reactions occur homogeneously in the organic phase (Starks, Liotta et al. 1994), and the rates of these reactions would likely be decreased by adding CO_2. However, GXL/aqueous systems could be beneficial to PTC reactions that have an interfacial mechanism in organic/water systems, like alkylations, which require transfer of hydroxide ion into the interface. Some alkylating agents are sensitive to hydrolysis by water, so some care would be required in choosing the reaction. An example reaction is the methylation of deoxybenzoin, shown in Figure 6.1 (Halpern, Sasson et al. 1982). The ratio of C-alkylation to O-alkylation has been shown to be dependent on solvent polarity and catalyst structure, which could be used to further elucidate any changes in mechanism caused by added CO_2 in the GXL phase.

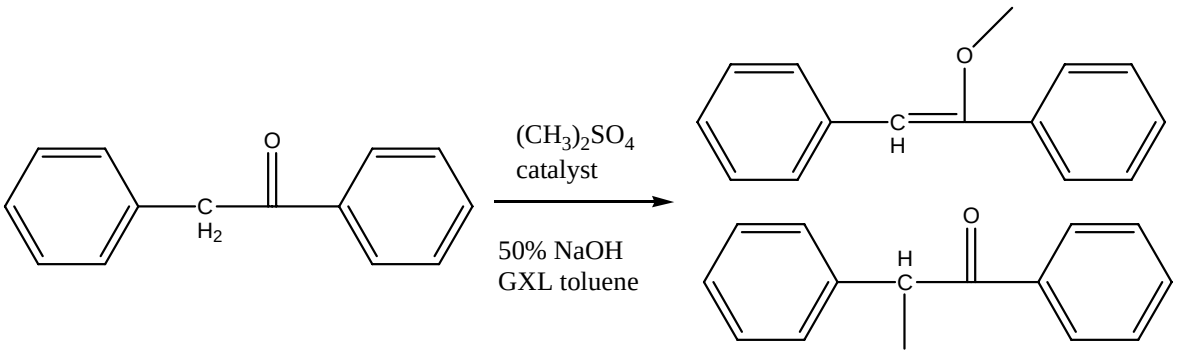

Figure 6.1: Methylation of deoxybenzoin with dimethyl sulfate

The accumulation of catalyst at the GXL/water interface could lead to interesting effects for asymmetric quaternary ammonium salts (Figure 6.2). These catalysts are similar in structure to surfactants and may form emulsions between water and GXLs as CO_2 is added and the interfacial concentration increases. In theory, these emulsions could then be broken simply by depressurization. For some of these catalysts, such as hexadecyltrimethyl ammonium salts, the tendency to lower interfacial tension is so strong that it already forms emulsions in some systems (Starks, Liotta et al. 1994). Therefore, the catalysts used in reversible emulsions would have to be chosen carefully so that they do not form emulsions in the pure organic/water system, but are surfactant-like enough that they do with increases in interfacial concentration. Catalysts with six- to twelve-carbon alkyl groups would probably work best.

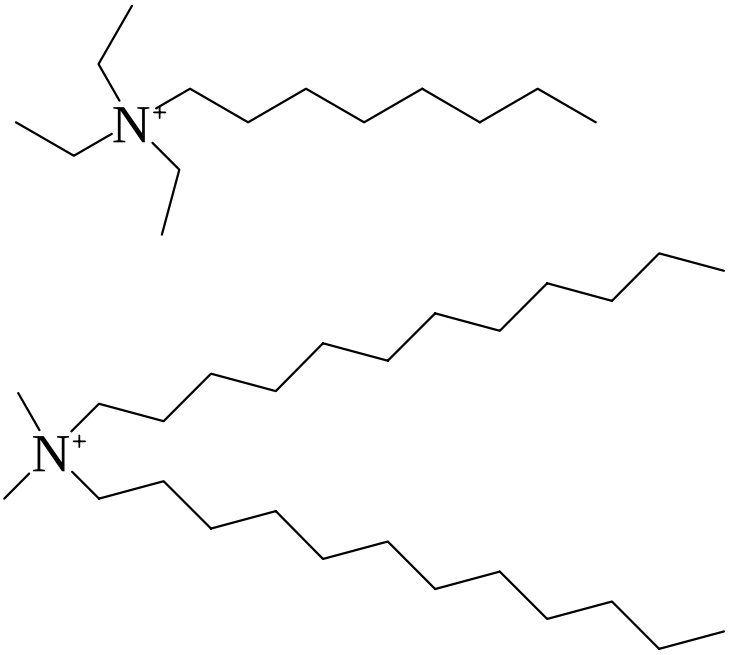

Figure 6.2: Asymmetric quaternary ammonium cations, octyltrimethylammonium (above) and didodecyldimethylammonium (below).

Emulsions are used both industrially, as in emulsion polymerization, and in synthetic organic chemistry to increase contact between immiscible phases. In either case, the products must be recovered from the emulsion for further reaction or isolation. This is typically done by adding heat to break the emulsion. An emulsion that could be broken by depressurization could be especially beneficial to systems with thermally sensitive products.

Phase-Transfer Catalysis with Chiral Catalysts

In this work, the alkylations of phenylacetonitrile and methylbenzylcyanide with the chiral phase-transfer catalyst N-benzylcinchonidinium bromide under solid-supercritical fluid conditions were performed. The reactions resulted in racemic mixtures in both cases. These findings are consistent with literature data for PTC reactions with chiral catalysts, which showed that no enantiomeric excesses (e.e.'s) are achieved for

solid-liquid conditions, while liquid-liquid reactions are typically more successful. It appears that the chiral catalyst is unable to align properly with the reactant under these conditions.

SCF/aqueous PTC systems may be more analogous to the systems that have been shown to result in good e.e.'s in the literature (Dolling, Davis et al. 1984). These systems would still have the benefits of SCF solvents such as increased transport, ease of product recovery, and replacement of more harmful solvents. Reactions such as the indanone alkylation shown in Figure 6.3 could be good for proof-of-concept experiments since they have been reported to have high e.e.'s with these catalysts.

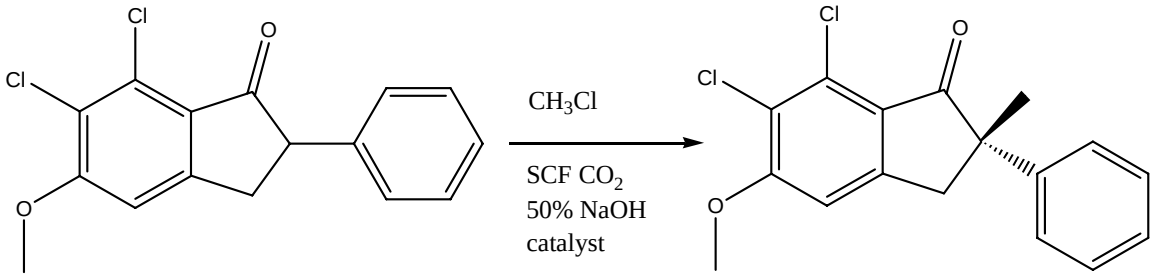

Figure 6.3: Asymmetric methylation of 6,7-dichloro-5-methoxy-2-phenyl-1-indanone.

References

Dolling, U. H., P. Davis, et al. (1984). "Efficient catalytic asymmetric alkylations. 1. Enantioselective synthesis of (+)-indacrinone via chiral phase-transfer catalysis." Journal of the American Chemical Society **106**(2): 446-7.

Halpern, M., Y. Sasson, et al. (1982). "Hydroxide-ion initiated reactions under phase-transfer-catalysis conditions. IV. Effect of catalyst structure." Tetrahedron **38**(21): 3183-7.

Starks, C. M., C. L. Liotta, et al. (1994). Phase-Transfer Catalysis: Fundamentals, Applications, and Industrial Perspectives.

APPENDIX A

GEL-BASED FILTER FOR REMOVING ODORS FROM AIR

In a project led by Charlene Bayer at Georgia Tech Research Institute (GTRI), a multi-disciplinary team worked to develop air filter media with chemical functionalities that would react with components in an inlet air stream to remove unwanted chemicals and odors. Filters were to be developed and optimized for two different applications. One application was the removal of tobacco smoke odor from hotel rooms using the filters installed in hotel room air conditioning and heating units. The other application was the removal of toxic chemicals from building filtration systems.

The basic filter design consisted of a gel, possibly supported on a matrix, containing sequestering agents that would chemically react with the contaminants to remove them from the air. The two applications inherently prescribe different requirements for the filter. In order to optimize for the two different systems, full understanding of the chemistry and mass transfer processes involved is necessary. The work done by the group includes mathematically modeling filter performance, field testing at hotel rooms for chemical species present in environmental tobacco smoke, selecting and testing possible sequestering agents, developing the configuration of the filter, and testing of the filter for performance against contaminated air streams. My contribution to the project was in the areas of gel formulation development, sequestering agent selection and testing, and filter matrix design.

Apparatus

The sequestering agent beads were packed in small glass tubes (1/8 inch diameter) and tested for capture of the challenge compounds by flowing an air stream saturated with the compound through it and measuring the outlet concentration by FID response. The air stream was saturated by bubbling through the compound. The set-up is illustrated in Figure A.1.

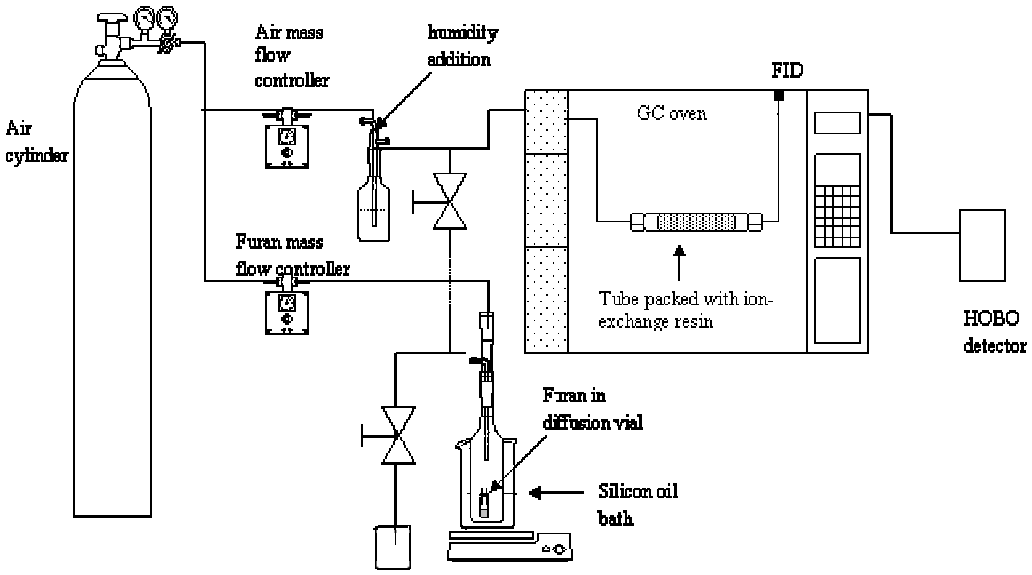

Figure A.1: Apparatus for testing sequestering agent beads.

Small filters were constructed and tested in the same manner in a small chamber which replaced the glass tube in the previous experiments (Figure A.2).

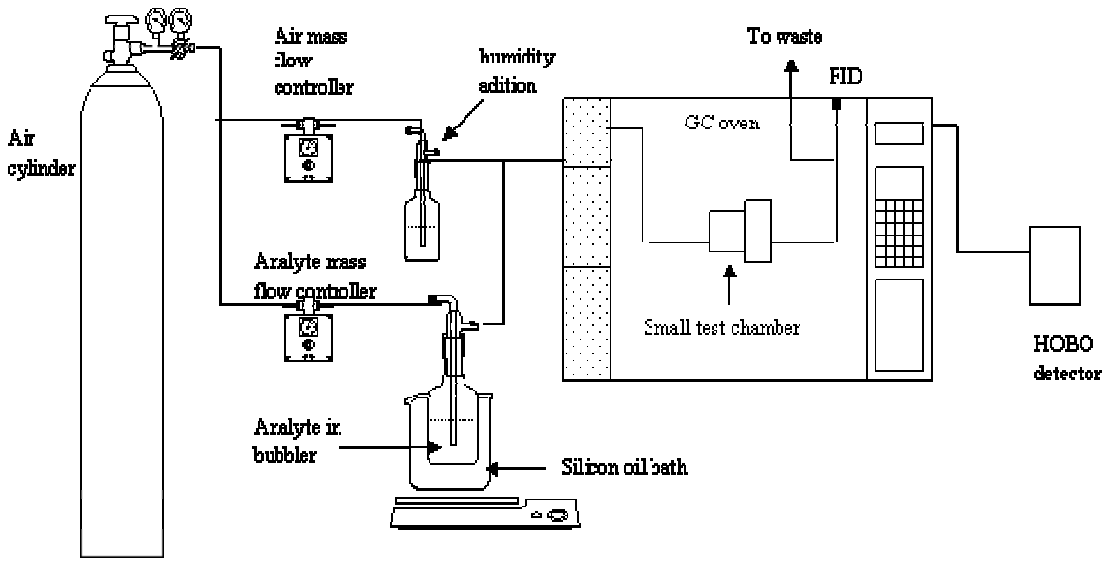

Figure A.2: Apparatus for testing small filters.

Results and Discussion

Sequestering Agent Selection and Testing

Ion exchange resins were used as the sequestering agents in the filters. Beads of highly acidic Dowex HCR-S and highly basic Dowex 550-A were tested first in a packed tube for capture of the challenge chemicals from air and later incorporated into each of the gel formulations and tested again. The beads were added at 5% by weight to the gels either individually or at a 1:1 ratio by weight. Both types of beads showed some capture of challenge compounds.

Gel Formulation Development

Original Formulation

The first gel formulation used was a proprietary polyacrylamide-based formula. Synthesizing it required polymerization of an acrylamide monomer and resulted in odors

and possible health hazards due to unreacted monomer. The time constraints imposed by the polymerization also made manufacturing test filters difficult since the reaction occurred so quickly. New formulations based on purchased polyacrylamide beads were investigated to alleviate these problems.

Polyacrylamide Gels

Several gel formulations involving polyacrylamide and water were tested. Other species were also added to try to achieve the favorable consistency of the original gel, while eliminating its undesirable qualities.

First, mixtures containing polyacrylamide concentrations from 25-75% were prepared. In these cases, the solvents used were water, glycerol, and a 50% by weight mixture of glycerol and water. For the higher polymer concentrations, there was not enough solvent present to achieve a liquid mixture. The 25% polymer in water and the water/glycerol mixture seemed to have a consistency close to that of the previous gel formulation, so mixtures at lower polymer concentrations were also tested.

The next step was to determine whether the mixtures would retain their water concentrations when exposed to the atmosphere. The weights of several samples of the 25% polyacrylamide mixture were measured periodically after being left on the benchtop to allow the water concentration to equilibrate. After several days, the water concentration decreased from 75% to 25% in the samples. In this state, the resulting gel was very hard and glassy.

To improve the final consistency of the gel, other species were added to the formula. Sodium sulfate was added to approximately 1% in a mixture with 15% polyacrylamide in water. A similar sodium bicarbonate solution was also prepared, and

samples of both were left on the benchtop for several days. The samples again became very hard and glassy, indicating that the salts did not improve water retention in the gel.

The formulation was then adjusted to include polyacrylamide, water, and sorbitol as a replacement for the glycerol in the orginal to improve the consistency and water retention properties. These gel formulations were found to retain water well. They were also tested for the amount of water uptake observed when the gel is exposed to a 100% relative humidity environment at 82°C. While some of the gels remained virtually unchanged, some of the formulations absorbed large amounts of water and became much less viscous. The possibility of exploiting this behavior in processing and manufacturing was studied.

Strongly acidic sequestering agent beads were added to the gel formulations that seemed to show promise. They failed upon testing in the small chamber for removal of 2-vinylpyridine. Upon further analysis, it was determined that the gel was actually basic due to the free amine groups in polyacrylamide. Gels were then prepared by adding various amounts sulfuric acid to titrate them back to an acidic state. However, these filters were not effective either.

Samples of commercial solid polyacrylamide at various molecular weights were obtained and used to prepare gels in the same fashion as the previous ones. Gels containing 5%, 10%, 15% and 20% polyacrylamide by weight, with water:sorbitol ratios of 50:50, 60:40 and 80:20 were prepared. These samples were exposed to the atmosphere and monitored for water loss.

The gel texture of the 5% PA Jayfloc 3452 APAM (brand name) sample appeared to have many of the desired characteristics, so it was coated on small aluminum filters,

both with and without sequestering agent beads included. It coated evenly, and there appeared to be enough holes to allow for air passage, though the holes were big enough to make channeling a concern. Without beads, it showed a very small amount of capture. With beads, it showed even less. Samples of these gels were set out to monitor water loss, and it was found that the filter samples containing beads dried out faster than those without beads. While the percentage of water lost did not appear to be very significant, qualitative investigation of the samples shows that the gel without beads remained wet and sticky while the one with the beads became very coarse and dry. Thus, the diffusive properties had probably changed. The gel was too dry for the target compounds to diffuse into them properly. This led to the development of a newer, wetter formulation.

The next formulation that was used was Jayfloc 3461 CPAM, in a modified version of the formula containing 5% polyacrylamide by mass and an 80:20 ratio of water to sorbitol. These test filters also coated very evenly, though the sample with sequestering agent beads started out too watery and had to be allowed to stand for a few minutes before it would coat properly. The samples with beads were tested (the non-bead ones were not tested) and the results appeared promising at first with about 70% capture. At the end of the hour, the capture went back down to 20-30%. Upon inspection it was found that once again, the filters were again too dry to allow proper diffusion.

It was also determined, at first by qualitative observation, that the 80:20 water:sorbitol samples dried out faster than the 50:50 samples. This was probably due to the fact that increased sorbitol caused the gel to retain water. Thus gels made from the 3461 polymer with a 50:50 water:sorbitol ratio and sequestering agent beads were coated onto filters and tested in the small chamber with 2-vinylpyridine. The results showed a

significant reduction in the signal from the FID on the outlet of the small chamber, indicating some capture of the 2-vinylpyridine.

Some samples of gels using Jayfloc 3461 were prepared and put into foil pans to dry, with the goal that they would become gel "cakes" that were firm enough to hold their shape, yet wet enough to have good capture. This did not occur. They were too sticky to remove from the pan. Also, other observations showed that such a high fraction of polyacrylamide compared to sorbitol dried out too much when treated with beads and subsequently tested.

Small aluminum filters were coated with gel made from each of the types both with and without the addition of the sequestering agent beads. These filters were tested in the small chamber for capture of a nitrogen base.

Gels prepared with each of the new polyacrylamides were also monitored for water loss and equilibrium water concentration when exposed to the atmosphere. Analysis of these results shows that the average final water concentration, which is related to the softness and flexibility of the gel, was not significantly different for gels made from the various types of polyacrylamide. The average final water concentration was highest in the 3455 gel at 23.1% and lowest in the 3461 gel at 18.0%.

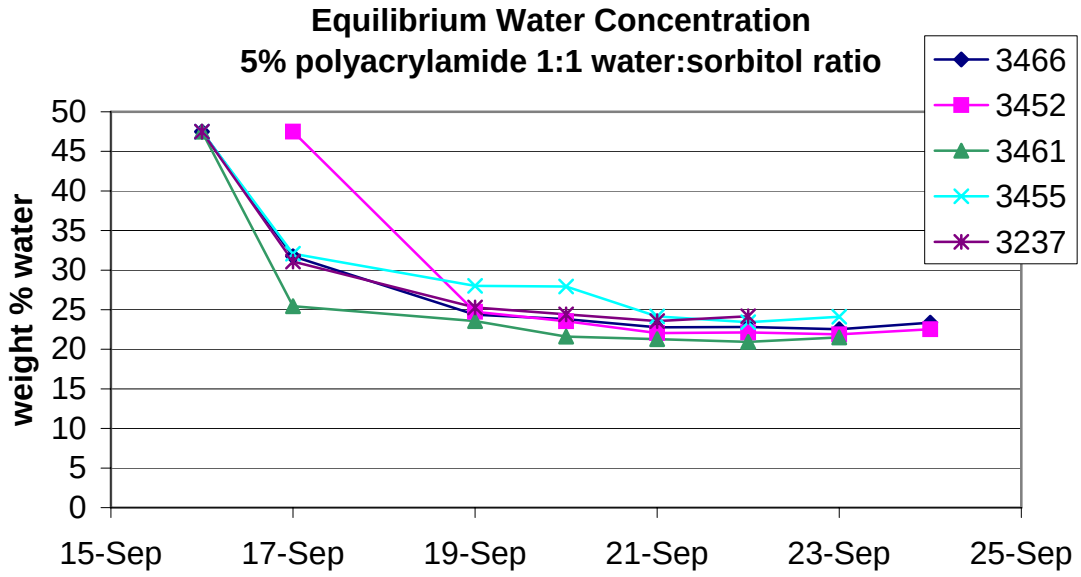

Figure A.3: Weight percent water as a function of time exposed to the atmosphere for 5% polyacrylamide gels with a 1:1 ratio of water to sorbitol made with several types of polyacrylamide.

The gels that were used for coating the filters that were tested in the small chamber for capture of 2-vinylpyridine consisted of 5% polyacrylamide with a water to sorbitol ratio of 1:1. A plot of water concentration versus time for each of the gels with this formulation shows the same trend stated above, as shown in Figure A.3.

The gels discussed above contained polyacrylamide, water, and sorbitol. After prolonged exposure to air in the small chamber, these gels were found to dry out excessively and become very hard. The next formulation change was to coat filters with gels made from polyacrylamide, water, sorbitol and glycerol. Preliminary evidence indicated that these gels did not become as hard and dry as previous formulations when tested in the small chamber.

Diffusion and Partitioning Experiments

Accurately modeling the behavior of the final filters required knowledge of the physical parameters that describe the transport of the analytes in the gel—diffusivity and partition coefficients.

The diffusivities of two dyes, azulene and methyl orange, into different gels made from each of the types of polyacrylamide were determined by visually measuring the distance the dye diffused into the gel as a function of time. Gels were prepared using each of the five types of polyacrylamide which contained polyacrylamide (PA), water and either glycerol, sorbitol, or both with the formulations shown in Table A.1, below.

Table A.1: Concentrations of gels used in diffusion experiments

	PA	**Water**	**Sorbitol**	**Glycerol**
1	5%	48%	24%	24%
2	5%	48%	0%	48%
3	5%	48%	38%	10%
4	5%	48%	48%	0%

Each of the gels shown above was prepared from each of the types of polyacrylamide for the azulene diffusion experiments, for a total of 20 samples. For the methyl orange diffusion experiments, no gels containing only sorbitol (formulation #4) were prepared, for a total of 15 samples.

In each case, the gels were prepared in 10 mL graduated cylinders and the solid dye was added to the surface. After several days, the distance the dye had diffused into the gel in centimeters was measured using calipers and recorded. The distance the dye

had diffused was assumed to be from the top of the gel to the point at which the color of the dye could no longer be seen.

This type of system can be modeled as diffusion into a semi-infinite media. The partial differential equation and boundary conditions applicable are shown in equation A-1.

$$\frac{\partial c}{\partial t} = D\frac{\partial^2 c}{\partial z^2}$$

$$t = 0, \text{all z}, c = c_\infty$$
$$t > 0, z = 0, c = c_0$$
$$t > 0, z = \infty, c = c_\infty$$

Equation A-1

The analytical solution for the system is given by Equation A.2, where c is the concentration of the dye in the gel, t is time in seconds, D is diffusivity in cm/s^2, z is distance into the gel in cm, c_0 is the concentration of the dye in the top layer of gel, and c_∞ is the concentration of the dye in the gel at infinite distance (or before diffusion begins), which in this case is zero, since there is no dye in the gel initially.

$$\frac{c - c_0}{c_\infty - c_0} = erf\,\frac{z}{\sqrt{4Dt}}$$

Equation A.2

The diffusivity of the dyes in each of the gels can be calculated with this information if an assumption is made about the percent decrease in dye concentration from the top of the gel to the point at which the color disappears. For methyl orange, it

was assumed that the concentration where the color could not be seen was 98% less than the concentration at the top of the gel. With this assumption, the diffusivities shown in Table A.2, below, were calculated.

Table A.2: Diffusivities of methyl orange into gels.

Polyacrylamide	Formulation	D (cm/s^2)
3452	2	1.04E-06
3461	2	1.00E-06
3237	2	9.25E-07
3455	2	9.17E-07
3466	2	6.78E-07
3455	1	6.24E-07
3452	1	6.04E-07
3461	1	5.44E-07
3237	1	5.05E-07
3466	1	4.50E-07
3452	3	3.96E-07
3455	3	3.62E-07
3237	3	3.49E-07
3466	3	3.17E-07
3461	3	2.64E-07

For azulene, the solubility of the dye in the gel is not as high as that of methyl orange, so the color exhibited by the dye in the samples was not as strong. From the appearance of the samples, it was assumed that the concentration where the color could not be seen was 50% less than the concentration at the top of the gel. With this assumption, the diffusivities shown in Table A.3 were calculated.

Table A.3: Diffusivities of azulene into gels

Polyacrylamide	Formulation	D (cm/s^2)
3237	2	4.17E-06
3455	2	3.45E-06
3466	2	3.30E-06
3461	2	2.57E-06
3237	1	2.21E-06
3466	1	2.06E-06
3452	2	1.98E-06
3461	1	1.68E-06
3452	1	8.95E-07
3237	3	8.31E-07
3466	3	7.61E-07
3455	1	5.97E-07
3461	3	5.08E-07
3237	4	3.02E-07
3466	4	2.02E-07
3452	3	2.01E-07
3461	4	1.97E-07
3455	3	1.57E-07
3455	4	1.36E-07
3452	4	7.52E-08

These calculations provided good initial estimates of the diffusivities, but in order to find the diffusivities more accurately, gel samples with known concentrations of methyl orange were prepared and used to determine the actual concentration of dye in the gel at different distances. This was accomplished by comparing the colors of the gels and recording the distance at which the gel appeared the same color as the gel with the known concentration. For each sample, the concentration was obtained at two points in the gel, allowing the diffusivity to be calculated without the assumption concerning the concentration decrease mentioned above. Table A.4, below, lists the diffusivities obtained by this method.

Table A.4: Diffusivities of methyl orange in the gels, calculated with two known concentration points for each sample.

Polyacrylamide	Formulation	D (cm/s^2)
3455	2	1.88E-06
3455	3	1.35E-06
3452	1	1.34E-06
3452	2	1.16E-06
3455	1	1.10E-06
3452	3	9.39E-07
3461	2	6.62E-07
3237	2	6.16E-07
3466	2	5.85E-07
3466	3	4.97E-07
3466	1	3.28E-07
3237	1	2.87E-07
3461	1	2.72E-07
3461	3	2.11E-07
3237	3	2.03E-07

Filter Design

Several filter designs were considered and tested, including supported and non-supported designs. The supported designs consisted of purchased or fabricated filters made of cotton, polymer, fiberglass, or aluminum coated with gel containing sequestering agent beads. The aluminum filters provided the best coating properties and resulted in the most successful small chamber tests. Coating polymeric or cotton twine with gel containing sequestering agent and then weaving it into a filter was also considered.

Small filters were prepared from the four types of media for testing in the small chamber. To prepare them, small circles of the media were cut to fit in the chamber and fit into a vacuum filtration apparatus. A dilute solution of gel containing sequestering agent beads was poured into the top of the apparatus and pulled through the test filter

with a vacuum pump. The beads and some of the gel remained trapped in the fibers of the filter after the solution was pulled through. These filters were allowed to dry and tested in the small chamber for capture of a nitrogen base.

A final filter form of gel containing the sequestering agents coated on polymeric fibers was also considered. To simulate this, polymeric and cotton twine fibers were coated with gel and woven into filters that will fit into the small chamber for testing against 2-vinylpyridine. These filters were tested, and the results of the tests are shown in Figure A.4 below.

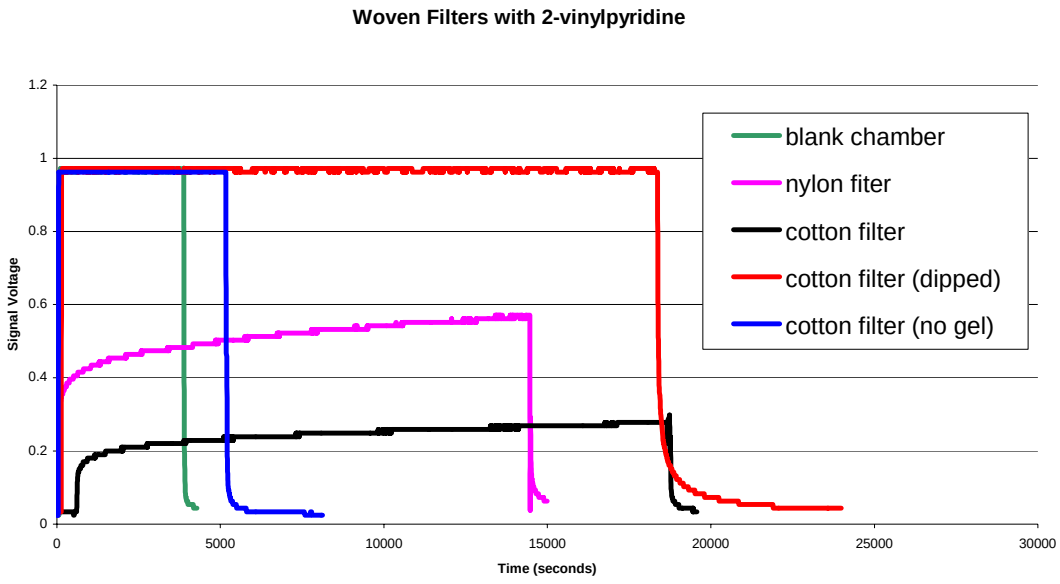

Figure A.4: Gel coated woven filters with 2-vinylpyridine

There was no removal of the 2-vinylpyridine compared to a blank chamber for either the cotton filter with no gel on it or the cotton filter that had been woven before being coated with the gel. Both the nylon filter and the cotton filter which had been coated before being woven showed removal of the 2-vinylpyridine from the air. At 121

ppm 2-vinylpyridine the nylon filter showed 78.3% removal and the cotton filter showed 89.6% removal.

Several unsupported types of filters were constructed with the goals of increasing the surface area and air contact in the filter and eliminating the need for a support matrix. The basic premise behind most of the different types was wetting the beads of solid polyacrylamide to induce "stickiness" on the surface, and creating filters from these beads. Sorbitol was also added to improve the adhesion of the beads and sequestering agent beads were mixed in to provide capture of the target compounds. Filters made of gel that had been "foamed" by CO_2 pressure were also attempted.

Four processes were attempted for constructing this type of filter. The first was to mix dry polyacrylamide and sorbitol beads in a small dish and then spray the mixture with a mist of water. A variation of this method was to mix the solids, but then to add them to the dish only in thin layers, misting each layer with water to induce adhesion before adding the next layer. The third process was to mix the solids in a small dish and to place the dish in a humid environment to allow the absorbtion of water. The fourth process attempted was to mix the solids in a large excess of water, and then to immediately lift the solids out of the water using filter paper.

Each of the methods described above was attempted using only polyacrylamide beads and then a mixture of polyacrylamide and sorbitol as the solid phase. The two processes that showed the most promise were the second and third processes, which involved spraying the solids with water in thin layers and exposing the solids to a humid environment, respectively. A filter including strongly acidic sequestering agent beads

was also prepared using the humidity method. While we were unable to observe significant capture using these filters, the results were promising.

The ability to create a foamed gel which could both retain its shape and allow air passage could make possible the design of a filter without the inclusion of an inert matrix for support of the gel and the sequestering agents. To observe the properties of a foamed version of the gel, 15.34 mL of CO_2 at 1500 psia and 15.7^{o}C was added to 2.55 g of gel in a pressure vessel. The pressure in the vessel was about 875 psi, which indicates that both liquid and vapor CO_2 were present. After 24 hours, the vessel was rapidly depressurized, removing the CO_2 and leaving the gel with large bubbles throughout. This gel was still very soft and did not retain its shape, however.

The same gel was repressurized using 15.32 mL of CO_2 at 1100 psia and 21.9^{o}C, and allowed to remain under pressure for 11 days. After depressurization, the resulting gel was very foamy, with many small bubbles, so that the gel appeared white in color. Over the next three days, the gel collapsed back nearly to its original size, although many of the bubbles remained.

For both experiments, the foam formed appeared to be a "closed-cell" foam, which would probably not allow air passage through. The possibility of instead creating an "open-cell" foam by manipulating various variables was investigated, but no viable method was found.

Conclusions

Work toward the development of an air filter media with chemical functionalities that would react with components in an inlet air stream to remove unwanted chemicals and odors shows that the basic premise of using a gel containing ion exchange resin sequestering agents holds promise of being successful. Sample filters of various configurations and gel formulas were constructed and tested for capture of select target compounds. Several of them showed some capture, suggesting that further research in manufacturing could result in a viable product. Much of the groundwork toward manufacturing optimization has also been laid with this research. A filter that met the required capture specifications was eventually produced, but has not yet been implemented industrially.

APPENDIX B

PHASE-TRANSFER CATALYSIS WITH A CHIRAL CATALYST IN SUPERCRITICAL FLUIDS

Previously, Wheeler, et al reported the first example of a phase-transfer-catalyzed alkylation reaction under supercritical fluid conditions (Wheeler, Lamb et al. 2002). The reaction was that of phenylacetonitrile and ethyl bromide in the presence of tetrabutylammonium bromide (TBAB) and potassium carbonate in supercritical ethane, shown in Figure B.1 below. This reaction was chosen because it yields an important precursor in pharmaceutical synthesis. The product of this reaction possesses a chiral center, which is present as a racemic mixture when catalyzed by TBAB. In the pharmaceutical industry, the ability to synthesize enantiomerically pure compounds is very important. Reported work using chiral quaternary ammonium salts as enantioselective phase-transfer catalysts prompted a study of the application of these types of catalysts to reactions performed in supercritical fluids (Dolling, Davis et al. 1984; Dolling, Hughes et al. 1987; Hughes, Dolling et al. 1987; Corey, Xu et al. 1997). Chiral phase transfer catalysis has also been used to synthesize amino acids (Shirakawa, Tanaka et al. 2004) and many other types of compounds.

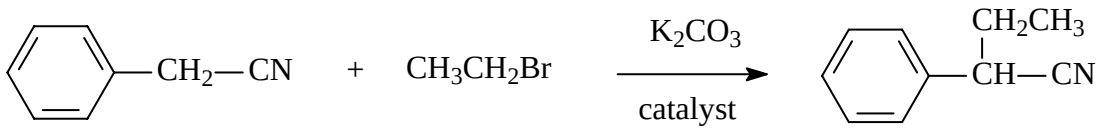

Figure B.1: Alkylation of phenylacetonitrile with ethyl bromide

In this work, two enantioselective alkylations in supercritical fluids were attempted. The first is of phenylacetonitrile, and the second is of methylbenzylcyanide. The chiral phase transfer catalyst in both cases was N-benzylcinchonidinium bromide, shown in Figure B.2.

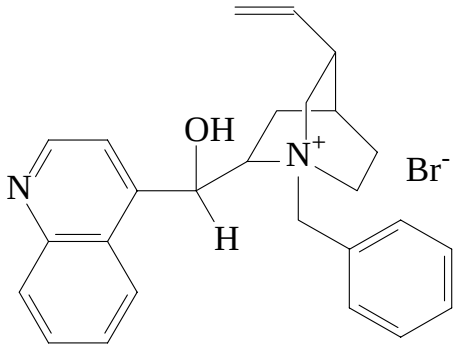

Figure B.2: Chiral quaternary ammonium salt N-benzylcinchonidinium bromide.

Experimental Methods

Materials

Ethane was obtained from Air Products (CP grade). Reactants phenylacetonitrile (99+%), methyl benzyl cyanide (98%), and ethyl bromide (99+%), were obtained from Sigma Aldrich, and anhydrous potassium carbonate (A.C.S. Reagent Grade) was obtained from J.T. Baker. The chiral phase-transfer catalyst N-benzylcinchonidinium bromide (97%) was also obtained from Sigma-Aldrich.

Apparatus

Figure B-3 shows a schematic of the reaction apparatus. All reactions were performed in a high-pressure stirred reactor (Parr Instrument Company, Model 4561).

The reactor had a maximum working pressure of 208 bar, and a maximum working temperature of 350°C, and was stirred by a paddle-type impeller on a magnetic drive (Parr Instrument Company, Model A1120HC). Stainless steel balls were added to the reactor to increase agitation. The seal between the stirrer and the reactor head was made with a silver gasket, and a teflon gasket made the seal between the reactor body and reactor head. The internal volume of the reactor was approximately 285 mL. Temperature, pressure, and stirring rate were monitored and controlled by a PID temperature controller and tachometer (Parr Instrument Company, Model 4842) with a digital pressure transducer (Heise, Model 901B). The reactor was fitted with a rupture disk to ensure the pressure in the reactor remained below the reactor pressure rating.

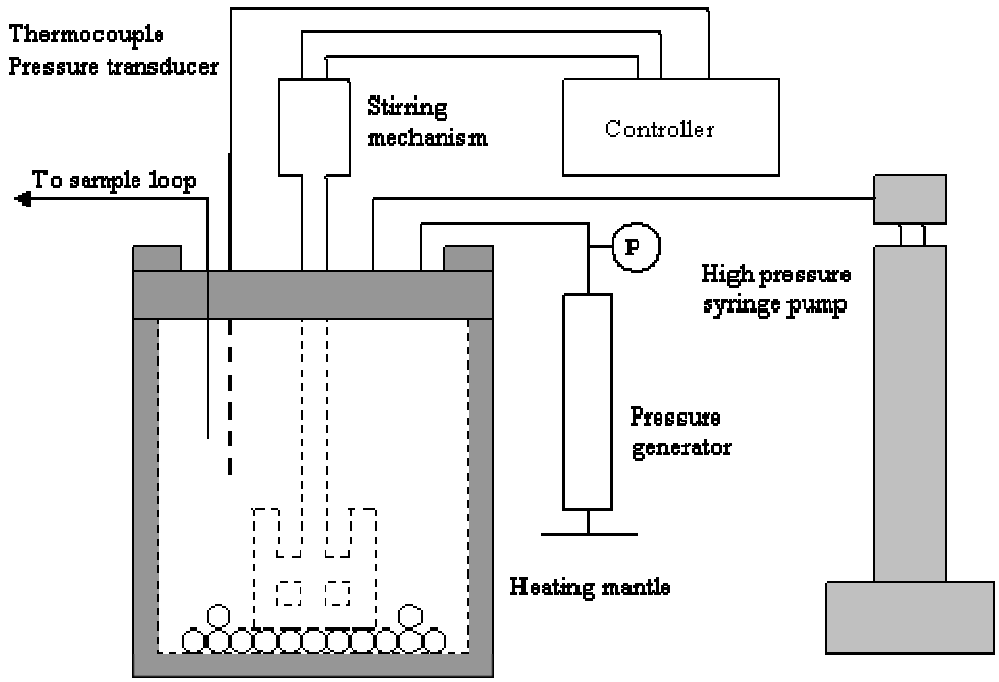

Figure B.3: Schematic of PTC reaction apparatus

The supercritical phase was sampled using a dip tube extending approximately 3 cm into the reactor connected to a six-port sampling valve (Valco Instruments Co. Inc.)

fitted with a 250 microliter sample loop. The dip tube had a filter on the end inside the reactor to prevent solids from entering the line. The reactor was pressurized with ethane using a high pressure syringe pump (Isco, Inc., Model 500D). An HPLC pump was used to flush the sample loop after each sample. The phenylacetonitrile or methylbenzyl cyanide were delivered to the reactor using a high pressure generator (High Pressure Equipment Company, Model 87-6-5) connected to a port on the reactor head.

Procedure

Ethyl bromide and potassium carbonate were both used at five times the amount of the limiting reagent, phenylacetonitrile or methylbenzyl cyanide. The catalyst was used at 10% the amount of limiting reagent.

The reactor was loaded with solid potassium carbonate and catalyst and stirred overnight to achieve a uniform particle size. During this stirring, the system was maintained at 35°C and continually flushed with nitrogen to remove any water present. The reactor was then loaded with ethyl bromide, sealed, and simultaneously heated to 75°C and pressurized to 150 bar while stirring at approximately 300 rpm. Once the desired conditions were reached, the limiting reagent was added by a high pressure hand pump to start the reaction.

Samples were taken in triplicate at regular intervals through the six-port valve, illustrated in Figure B.4. For each sample, the valve was first switched to the position that allowed the reactor contents to flow through the sample loop and out to waste (position A). The valve to the waste reservoir was opened, and the reactor contents were allowed to flush for several seconds. The valve was then closed, containing the reactor contents in the loop, and the HPLC pump switched on to allow solvent, acetone in this

case, to flow into a 5 mL flask through the sample collection tube. After a small amount of acetone was collected, the six-port valve was switched to the position that allowed the loop contents to be flushed through the sample collection tube by the acetone into the collection flask (position B). When the sample had been diluted to 5 mL, the HPLC pump was switched off.

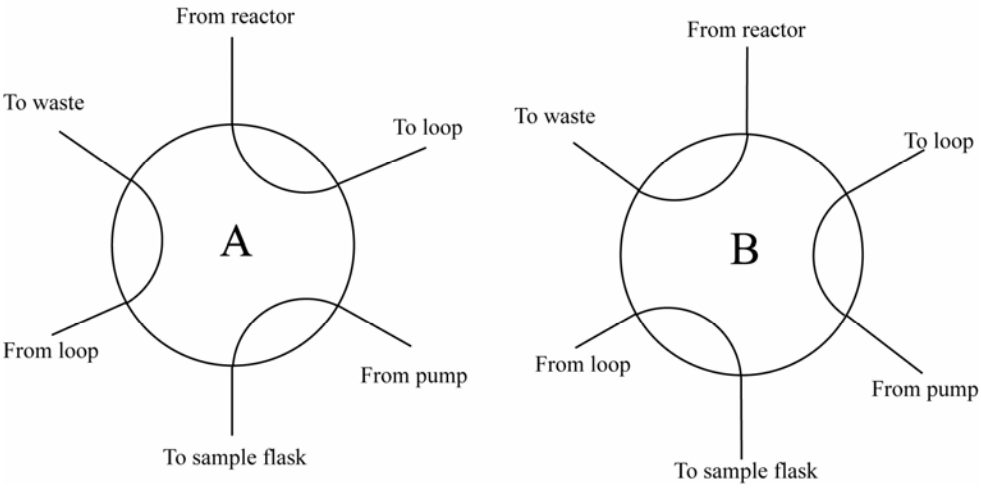

Figure B.4: Sampling system

The samples were analyzed by a gas chromatograph (Hewlett-Packard 6890) equipped with a flame-ionization detector. The responses of the reactants and products were calibrated prior to analysis. Selected samples were also analyzed by gas chromatograph fitted with a chiral column. This was done by Teresa Chamblee at the analytical labs at Coca-Cola.

Results and Discussion

We attempted to perform the enantioselective alkylation of phenylacetonitrile with ethyl bromide, also in the presence of potassium carbonate in supercritical ethane at 150 bar and 75°C with the chiral phase-transfer catalyst N-benzylcinchonidinium

bromide. These results of three separate runs (in different colors) are shown in Figure B.5. Conversions of 80-85% were achieved after 24 hours. The average pseudo-second-order rate constant was 4.81×10^{-6} L/mol-s.

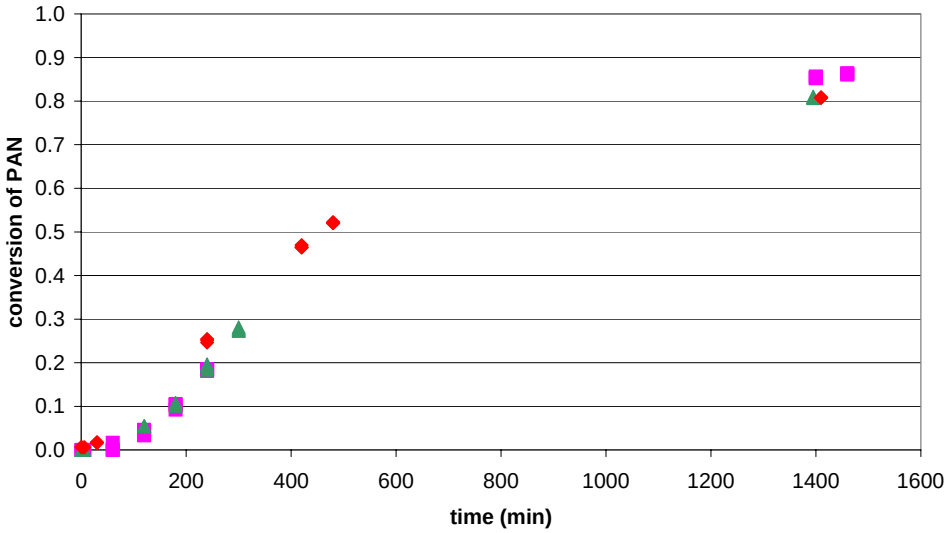

Figure B.5: Conversion of phenylacetonitrile with 10% N-benzylcinchonidinium bromide.

The product of the reaction still possessed an acidic proton at the chiral center, so there existed the possibility that the product could racemize after reaction, since base was still present in the reaction vessel. In order to eliminate this possibility, we tried the alkylation of methyl benzyl cyanide (MBC) with ethyl bromide (Figure B.6). MBC possesses only one proton on its chiral center, and should not be able to rearrange once it has been alkylated.

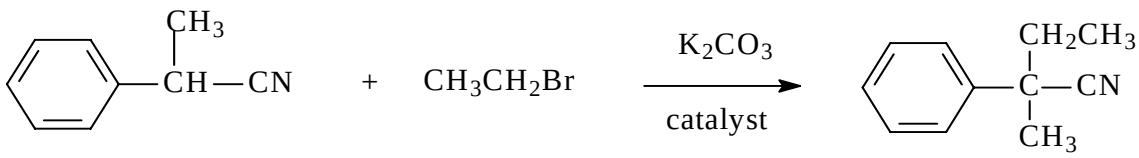

Figure B.6: Alkylation of methyl benzyl cyanide with ethyl bromide

After 48 hours at 150 bar and 75°C, approximately 20% conversion of the MBC was achieved. The final product samples were analyzed on a chiral gas chromatograph column with a mass spectrometer detector (Figure B.7). Two product peaks were found in approximately equal proportions. These were presumably the responses to each of the enantiomers, meaning that both enantiomers were present and that no selectivity had been achieved. Diez-Barra, et. al. report chiral Michael additions using a very similar catalyst under liquid-liquid and solid-liquid (solvent-free) PTC conditions (Diez-Barra, de la Hoz et al. 1998). The solvent-free condition best correlates to the supercritical fluid-solid system described in this work. They found that while modest enantiomeric excesses (e.e.'s) were achieved under liquid-liquid conditions, no e.e. was achieved under solvent-free conditions. They speculated that the catalyst was not able to differentiate between the faces of the enolates under those conditions. Our results are also consistent with this theory. Other reports of successful enantioselective PTC reactions that have been found in the literature were only conducted in liquid-liquid systems (Dolling, Davis et al. 1984; Dolling, Hughes et al. 1987; Hughes, Dolling et al. 1987; Corey, Xu et al. 1997).

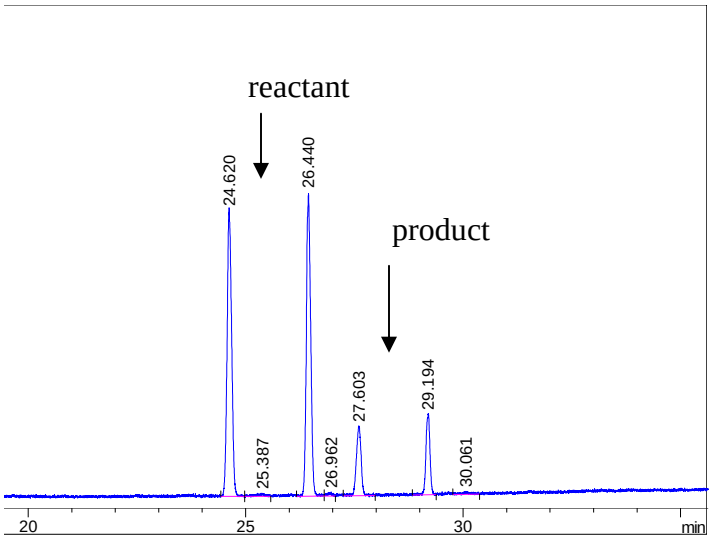

Figure B.7: Results from chiral chromatograph for MBC alkylation.

Conclusions

The alkylations of phenylacetonitrile and methylbenzylcyanide with the chiral phase-transfer catalyst N-benzylcinchonidinium bromide under solid-supercritical fluid conditions resulted in racemic mixtures in both cases. These findings are consistent with literature data for PTC reactions with chiral catalysts, which showed that no enantiomeric excesses are achieved for solid-liquid conditions, while liquid-liquid reactions are typically more successful. It appears that the chiral catalyst is unable to align properly with the reactant under these conditions.

References

Corey, E. J., F. Xu, et al. (1997). "A Rational Approach to Catalytic Enantioselective Enolate Alkylation Using a Structurally Rigidified and Defined Chiral Quaternary Ammonium Salt under Phase Transfer Conditions." Journal of the American Chemical Society **119**(50): 12414-12415.

Diez-Barra, E., A. de la Hoz, et al. (1998). "A study on the phase transfer catalyzed Michael addition." Tetrahedron **54**(9): 1835-1844.

Dolling, U. H., P. Davis, et al. (1984). "Efficient catalytic asymmetric alkylations. 1. Enantioselective synthesis of (+)-indacrinone via chiral phase-transfer catalysis." Journal of the American Chemical Society **106**(2): 446-7.

Dolling, U. H., D. L. Hughes, et al. (1987). "Efficient asymmetric alkylations via chiral phase-transfer catalysis: applications and mechanism." ACS Symposium Series **326**(Phase Transfer Catal.: New Chem., Catal., Appl.): 67-81.

Hughes, D. L., U. H. Dolling, et al. (1987). "Efficient catalytic asymmetric alkylations. 3. A kinetic and mechanistic study of the enantioselective phase-transfer methylation of 6,7-dichloro-5-methoxy-2-phenyl-1-indanone." Journal of Organic Chemistry **52**(21): 4745-52.

Shirakawa, S., Y. Tanaka, et al. (2004). "Development of a Recyclable Fluorous Chiral Phase-Transfer Catalyst: Application to the Catalytic Asymmetric Synthesis of a-Amino Acids." Organic Letters **6**(9): 1429-1431.

Wheeler, C., D. R. Lamb, et al. (2002). "Phase-Transfer-Catalyzed Alkylation of Phenylacetonitrile in Supercritical Ethane." Industrial & Engineering Chemistry Research **41**(7): 1763-1767.

APPENDIX C

VALIDATION OF TAYLOR-ARIS DISPERSION MEASUREMENTS

Introduction

The validation work included in this appendix was performed by Malina Janakat and Dr. Xiuyang Lu, a visiting professor from Zhejiang University in Hangzhou, China. The experimental and analytical methods used are outlined in Chapter 3 of this thesis.

Diagnostics

Influence of Detection Wavelength

The influence of wavelength on the diffusion coefficient of benzene in methanol at 313 K and 100 bar is shown in Figure C.1. From the results we can see that different wavelengths give different results. Since the detector has the ability to measure up to five wavelengths simultaneously, it was very easy to compare the results of several wavelengths and ensure that they were ascertained under identical conditions. This is important to point out because while we determined that the best place to detect benzene is at 254 nm, the literature tells us that benzene should be detected at either 210 nm (Sassiat, Mourier et al. 1987) or 239 nm (Funazukuri, Kong et al. 2000). From our studies, however, we determined that 210 nm is unsuitable for these purposes and that 239 nm works, but 254 nm produces a stronger signal.

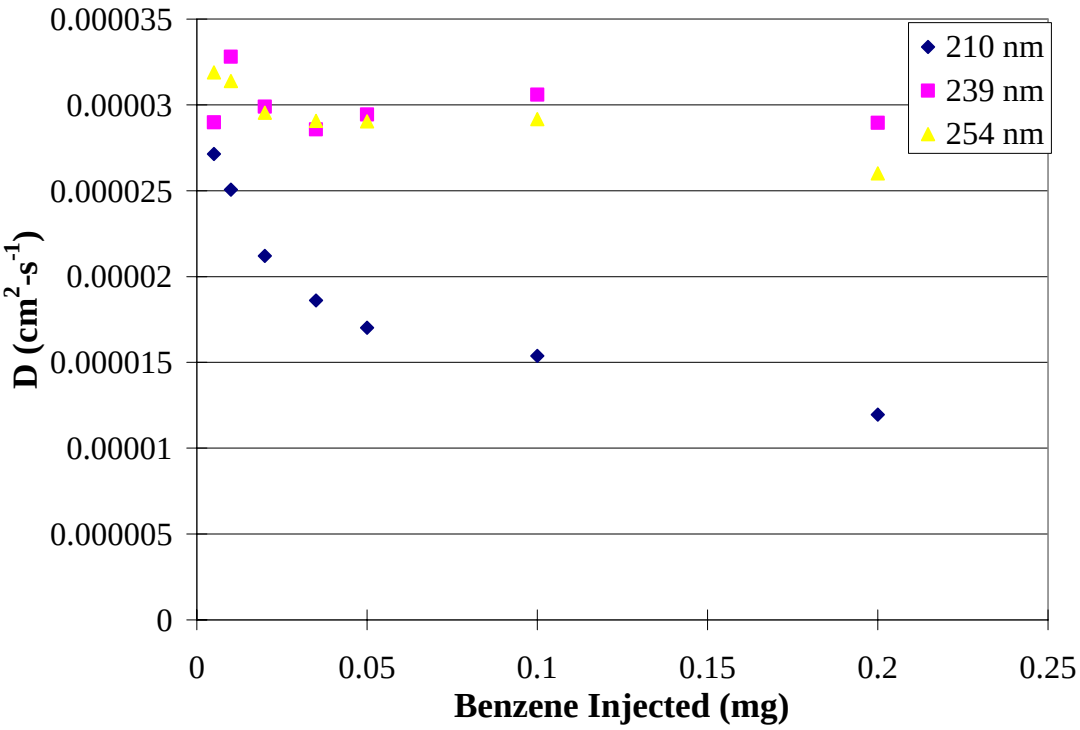

Figure C.1: Influence of detector wavelength and injected amount of solute on the diffusion coefficient of benzene in methanol, 313 K, 100 bar, $v_{Methanol}$=0.2 ml/min.

Influence of Amount of Solute Injected

Diffusion coefficient data must be measured at infinite dilution in order to eliminate effects from self-diffusion of the solute (Cussler and Editor 1996). In practice, infinite dilution is very difficult to achieve because it is typically below the detection limits of any instrument. Thus it was important to determine the appropriate operating range to be as close to infinite dilution as possible while still working in the range where the intensity is linear with the concentration. The limits of the detector were tested by measuring the diffusion coefficients of four compounds – benzene, toluene, 2-naphthol and phenol – as a function of injected quantity. Data for benzene are already presented above in Figure C.1, data for the remaining compounds are shown in Figures C.2 through C.4.

Comparison of these four figures indicates that benzene is the most sensitive of the four compounds to the amount of solute injected. At higher injected quantity, the diffusion coefficient of benzene (Figure C.1) decreases due to the interactions between solute molecules; the system is not sufficiently dilute and self-diffusion is occurring. At lower injected quantities the diffusion coefficient increases sharply. We have not determined a definitive explanation but speculate that the peak areas are so low as to be below the limits of the detector or that there is mixing within the detector that becomes problematic when the solute is very dilute. Knowledge of such behavior is important in the design of future experiments with the equipment.

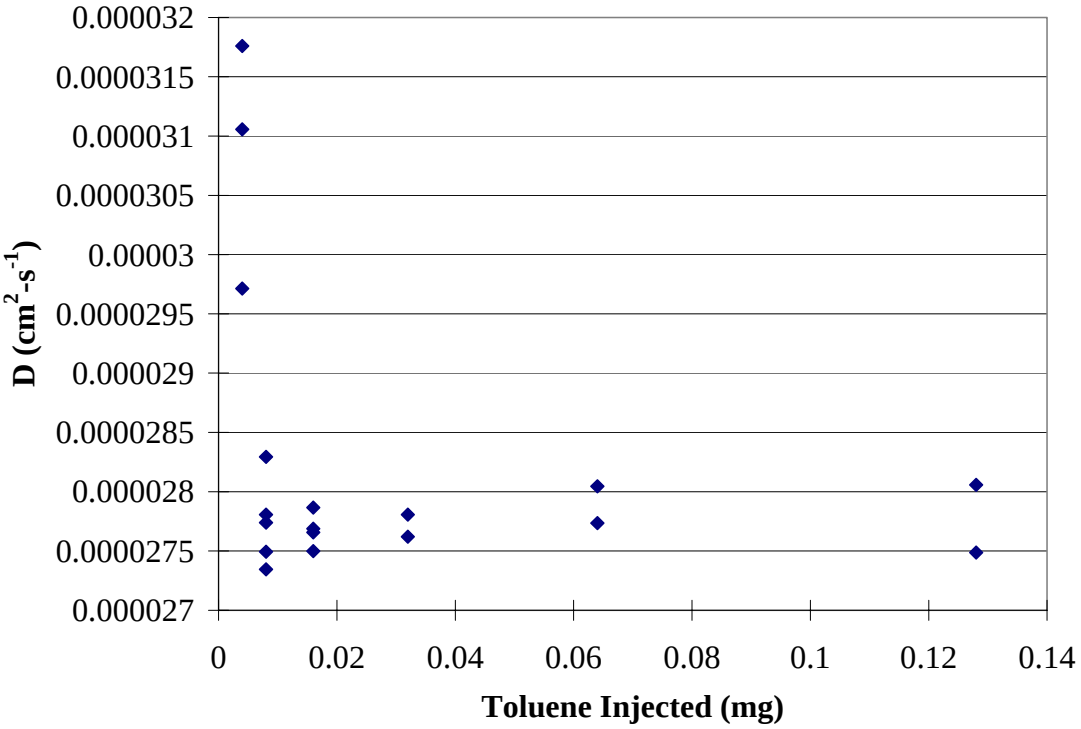

Figure C.2: Influence injected amount of solute on the diffusion coefficient of toluene in methanol, 313 K, 100 bar, $v_{Methanol}$=0.2 ml/min, 260 nm.

Toluene (Figure C.2) and 2-naphthol (Figure C.3) show similar behaviors at low concentrations, but do now show the same decrease at higher solute amounts. Their threshold for self-diffusion seems to be beyond the limits tested in this study. Phenol does not show either behavior (Figure C.4), indicating that the entire injection range would be suitable for measurement.

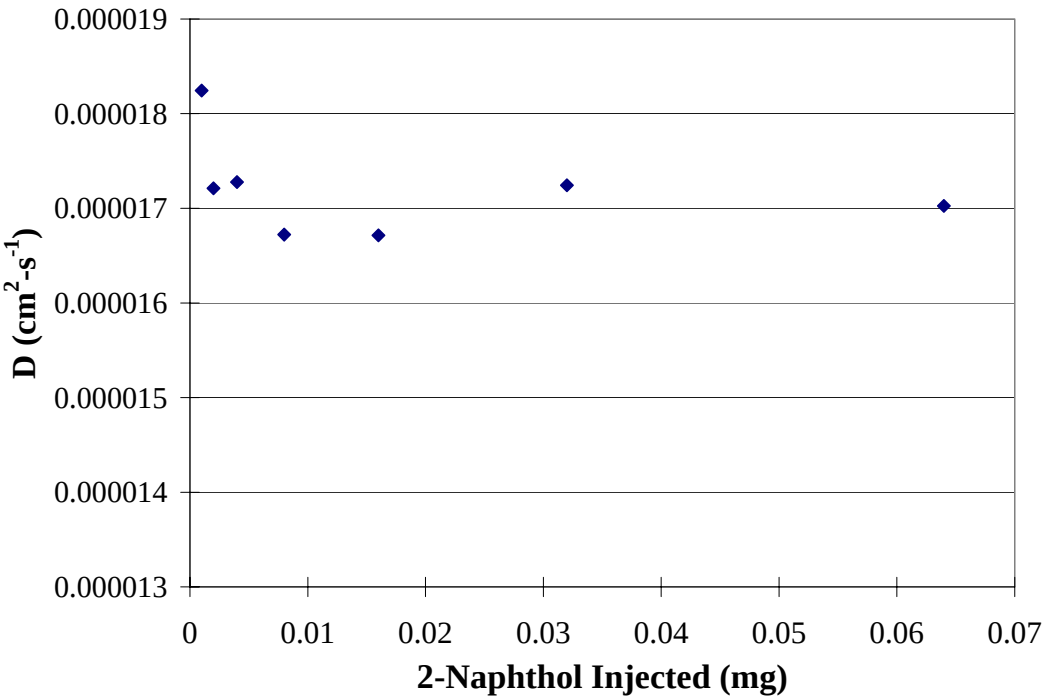

Figure C.3: Influence injected amount of solute on the diffusion coefficient of 2-naphthol in methanol, 313 K, 100 bar, $v_{Methanol}$=0.2 ml/min, 274 nm.

We also looked at the linearity of the detector with regard to peak area versus injected quantity. Data for the peak area of phenol as a function of injected quantity are in Figure B.5. We wanted to make sure that we were running our experiments in the area where the detector is linear. Based on this and the measurements above, it seems that the appropriate operating range for the peak area should be between 10,000-100,000 mAu-

sec. Anything lower and the concentration might become too low and fall into that 'upturn' area. Anything higher and self-diffusion might occur.

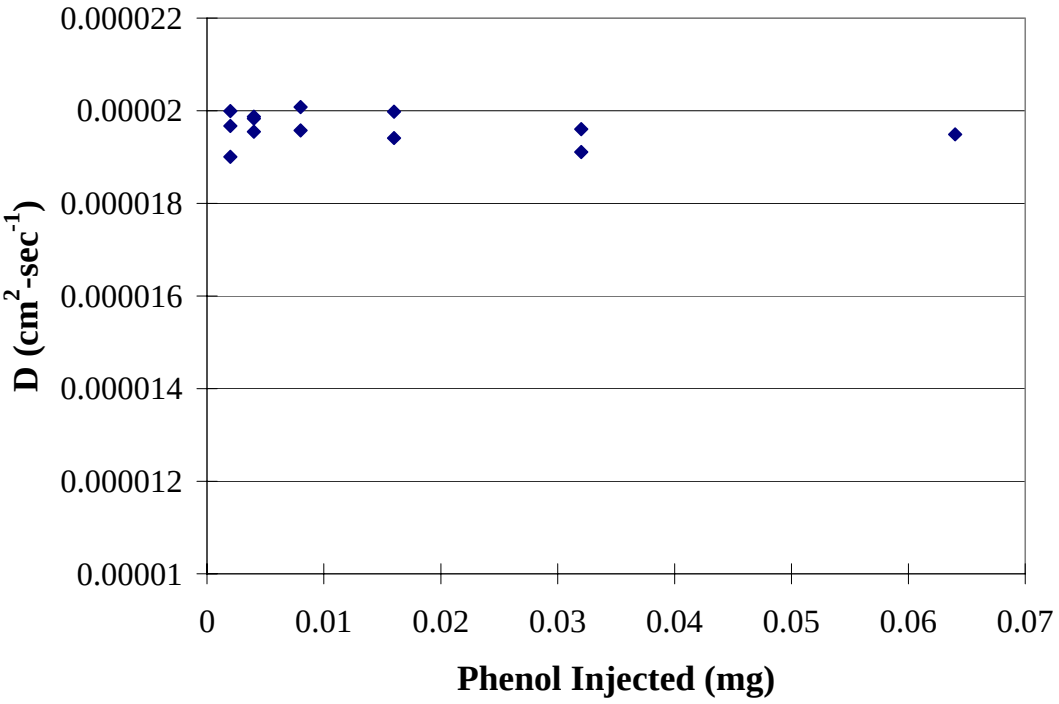

Figure C.4: Influence injected amount of solute on the diffusion coefficient of phenol in methanol, 313K, 100 bar, $v_{Methanol}$=0.2 ml/min, 272 nm.

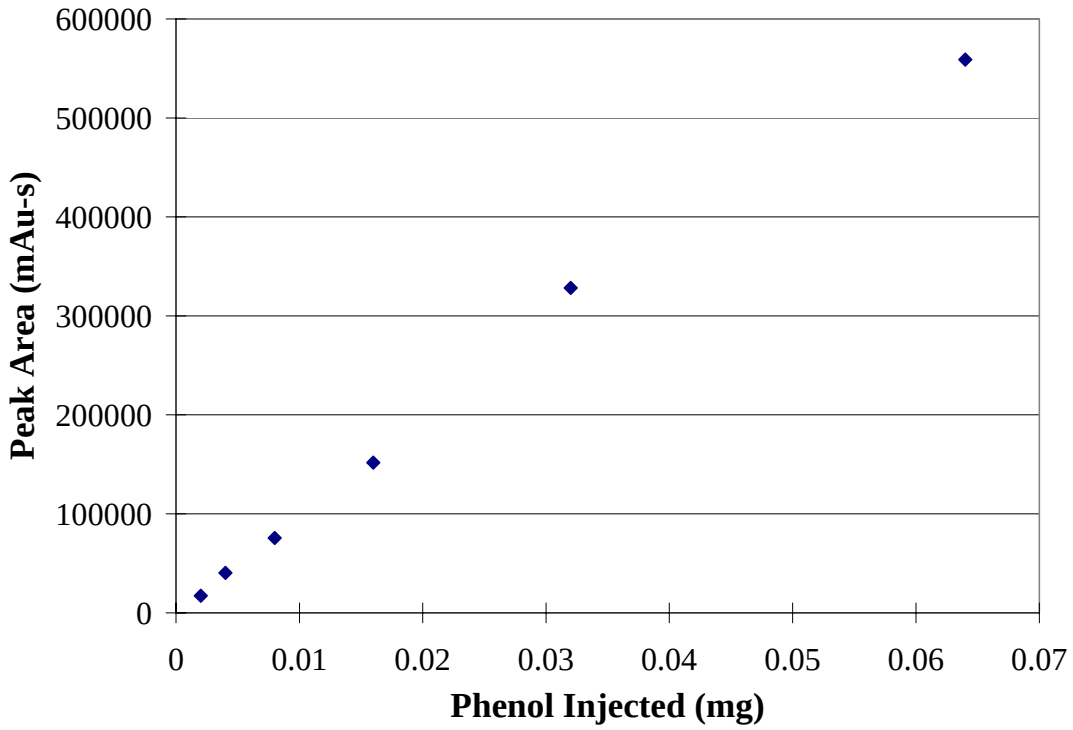

Figure C.5: Influence injected amount of phenol on the peak area 313 K, 100 bar, $v_{Methanol}$=0.2 ml/min, 272 nm.

Influence of Flow Rate

It is important to choose the flow rate of the mobile phase carefully because the flow profile must be laminar for the Taylor-Aris dispersion technique to be valid. Since the flow is through a coiled tube and not a straight tube, having a Reynolds number of less than 2100 was not the only determining factor in choosing a flow rate. It was also important that the square root of the product of the Dean and Schmidt numbers be less than approximately 10. This means that the flow rate must be less than approximately 2.5 ml/min for methanol. However, the calculations were based on assumptions for a coiled tube that may not have been valid for 100 feet of length and imperfect circles. The influence of flow rate on the diffusion coefficient for benzene in methanol was measured

at 313 K and 100 bar and appears in Figure C.6. The data confirm the calculation and indicate that 0.25 ml/min is the maximum flow rate for methanol under the operating conditions. Beyond that limit the flow may no longer be laminar and dispersion due to turbulent flow makes it difficult to decipher diffusion coefficients from the resulting data.

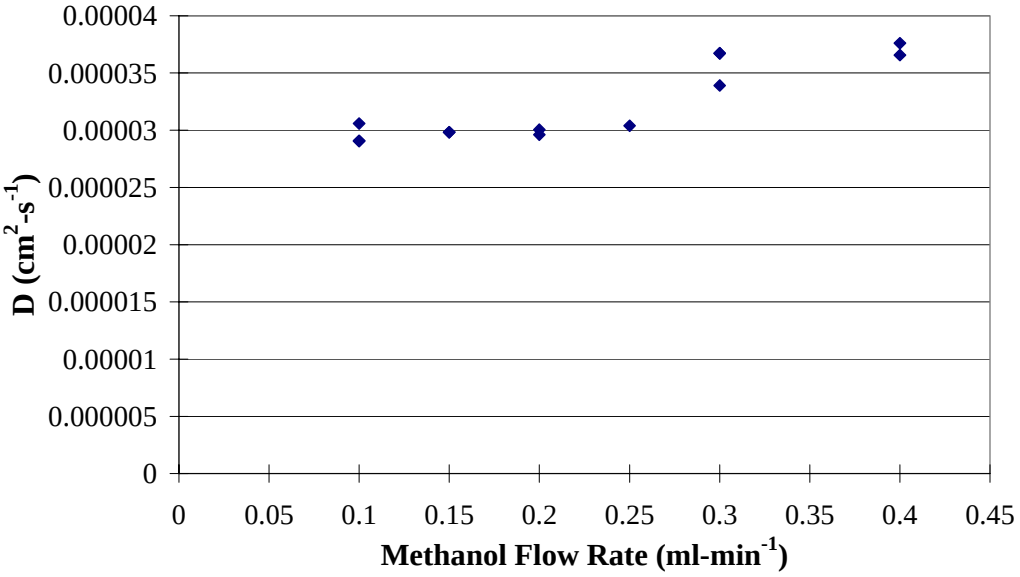

Figure C.6: Influence of methanol flow rate on the diffusion coefficient of benzene, 313 K, 100 bar, 0.01 mg injection.

Influence of Pressure

The influence of hydrostatic pressure in the mobile phase on the diffusion coefficients of benzene in methanol at 295 K are shown in Figure C.7. As pressure is increased, the diffusion coefficient decreases. This is expected from a fundamental standpoint. More importantly, the behavior is linear within the range of the experiments.

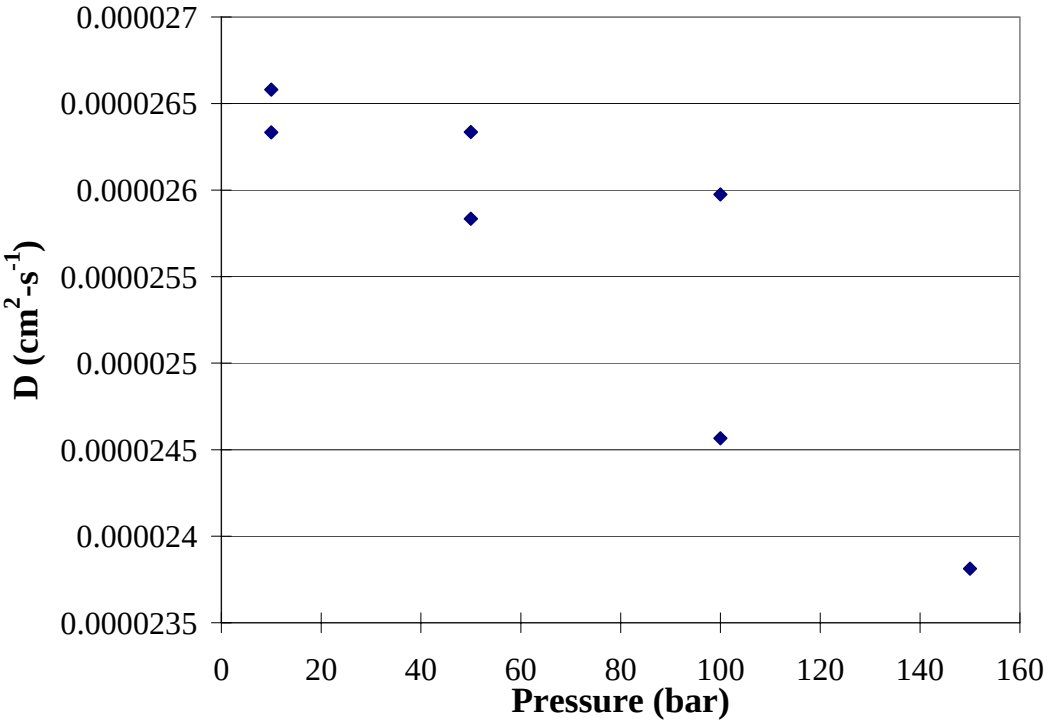

Figure C.7: Influence of hydrostatic pressure of methanol on the diffusion coefficient of benzene, 313 K, 0.01 mg injection, $v_{Methanol}$=0.2 ml/min.

Influence of System Temperature

The influence of system temperature on the diffusion coefficients of benzene and toluene in methanol are shown in Figures C.8 and C.9, respectively. In both cases, the diffusion coefficient increases linearly with temperature for the range of temperatures studied.

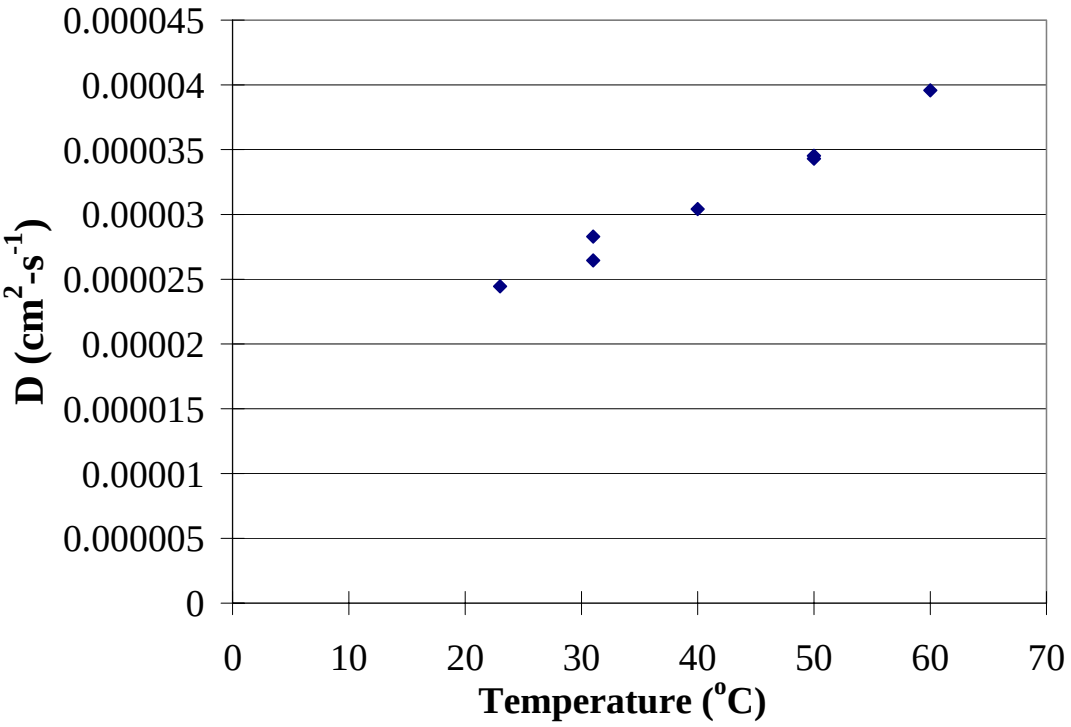

Figure C.8: Influence of temperature of methanol on the diffusion coefficient of benzene, 100 bar, 0.01 mg injection, $v_{Methanol}$=0.2 ml/min.

Influence of Chiller Temperature

Since the syringe pumps for the methanol and CO_2 were to be chilled so that their density could be known and to ensure that liquid CO_2 was being dispensed into the system, it was necessary to understand the impact of the chiller temperature on the resulting diffusion coefficient. If the chiller had any impact it would need to be corrected for. Data for the diffusion coefficient of toluene as a function of chiller temperature are shown in Figure C.10. It is obvious that the influence of chiller temperature on the diffusion coefficients of toluene in methanol at 323 K and 100 bar is negligible, which indicates that the pre-heater is sufficient for heating the mobile phase to the requisite temperature.

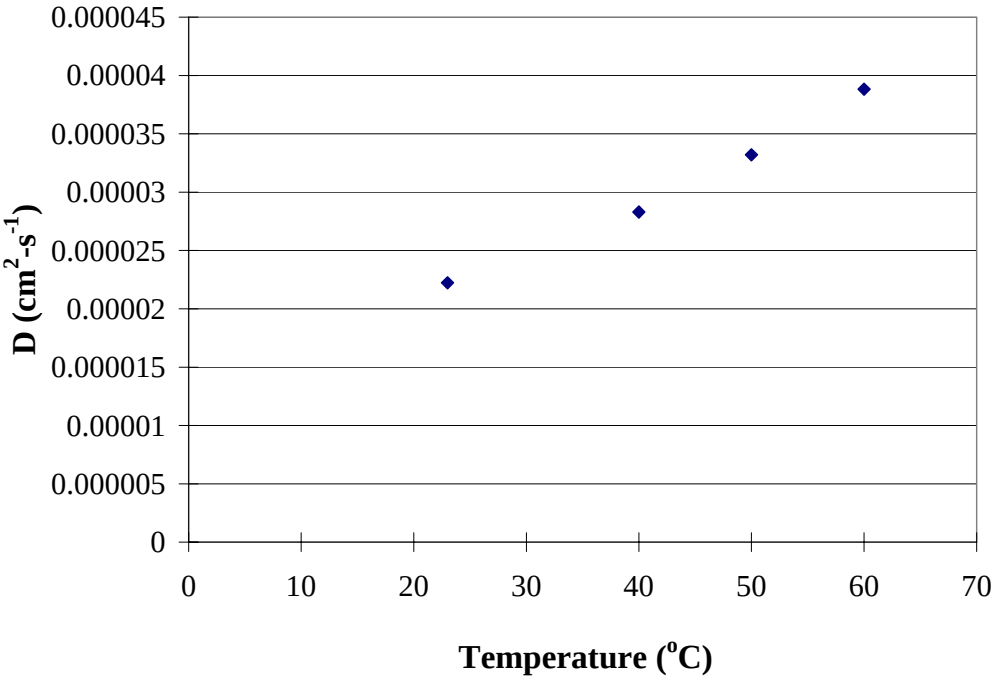

Figure C.9: Influence of temperature of methanol on the diffusion coefficient of toluene, 14 bar, 0.01 mg injection, $v_{Methanol}$=0.2 ml/min.

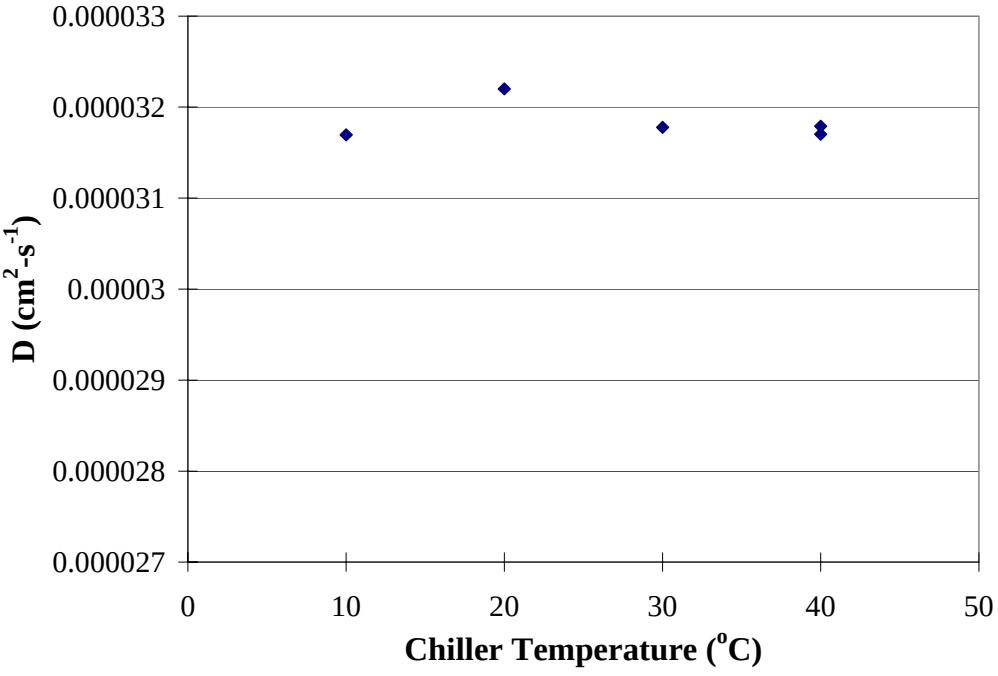

Figure C.10: Influence of chiller temperature on the diffusion coefficient of toluene, 313 K, 100 bar, 0.01 mg injection, $v_{Methanol}$=0.2 ml/min.

Upon validation of the above parameters, data of the solids were compared with that of the literature and data for the diffusion of benzene in mixtures of methanol and carbon dioxide were measured and confirmed. These are discussed in detail in Chapter 3.

Summary of system requirements

- Results are very sensitive to the detection wavelengths, especially for solutes with sharp peaks in their spectrum such as benzene. Careful selection of the wavelength should be made, and the UV detector linearity at selected wavelength should be checked.
- Although a definitive explanation as to why the diffusion coefficients go up sharply at lower injected quantities has not been found, being aware that the problem exists makes it easier to avoid. The injection quantity should be checked for all solids in methanol before taking data in mixtures.
- The peak area should be considered in the selection of the injected quantity. Based on studies for the above compounds, the peak area should be in the range of 10,000-100,000 mAU-sec as well as satisfying the above criterion.
- A Gaussian curve is assumed for the calculation of the diffusion coefficient from the response curve. Thus it is important to ensure that the response curve is Gaussian.

Determination of system requirements

Since our work involved compounds that had not yet been studied via the Taylor-Aris dispersion method, it was important to determine the appropriate wavelength and injection quantity for each solid. For each of the remaining four solutes, their UV signatures in methanol were obtained from the literature (Silverman, Bassler et al. 1963) where available and all were measured via a separate (not on the SFC) UV spectrophotometer. A series of stock concentrations ranging from 1-32 mg solute/ml methanol were prepared and run through the system at the desired operating conditions (40 °C, 150 bar, 0.2 ml/min mobile phase). Since the data acquisition software has the ability to analyze up to five wavelengths simultaneously, each solute was measured at five different wavelengths and the one which gave the best results based on shape and area of resulting peak was chosen. Parameters determined for all solutes studied are summarized in Table C.1.

Table C.1: Best wavelength for each solute.

Solid	Wavelength (nm)	Concentration (mg/ml)
Benzene	251	32
Pyridine	252	1
Pyrimidine	241	1
Pyrazine	260	2
1,3,5-Triazine	270	4

References

Cussler, E. L. and Editor (1996). Diffusion: Mass Transfer in Fluid Systems, Second Edition.

Funazukuri, T., C. Y. Kong, et al. (2000). "Infinite-dilution binary diffusion coefficients of 2-propanone, 2-butanone, 2-pentanone, and 3-pentanone in CO2 by the Taylor dispersion technique from 308.15 to 328.15 K in the pressure range from 8 to 35 MPa." International Journal of Thermophysics **21**(6): 1279-1290.

Sassiat, P. R., P. Mourier, et al. (1987). "Measurement of diffusion coefficients in supercritical carbon dioxide and correlation with the equation of Wilke and Chang." Analytical Chemistry **59**(8): 1164-70.

Silverman, R. M., G. C. Bassler, et al. (1963). Spectroscopic Identification of Organic Compounds. New York, John Wiley & Sons.

APPENDIX D

EXTRACTION-SPECTROPHOTOMETRIC ANALYSIS OF PHASE TRANSFER CATALYSTS

An extraction-spectrophotometric analysis technique developed by Yamamoto was used to measure the partition coefficients of tetrahexylammonium bromide in Chapter 4 (Yamamoto 1995). The method was modified slightly to measure the concentration of the salt in an organic solvent, toluene, as well as in aqueous solution.

In this analysis technique, bromophenol blue (BPB) sodium salt (Figure D.1), a sulphonephthalein diprotic acid dye, dissociates to form a yellow monovalent anion and a blue divalent anion. These dye anions interact with quaternary ammonium ions in aqueous solution. These ion associates can be extracted into chloroform and analyzed by UV to determine the concentration of the quaternary ammonium salt in the original solution.

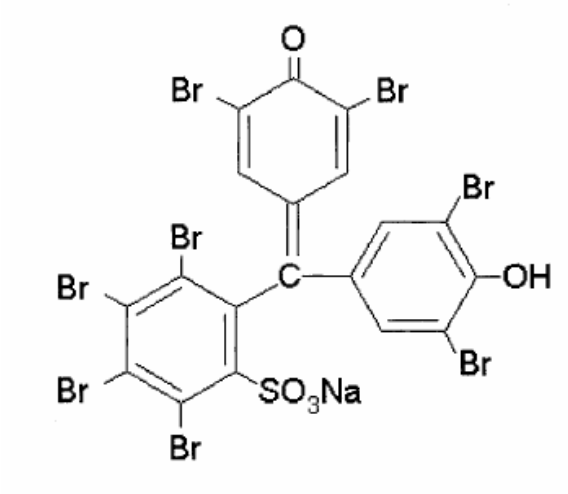

Figure D.1: BPB sodium salt structure

For each experiment, stock solutions of phosphate buffer (pH 8.0) and BPB (5 x 10^{-4} M in phosphate buffer solution) were prepared. The buffer was necessary so that BPB (pKa = 4.10) was extracted mainly as a divalent anion in the ion associate. The BPB was found to be unstable in solution after more than a day, so a new solution was made for each experiment.

The aqueous samples from the reactor were diluted to 10 mL with buffered water. Two mL of each diluted sample were mixed with 2 mL of BPB solution and 4 mL of chloroform in a capped vial. The organic samples were diluted to 5 mL with chloroform. Those 5 mL were mixed with 5 mL of BPB solution in capped vials. All samples were allowed to equilibrate on a rotisserie stirrer for 24 hours. The literature method required mixing for 30 minutes, but waiting 24 hours was found to give more reproducible results in this work.

After equilibration, the upper (water) phase was removed from each vial, and the lower (chloroform) phase was analyzed by UV. The absorption spectra of the 1:2 ion associate (λ_{max} = 606 nm), which had previously been calibrated with THxAB concentration, was measured against pure chloroform. A sample spectra is shown in Figure D.2.

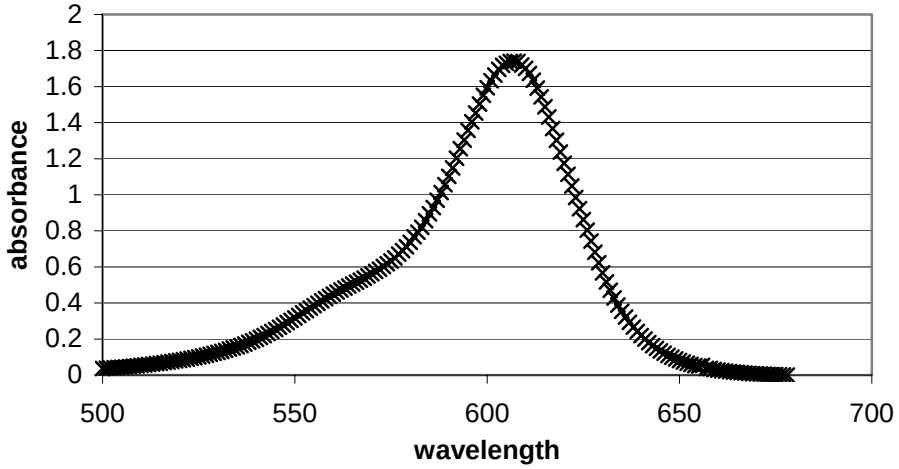

Figure D.2: Sample spectra of BPB:Q^{+}_{2} complex in distribution experiments.

References

Yamamoto, K. (1995). "Sensitive determination of quaternary ammonium salts by extraction-spectrophotometry of ion associates with bromophenol blue anion and coextraction." Analytica Chimica Acta **302**(1): 75-9.

VITA

Natalie B. Maxey

Natalie Renee Brimer was born on August 9, 1978 to Sam and Judy (Guynes) Brimer of Pollock, Louisiana. The oldest of three daughters, she graduated co-valedictorian with her future husband, Kirk Maxey, from Grant High School in Dry Prong, Louisiana. Natalie attended Louisiana Tech University and graduated summa cum laude with a Bachelor of Science in Chemical Engineering in 2000. She and Kirk were also married that year. She attended graduate school at Georgia Institute of Technology in Atlanta, Georgia, where she researched under the guidance of Dr. Charles Eckert of Chemical and Biomolecular Engineering and Dr. Charles Liotta of Chemistry and Biochemistry. She will complete a Ph.D. in Engineering in May 2006.